New Jersey Institute of Technology
Digital Commons @ NJIT

Theses | Electronic Theses and Dissertations

5-31-1993

Investigation of the effects of methyl chloride addition on premixed, laminar, methane/air flat flames

Limin Wang
New Jersey Institute of Technology

Follow this and additional works at: https://digitalcommons.njit.edu/theses

 Part of the Chemical Engineering Commons

Recommended Citation

Wang, Limin, "Investigation of the effects of methyl chloride addition on premixed, laminar, methane/air flat flames" (1993). *Theses*. 1787.
https://digitalcommons.njit.edu/theses/1787

This Thesis is brought to you for free and open access by the Electronic Theses and Dissertations at Digital Commons @ NJIT. It has been accepted for inclusion in Theses by an authorized administrator of Digital Commons @ NJIT. For more information, please contact digitalcommons@njit.edu.

Copyright Warning & Restrictions

The copyright law of the United States (Title 17, United States Code) governs the making of photocopies or other reproductions of copyrighted material.

Under certain conditions specified in the law, libraries and archives are authorized to furnish a photocopy or other reproduction. One of these specified conditions is that the photocopy or reproduction is not to be "used for any purpose other than private study, scholarship, or research." If a, user makes a request for, or later uses, a photocopy or reproduction for purposes in excess of "fair use" that user may be liable for copyright infringement,

This institution reserves the right to refuse to accept a copying order if, in its judgment, fulfillment of the order would involve violation of copyright law.

Please Note: The author retains the copyright while the New Jersey Institute of Technology reserves the right to distribute this thesis or dissertation

Printing note: If you do not wish to print this page, then select "Pages from: first page # to: last page #" on the print dialog screen

NJIT New Jersey's Science & Technology University

The Van Houten library has removed some of the personal information and all signatures from the approval page and biographical sketches of theses and dissertations in order to protect the identity of NJIT graduates and faculty.

ABSTRACT

Investigation of the Effects of Methyl Chloride Addition on Premixed, Laminar, Methane/Air Flat Flames

by
Limin Wang

Temperatures and the concentrations of stable species, such as CO, CO_2, CH_4, and CH_3Cl, have been measured over the height above burner at equivalence ratio of 0.79 (fuel lean) and 1.20 (fuel rich) for premixed, laminar CH_4/air and CH_3Cl/CH_4/air flat flames. A water-cooled quartz sampling micro-probe and gas chromatographic analysis were used for the concentration measurements. Chemical kinetic modeling of these flames with a 279-reaction, 63-species elementary reaction mechanism is performed using the CHEMKIN premixed flat flame code. The results of rate-of-production calculations are analyzed to determine the most important reaction pathways responsible for destruction of the fuels, and the production and consumption of the intermediates. Experimental data show that CH_4/air flames doped with CH_3Cl have higher CO/CO_2 concentration ratios over almost all heights above the burner at the same equivalence ratio, which is consistent with the modeling prediction.

INVESTIGATION OF THE EFFECTS OF METHYL CHLORIDE ADDITION ON PREMIXED, LAMINAR, METHANE/AIR FLAT FLAMES

by
Limin Wang

A Thesis
Submitted to the Faculty of
New Jersey Institute of Technology
in Partial Fulfillment of the Requirements for the Degree of
Master of Science in Chemical Engineering

Department of Chemical Engineering,
Chemistry, and Environmental Science

May 1993

APPROVAL PAGE

Investigation of the Effects of Methyl Chloride Addition on Premixed, Laminar, Methane/Air Flat Flames

Limin Wang

Dr. Robert B. Barat, Thesis Advisor (Date)
Assistant Professor of Chemical Engineering, NJIT

Dr. Joseph W. Bozzelli, Committee Member (Date)
Distinguished Professor of Chemistry, NJIT

Dr. Richard S. Magee, Committee Member (Date)
Professor of Chemical and Mechanical Engineering, and Executive Director of the Hazardous Substance Management Research Center

BIOGRAPHICAL SKETCH

Author: Limin Wang

Degree: Master of Science in Chemical Engineering

Date: May 1993

Undergraduate and Graduate Education:

- Master of Science in Chemical Engineering
  New Jersey Institute of Technology, Newark, NJ, 1993

- Bachelor of Science in Chemical Engineering
  East China University of Chemical Technology, P. R. China, 1985

Major: Chemical Engineering

Presentations and Publications:

Limin Wang and Weichun Chen,"OH Radical Measurement by Laser Induced Fluorescence." *Society for the Advancement of Material & Process Engineering.* NJIT Minitech, Newark, New Jersey, April 10, 1992.

Limin Wang, Philippe Jalvy, and Robert Barat,"The Impact of Chlorine on a Premixed, Fuel-Lean Methane/Air Laminar Flat Flame." Submitted to *Combustion Science and Technology.* April, 1993.

Limin Wang and Robert Barat,"The Impact of Chlorine on a Premixed, Fuel-Rich Methane/Air Laminar Flat Flame." Submitted to *Combustion and Flame.* May, 1993.

This thesis is dedicated to my parents,
Xing-Kang Wang and Zhi-Ying Xu,
and my best friend, Jim Vance

ACKNOWLEDGMENT

The author wishes to express her sincere gratitude to her advisor, Dr. Robert B. Barat, for his guidance, friendship, and moral support throughout this research work.

Special thanks to Dr. Joseph W. Bozzelli and Dr. Richard S. Magee for serving as members of the committee.

The author is grateful to the Northeast Hazardous Substance Research Center, an Environmental Protection Agency Research Center for Federal Regions I and II, for providing the funding of the research.

The author also appreciates the timely help and suggestions from the members of the NJIT faculty.

Finally, the author would like to thank Philippe Jalvy, Dustin Ho, Weichun Chen, and Hasan Karim for their sincere support during this study.

TABLE OF CONTENTS

LIST OF TABLES

LIST OF FIGURES

Figure **Page**

CHAPTER 1
INTRODUCTION

1.1 Background of the Project

Hazardous waste incineration plays an essential role in environmental protection and improvement. It is a viable disposal alternative for organic hazardous waste since it is applicable to a large number of organic pollutants, it detoxifies the waste, and it has the potential for energy recovery. Basically, the incineration process involves the conversion of organic waste materials to CO_2, H_2O, HCl, SO_2, and low volume inert ash material via high temperature oxidation. However, our recent understanding of the chemistry of combustion is still not adequate to predict the nature and amounts of trace organics from incinerators. In order to comply with more stringent regulations required by the government, many efforts have been made in the scientific research to eliminate the formation of products of incomplete combustion and control pollutant emissions into the environment.

Understanding the combustion characteristics of chlorinated hydrocarbons (ClHCs) is very important in the context of hazardous waste incineration. Because of the widespread use of ClHCs as industrial solvents and degreasers, ClHC-containing wastes are often incinerated, providing ultimate disposal and mitigating potential ground water contamination. Fire safety is a related area of concern to public officials. Chlorinated hydrocarbons are often used in the manufacture of plastics for wall and furniture coverings, plumbing materials, wiring insulation, etc. In the event of fire, ClHC-containing materials will be burned and can produce toxic substances.

To obtain a better knowledge of the properties of potentially toxic pollutants which are formed in combustion systems burning chlorinated hydrocarbons, the flame structures of simpler ClHCs must be better established and a fundamental understanding of the chemical and physical mechanisms of waste incineration must be developed. Flame structure studies are necessary and important for the development and subsequent verification of detailed chemical models describing the combustion of ClHCs. These mechanisms, once developed, can then be used to predict the combustion behavior of ClHCs in complex mixtures.

1.2 Scope of the Study

In this study, premixed, laminar, flat flames for both CH_4/air and CH_3Cl/CH_4/air fuel mixtures at atmospheric pressure were investigated to observe the effects of CH_3Cl addition on CH_4/air flames. The concentration profiles of stable species, such as CO, CO_2, CH_4, and CH_3Cl were obtained for different equivalence ratios (ϕ) and different CH_3Cl loadings. Also, the CO/CO_2 concentration ratio along the height above burner was generated for each flame. The following cases of fuel lean and fuel rich flames were studied:

1. ϕ=0.79,

1) CH_3Cl/CH_4=0, 2) CH_3Cl/CH_4=0.25, 3) CH_3Cl/CH_4=0.50

2. ϕ=1.20,

1) CH_3Cl/CH_4=0, 2) CH_3Cl/CH_4=0.25, 3) CH_3Cl/CH_4=0.50

A chemical mechanism (Ho et al., 1992) of 279-reaction and 63-species was used with the Sandia National Laboratories one-dimensional premixed laminar flat flame code (Sandia Report, 1985) to simulate the flame. The reaction mechanism is based upon fundamental thermodynamic

and kinetic principles. The modeling results of rates-of-production were also analyzed to determine the most important reaction pathways. This effort provided important insight into the chemistry of ClHC incineration.

A water-cooled quartz sampling microprobe and gas chromatographic analysis were employed for the concentration measurements. Temperature profiles of the different flames were made by using a Pt/Pt-13%Rh thermocouple. These profiles and the feed conditions were input to the model.

CHAPTER 2
LITERATURE SURVEY

Chlorinated compounds are known to inhibit hydrocarbon combustion processes and promote the formation of soot in flames. Over the past several years, much research work has been done on chlorinated hydrocarbon combustion.

A number of studies were conducted to investigate flame inhibition by small amounts of chlorinated compounds seeded into conventional hydrocarbon flames (Wilson, 1965, Biordi, 1973). These studies suggested that the major effect of the chlorine inhibitor was to react preferentially with H atoms rather than allowing H atoms to participate in the normal chain branching reaction ($H + O_2 = OH + O$). The effect is to reduce burning velocities and delay the point of ignition.

The flame speeds of premixed $ClHC/CH_4$/air mixtures were measured and reported by Valeiras (1984). Increasing chlorine content was shown to decrease the flame velocity and shift the maximum flame velocity from fuel rich toward fuel lean flames.

Chemical species and temperature profiles for laminar dichloromethane-methane-air flat flames with variable Cl/H loading have been reported by Senser et al. (1987). Significantly higher levels of C_2H_2, a known soot precursor, were found in ClHC flames as compared with analogous CH_4 flames.

Senkan and Karra (1987) explored the impact of chlorine on the combustion chemistry of hydrocarbons by undertaking systematic comparative studies of the structures of sooting CH_3Cl/CH_4 and CH_4 flames. Their results have shown that chlorine has a considerable effect on

flame chemistry, as evidenced by the enhanced formation of C_2 hydrocarbons, in particular C_2H_2 and C_2H_4, and CO. These species form earlier and at substantial levels in flames containing CH_3Cl when compared to those involving only CH_4, although the equivalence ratio of the latter flame was considerably higher.

Incipient soot formation in CH_2Cl_2/CH_4/air premixed flames were studied by Senser and Janssen (1991). They indicated that, at constant temperature, chlorine increases the rate of precursor formation and reduces the rate of precursor oxidation via reduction in the OH concentration.

The inhibition of a fuel lean C_2H_4/air flame in a jet stirred combustor by methyl chloride was investigated through experimental and mechanistic analyses by Barat et al. (1990). The results showed that the temperature of fuel lean C_2H_4/air combustion in a toroidal jet stirred combustor (TJSC) was progressively lowered as CH_3Cl increased, resulting in the transition to marginal instability. The addition of a small amount of CH_3Cl to the feed resulted in the transition of the TJSC from a state of near-marginal stability to one of significant localized blowout. The cause of this enhanced instability is an inhibition of CO burnout due to the consumption of OH by HCl. The termination channel of the reaction Cl + HO_2 (products HCl + O_2) further inhibits CO burnout because HO_2 is a source of OH.

The thermal decomposition of CH_2Cl_2 in H_2/O_2/Ar bath gas in a tubular flow reactor was studied by Ho et al. (1992). Their results indicated that a competition for OH between CO and HCl results in a reduction of CO conversion to CO_2.

CHAPTER 3
EXPERIMENTAL METHOD

3.1 Experimental Apparatus and Technique

A diagram of the experimental apparatus is shown in Figure 1. The premixed, laminar, flat flames of CH_4/air and CH_3Cl/CH_4/air are stabilized on a stainless steel, water cooled, porous Mckenna flat flame burner (refer to Figure 38 in Appendix B) of 60 millimeters diameter. A nitrogen shroud ring isolates the flame from the surrounding air. The burner is mounted on a precision laboratory jack. It can be moved vertically to allow the flame temperature and concentration profiles to be measured along the height above burner (HAB). All experiments are conducted at atmospheric pressure.

Reactant fuels are supplied from gas cylinders, and then mixed with the air before entering the burner. The total mass flow rates of the fuel and air mixture through the burner surface are held approximately constant at 0.0105 g/cm^2-sec. The cold gas velocity is between 8.2 cm/sec and 8.6 cm/sec. The velocity of nitrogen shroud gas is 7.7 cm/sec approximately. The gas flow rates of fuel, air, and nitrogen are measured and regulated through calibrated rotameters. Calibrations were carried out under the fixed inlet pressure of 20 psig and the temperature of 20 ^{0}C for each gas. The flow meters were oriented with their control valves mounted on the outlet. The methane, methyl chloride, and nitrogen used in the experiments are high purity grade (99.98%). The flowmeter calibration curves are shown in Appendix A.

The combustion products are exhausted through the ventilation system. The gaseous product HCl is scrubbed with a water spray in the

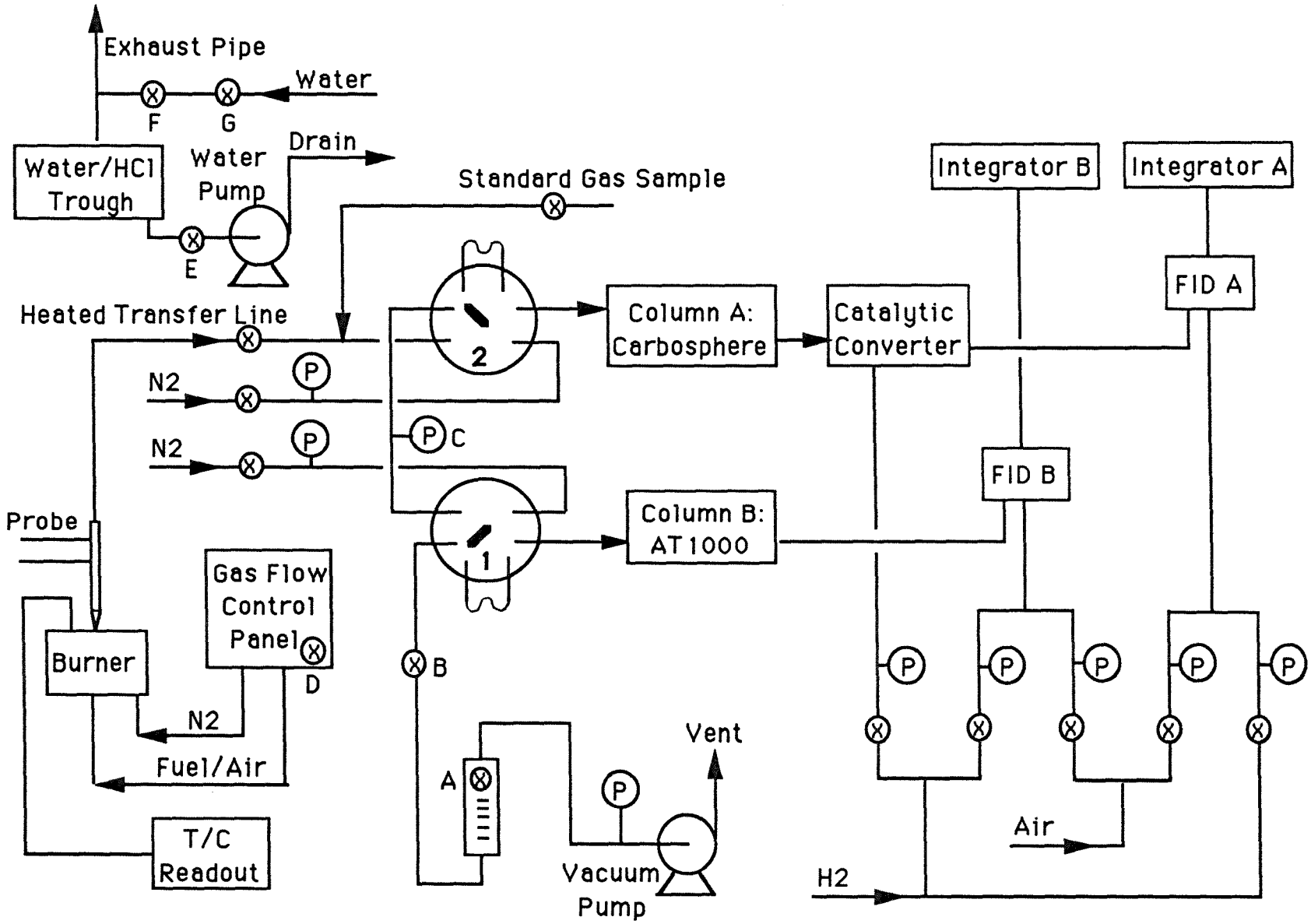

Figure 1 A Schematic Diagram of Experimental Apparatus

exhaust pipe, and then trapped in a water-drained trough far above the flame.

A water-cooled quartz micro-probe and Varian 3400 gas chromatograph (GC) are used for gas sampling and analysis respectively. Gas samples are pulled through the quartz microprobe, situated in the center of the flame, by means of a mechanical vacuum pump. In order to avoid water vapor condensation of the gas samples, the line between the microprobe and GC is externally heated. The probe is held fixed, while the burner is vertically translated.

In our GC analysis system, nitrogen is used as a carrier gas. Two six-port VALCO gas sampling valves are employed to introduce the gas samples into the GC columns. The two configurations of a six-port valve are shown below:

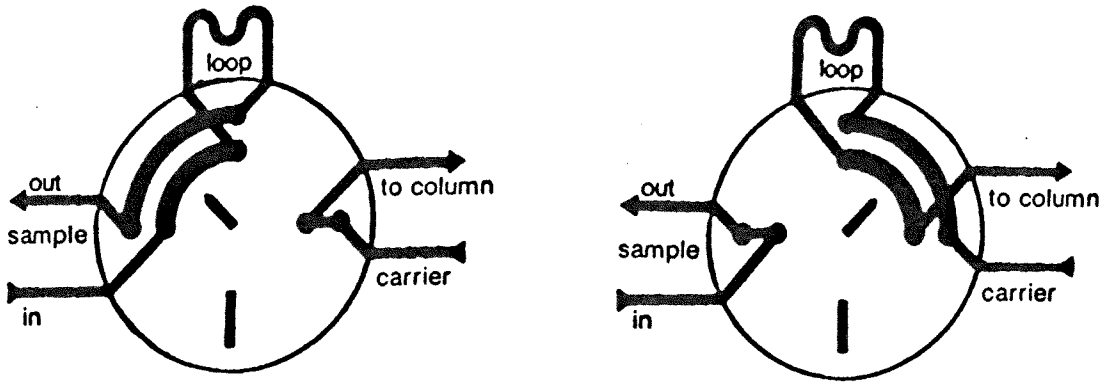

Collection Position Injection Position

Figure 2 Configuration of Six-Port Valve

The gas samples are collected in the sample loops to a fixed pressure (5 inHg) as measured on the pressure gauge C (Figure 1) and then injected into the packed columns in the GC. There are two 1/8" O.D. columns in the GC: column A is packed with Carbosphere (80/100) for CO, CO_2 and light hydrocarbons separation, and column B is packed with 1% AT-1000 on Graphac (60/80) for chlorinated hydrocarbon separation. The length of each column is six feet. After the sample is separated in column A, CO and CO_2 are methanated with H_2 over a ruthenium catalyst converter, which is heated to 300 ^{0}C. The sample is then detected by a flame ionization detector (FID A). The signal peaks from FID A are recorded and integrated by integrator A. After the sample is separated in column B, it is directly detected by FID B. The signals obtained by FID B are processed in integrator B.

Two GC column temperature programs are used for separation of samples from the CH_4/air flames and CH_3Cl/CH_4/air flames respectively.

For CH_4/air flames, the program is:

Initial temperature	90 ^{0}C	Holding time 1.7 min
Temperature ramp	15 ^{0}C/min	
Final temperature	110 ^{0}C	Holding time 2.0 min

For CH_3Cl/CH_4/air flames, the program is:

Initial temperature	70 ^{0}C	Holding time 3.0 min
Temperature ramp	15 ^{0}C/min	
Final temperature	110 ^{0}C	Holding time 2.0 min

The injection temperature is 150 ^{0}C and the detector temperatures are 300 ^{0}C for all cases.

The operating flow rates of nitrogen used as carrier gas for each column (Carbosphere and AT1000), air for each FID, and hydrogen for

each FID and converter in the GC system were also calibrated. These flow rates are shown in Table 1.

Table 1 Operating Conditions in GC System

Gas	Flow rate (ml/min)*	Pressure Gauge (psig)
N_2 (AT1000)	30	90
N_2 (Carbosphere)	30	20
H_2 (FID B)	30	
H_2 (FID A)	15	45 (for total H_2)
H_2 (Converter)	15	
Air (FID A & B)	300	50

*Standard temperature and pressure.

Flame temperature measurements were made using an OMEGA, uncoated, Type R, Pt/Pt-13%Rh thermocouple (shown in Appendix B). The thermocouple is supported by a fixed post and is positioned parallel to the burner surface, i.e. perpendicular to the direction of the gas flow. The burner is then raised or lowered with respect to the thermocouple to generate the temperature profiles. A radiation correction was not made.

3.2 Calibration of GC System

The GC system was calibrated with a Scotty IV analyzed standard gas mixture purchased from Scotty Specialty Gases (2330 Hamilton Blvd., South Plainfield, NJ 07080). The container of analyzed gases contains CO, CO_2, CH_2, C_2H_2, C_2H_4, and C_2H_6 with a concentration of 1% by volume in

nitrogen for each compound. The calibration procedures are almost the same as those used for analyzing gas samples from the flames. Though some differences exist, these are minor as described below. They do not affect the results.

When the GC analysis for the standard gas sample is performed, the outlet of the standard sample container is connected to the inlet of the sample loops in the GC (see Figure 1) and the valves on the container are kept closed. A vacuum pump is turned on to evacuate the sample loops. Then, the inlet valve of the pump is closed, and the sample loops are filled with the standard gas mixture by slowly opening the valves on the container, until the vacuum pressure reading on the gage reaches 5 inHg. Finally, the sample is injected to the GC with the VALCO valve.

Since the standard gas sample contained in the loops is static and the sample from the flame pulled by the vacuum pump flows continuously through the loops, a pressure drop in the loops with the flowing sample was a potential concern. The pressure drop was measured by installing one pressure gauge before the loop and the other after the loop. The readings shown on both gauges were effectively the same, 5.0 inHg and 5.2 inHg respectively. This indicated that the pressure drop in the loop can be neglected. Therefore, static filling the loops during a calibration is valid for analysis of flame samples flowed through the loops.

3.3 Calculation of Equivalence Ratio

The fuel equivalence ratio (ϕ) is defined as the actual fuel/oxygen molar concentration ratio in the feed mixture to the stoichiometric fuel/oxygen molar concentration ratio.

$$\phi = \{[\text{Fuel}] / [O_2]\ (\text{actual})\} / \{[\text{Fuel}] / [O_2]\ (\text{stoich.})\} \qquad (3.1)$$

In CH4/air flames, the overall reaction is:

$$CH_4 + 2O_2 = CO_2 + 2H_2O \qquad (a)$$

The equivalence ratio is calculated as follows:

$$\phi = \{[Fuel] / [O_2] (actual)\} / \{[Fuel] / [O_2] (stoich.)\}$$
$$= \{V_{CH_4} / V_{O_2} (actual)\} / \{1/2\}$$
$$= 2V_{CH_4} / V_{O_2} (actual)$$

where V_{CH_4} and V_{O_2} are the volumetric flow rate of CH_4 and O_2 respectively.

Since $V_{O_2} = 21\%$ Vair, So,

$$\phi = (2V_{CH_4}) / (21\% \text{ Vair}) = 9.52\, V_{CH_4} / \text{Vair} \qquad (3.2)$$

In CH3Cl/CH4/air flames, we have the following overall reactions:

$$CH_4 + 2O_2 = CO_2 + 2H_2O \qquad (a)$$

$$CH_3Cl + 3/2\, O_2 = CO_2 + H_2O + HCl \qquad (b)$$

Let $R = V_{CH_3Cl} / V_{CH_4}$, multiply (b) by R and combine with (a), we get

$$CH_4 + RCH_3Cl + (2+3R/2)O_2 = (1+R)CO_2 + (2+R)H_2O + RHCl$$

The equivalence ratio is:

$$\phi = \{(V_{CH_4} + V_{CH_3Cl}) / V_{O_2}\} / \{(1 + R) / (2 + 3R/2)\}$$
$$= \{(V_{CH_4} + RV_{CH_4}) / (21\%\text{Vair})\} / \{(1 + R) / (2 + 3R/2)\}$$
$$= 4.76\, (2 + 3R/2)\, V_{CH_4} / \text{Vair} \qquad (3.3)$$

Table 2 is the summary of the flame initial feed conditions. It shows the gas flow rate, the ratio of CH_3Cl to CH_4 (R), and calculated ϕ of fuel lean and fuel rich flames used in the experiments.

Table 2 Summary of Flame Conditions

ϕ	R	Vair (ml/min)*	V_{CH_4} (ml/min)*	V_{CH_3Cl} (ml/min)*	V_{N_2} (shroud) (ml/min)*
0.79	0	12830	1067	0	4830
0.79	0.25	12830	897	224	4830
0.79	0.50	12830	774	387	4830
1.20	0	12830	1617	0	4830
1.20	0.25	12830	1362	340	4830
1.20	0.50	12830	1176	588	4830

* Rotameters are calibrated at T = 25 ^{0}C and P = 20 psig.

3.4 Experimental Procedures

Before starting the flat flame burner, the analysis system is prepared for the gas sampling as follows: check the flow of nitrogen carrier gas to GC, and hydrogen and air for the GC detectors; heat the transfer line and the catalytic converter; start the GC program and ignite the FID detectors. Set up the integrators (refer to Appendix B). Then, position the water-cooled quartz micro-probe in the center of the burner and set up the flow rate of each gas according to the flame conditions summarized in Table 2.

When the GC is stabilized, start the flat flame burner. The sample is pulled through the quartz probe by a vacuum pump. Adjust the loop pressure to 5 inHg (gauge pressure) and inject the sample by switching the six-port valves, and then, quickly start the GC program. The peaks of the

species are recorded by the integrators (shown in Figures 40 and 41). Repeat the analysis at each position of HAB over a desired range.

In performing the gas sampling, the GC system should be checked frequently in case there is any leakage. It is also important to clean the GC columns by heating them at higher temperature (199 ^{0}C). Clean the Mckenna burner and the transfer line in the GC system after the completion of gas sampling to prevent HCl corrosion. Detailed operating steps are described in Appendix B.

CHAPTER 4
MODELING

The flames in this study are modeled by using a detailed reaction mechanism and the Sandia one-dimensional premixed flame code package, a Fortran program for modeling steady laminar one-dimensional premixed flames (Kee, et al., 1985). This model is capable of predicting temperature and species profiles in steady-state burner-stabilized and freely propagating premixed laminar flames. The equations governing steady, isobaric, quasi-one-dimensional flame propagation are written as follows (Kee, et al., 1985):

$$\dot{M} = \rho u A \tag{4.1}$$

$$\dot{M}\frac{dT}{dx} - \frac{1}{c_p}\frac{d}{dx}\left(\lambda A \frac{dT}{dx}\right) + \frac{A}{c_p}\sum_{k=1}^{K}\rho Y_k V_k c_{p_k}\frac{dT}{dx} + \frac{A}{c_p}\sum_{k=1}^{K}\dot{\omega}_k h_k W_k = 0 \tag{4.2}$$

$$\dot{M}\frac{dY_k}{dx} + \frac{d}{dx}(\rho A Y_k V_k) - A\dot{\omega}_k W_k = 0 \qquad (k=1, 2, ..., K) \tag{4.3}$$

$$\rho = \frac{p\overline{W}}{RT} \tag{4.4}$$

where x=the spatial coordinate, $\dot{M}$=the mass flow rate, T=the temperature, Y_k=the mass fraction of the kth species (there are K species), p=the pressure, u=the velocity of the fluid mixture, ρ=the mass density, W_k=the molecular weight of the kth species, $\overline{W}$=the mean molecular weight of the mixture, R= the universal gas constant, λ=the thermal conductivity of the mixture, c_p=the constant pressure heat capacity of the mixture, c_{pk}=the constant presure heat capacity of the kth species, $\dot{\omega}_k$=the molar rate of production by chemical reaction of the kth species per unit volume, h_k=the specific enthalpy of the kth species, V_k=the diffusion velocity of the kth species, and A=the cross-sectional area of the stream tube encompassing the flame.

These equations are solved by using finite difference discretization and the Newton method with the appropriate boundary conditions. In addition, the program runs in conjunction with the preprocessors for the chemical reaction mechanism, the thermodynamic properties, and the transport properties. It depends on data and subroutines from the CHEMKIN and transport packages (Kee, et al., 1985).

In this study, the model is used for computing species profiles for the burner-stabilized flame with a known mass flow rate and a known temperature profile obtained from the experimental measurements. The model can calculate the temperature profile by the energy conservation equation. But because of uncertainties in heat losses, it is better to use a measured temperature profile (if available) than that obtained by solving the energy conservation equation. There can be significant heat losses to the external environment, which are of unknown or questionable origin, and thus troublesome to model (Kee, et al., 1985). Therefore, in this work, only equations (4.1), (4.3), and (4.4) are used.

A detailed elementary reaction mechanism (See Appendix C) is used together with the code. It is based on an updated version of a set of reactions proposed by Ho et al. (1991). All the reactions in this mechanism are implicitly reversible. The model is run in the burner-stabilized flame mode. The temperature profiles obtained with a Pt/Pt-13%Rh thermocouple are introduced as an input parameter. The mole fractions of unburned gas mixture are used as the initial concentrations of the reactants. The composition of the final products is estimated based on the overall reactions with products of CO_2, H_2O, and HCl. A sample input file is shown in Appendix D. In this case, the mass flow rate through the burner is 0.0102 g/cm^2-sec. The pressure is 1.0 atmosphere. The unburned

reactant mole fractions are: O_2=0.1939, N_2=0.7293, and CH_4=0.0768. The estimated mole fractions of products are: CO_2=0.0768, H_2O=0.1536, O_2=0.0403, and N_2=0.7293. These estimates are used by the equation solver.

In order to obtain an important insight into the chemistry of chlorocarbons in hydrocarbon flames, the rate-of-production calculation, a subroutine created by Karim (1992), is applied with the flame code to get the rates of those reactions which directly produce or consume a certain species. The molar production rate $\dot{\omega}_k$ of species k is given by

$$\dot{\omega}_k = \sum_{i=1}^{I} \nu_{ki} q_i \qquad (4.5)$$

where ν_{ki} are the stoichiometric coeffecients and q_i are the rate of progress variables for the I reactions. The contributions to the rate of production of species k for reaction i is therefore simply

$$C_{ki} = \nu_{ki} q_i \ . \qquad (4.6)$$

Further details about how the reactions contribute to species production are found in the CHEMKIN user's manual. The contribution of each reaction to that species at each mesh point (indicating the height above burner) is normalized by taking the percentage of the net rate of production (ROP) or consumption to determine which reactions are more important. Contributions less than 10% are not reported. This cut-off is arbitrarily set by the user. The net production (positive) and consumption (negative) rates for that species at each mesh point are also provided. The output of the ROP calculations is shown in Appendix E. By performing and analyzing the rate-of-production calculation for the major species, the important reaction pathways are generated.

CHAPTER 5
RESULTS AND DISCUSSIONS

5.1 Comparison of Experimental and Modeling Results

Experimental and modeling studies are conducted with both $\phi = 0.79$ (fuel lean) and $\phi = 1.20$ (fuel rich) flames. ϕ is calculated based on the following overall reactions:

(a) $CH_4 + 2O_2 = CO_2 + 2H_2O$;

(b) $CH_3Cl + 3/2O_2 = CO_2 + H_2O + HCl$.

The molar feed ratios of CH_3Cl to CH_4 (R) are varied for a constant ϕ as follows:

1) R = 0; 2) R = 0.25; 3) R = 0.50.

This is achieved by reducing CH_4 and adding CH_3Cl, and adjusting the total flow rates to get temperature profiles nearly the same for three flames (R=0, R=0.25, and R=0.50) at each constant ϕ. From calculations, the total heating values of feed rates are also nearly the same for three flames (R=0, R=0.25, and R=0.50) at each constant ϕ. For $\phi = 0.79$ flames, the heating values of feed rates are −0.152 Kcal/mole, −0.154 Kcal/mole, and −0.154 Kcal/mole for R=0, R=0.25, and R=0.50 respectively. For $\phi = 1.20$ flames, the heating values of feed rates are −0.231 Kcal/mole, −0.233 Kcal/mole, and −0.235 Kcal/mole for R=0, R=0.25, and R=0.50 respectively. The total mass flow rates are held approximately constant at 0.0105 g/cm^2-sec for all flames. The CH_4/air flames serve largely as a base reference to make comparisons to CH_3Cl doped flames.

Figures 3 and 4 are the measured temperature profiles for fuel lean and fuel rich flames respectively. Both figures show that the temperature of CH_4/air flames is higher than CH_3Cl/CH_4/air flames in the preheat zone,

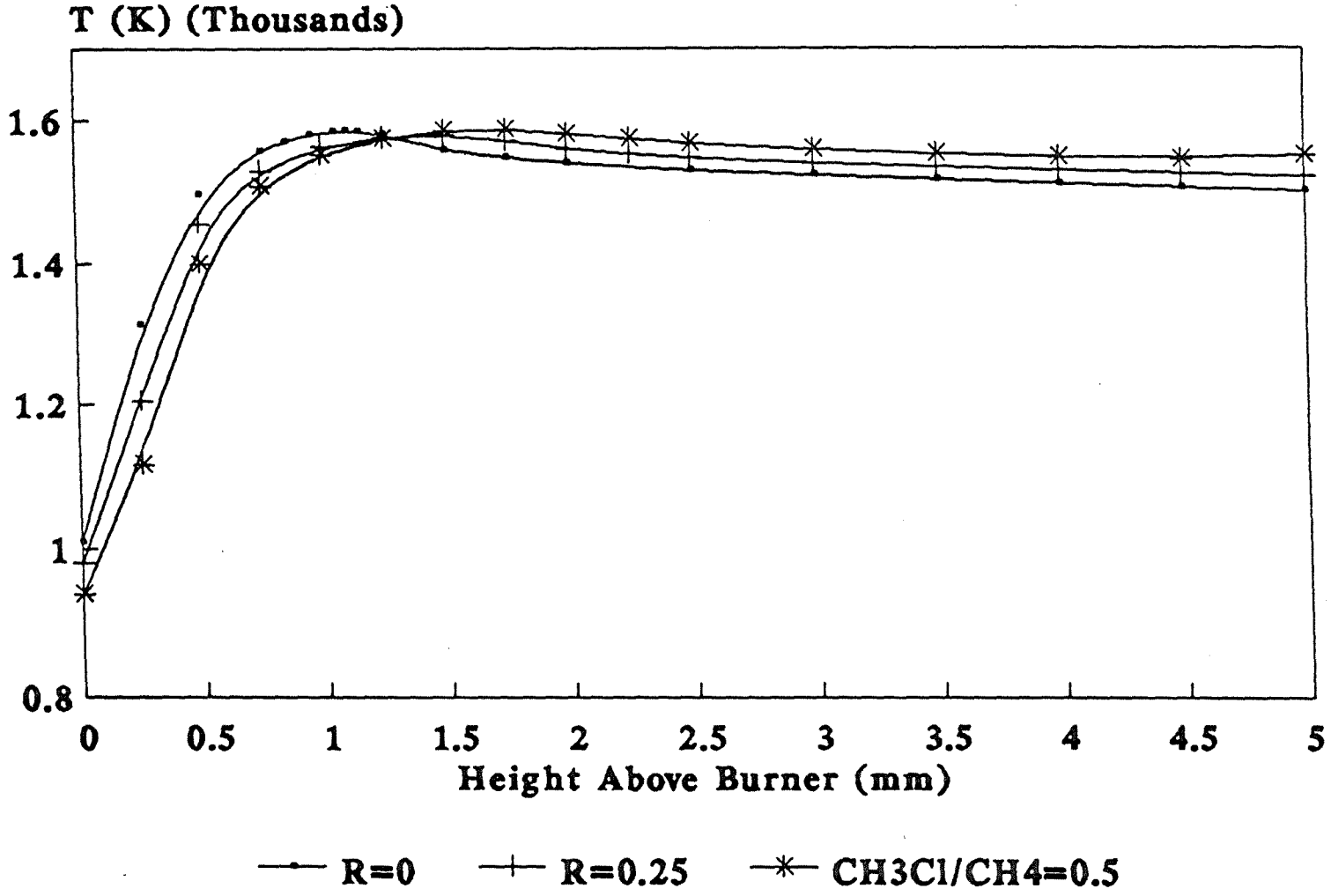

Figure 3 Temperature Profile for ϕ=0.79

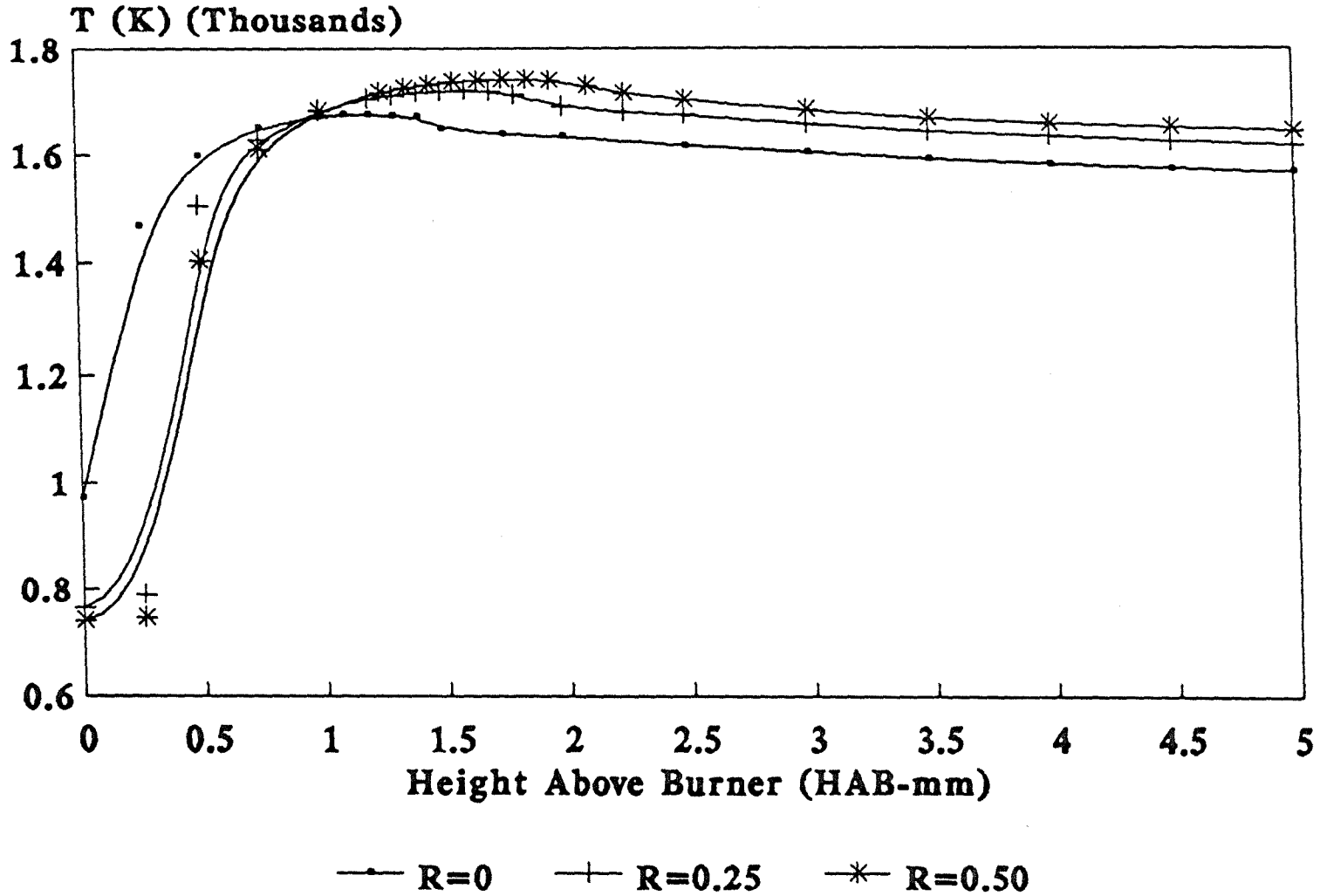

Figure 4 Temperature Profile for ϕ=1.20

and lower in the flame front and post flame zone. In the preheat zone, the feed gas is heated by conduction from the adjacent flame (reaction) zone. In additional, small free radicals such as H back-diffuse to initiate low temperature (<1000 K) chemistry. In the reaction zone (flame front), the reactants are consumed and intermediates produced (especially CO). This zone is characterized by large temperature gradients and heat release rate. In the post flame zone, intermediates such as CO are consumed as the flame approaches reaction equilibrium. Approximately, the preheat zone is from 0.0 mm to 0.8 mm HAB; the flame front is from 0.8 mm to 2.5 mm HAB; and the post flame zone is above 2.5 mm HAB. The temperature difference between CH_4/air and CH_3Cl/CH_4/air flames is only around 50 K (average), which is not significant. It is estimated that an uncertainty of ± 0.25 mm exists in the absolute position of the temperature profiles. This is observed while repeating the measurements.

The experimental and model predicted concentration profiles (mole fraction versus height above burner) of major species: CO, CO_2, CH_4, and CH_3Cl in each flame are compared in Figure 5 through Figure 10. The initial fuel and air feed are summarized in Table 2.

These results show a reasonable agreement between experimental data and model predictions, especially in the post-flame zone. The discrepancies between the model and measurements are most obvious near the burner surface (HAB = 0.0 mm). These discrepancies can be caused by both the experiments and the model, as both experimental and modeling investigation have their own limitations.

For experimental studies, it is difficult to achieve accurate measurements of species concentrations in the flame. For instance, in probe sampling, probe-surface interactions can occur. Labile species can be lost

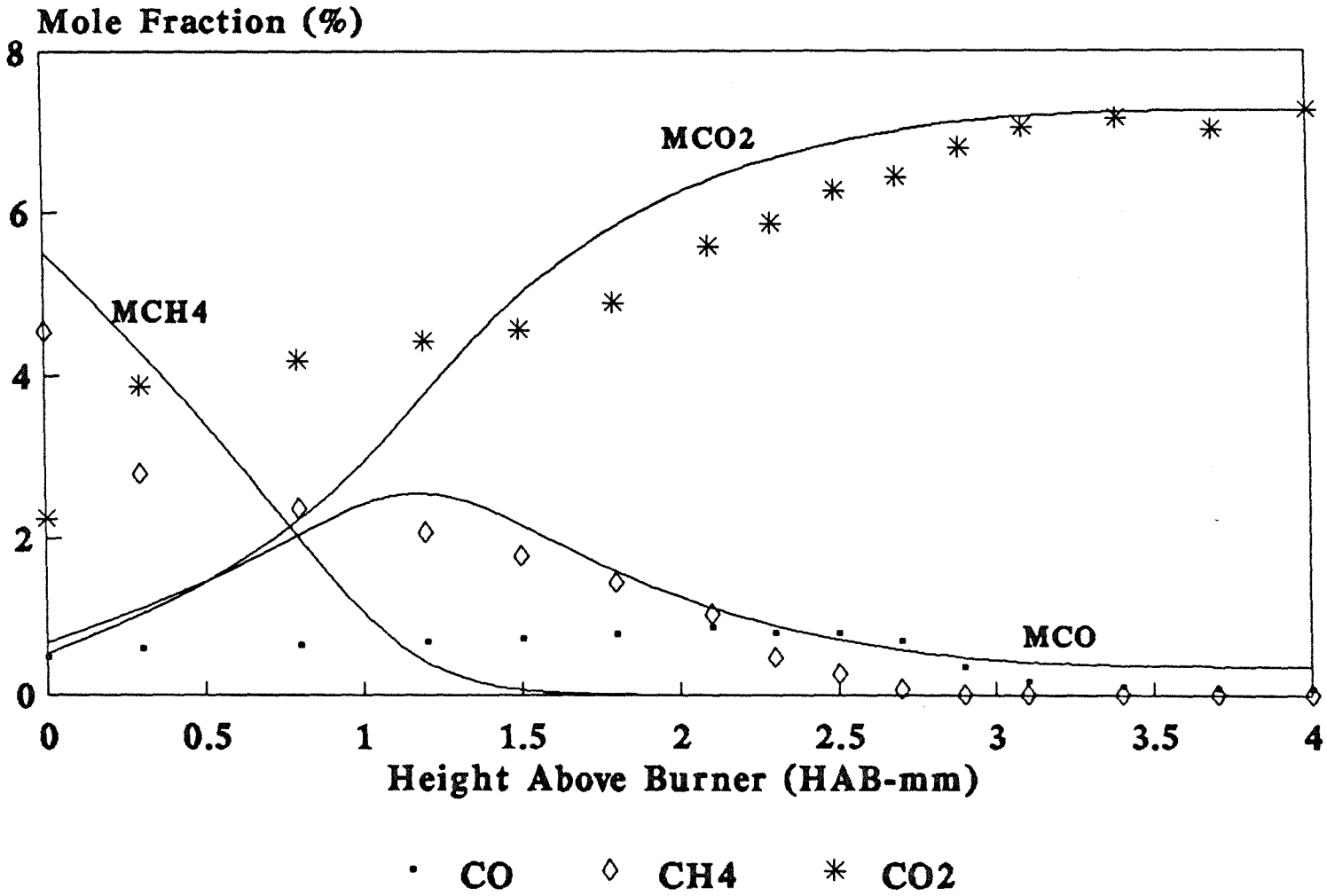

Figure 5 Comparison of Experimental & Model Results for ϕ=0.79, R=0

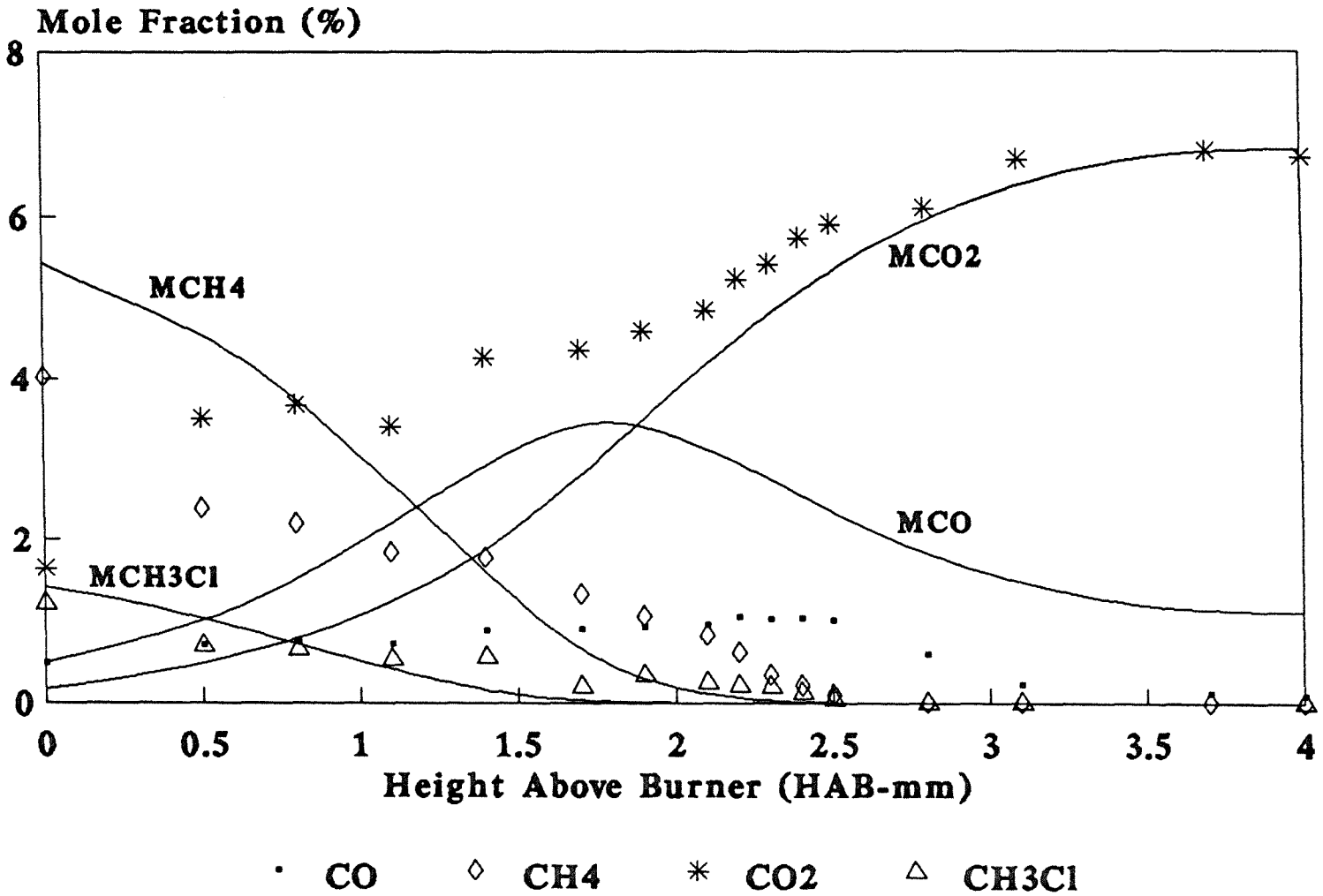

Figure 6 Comparison of Experimental & Model Results for ϕ=0.79, R=0.25

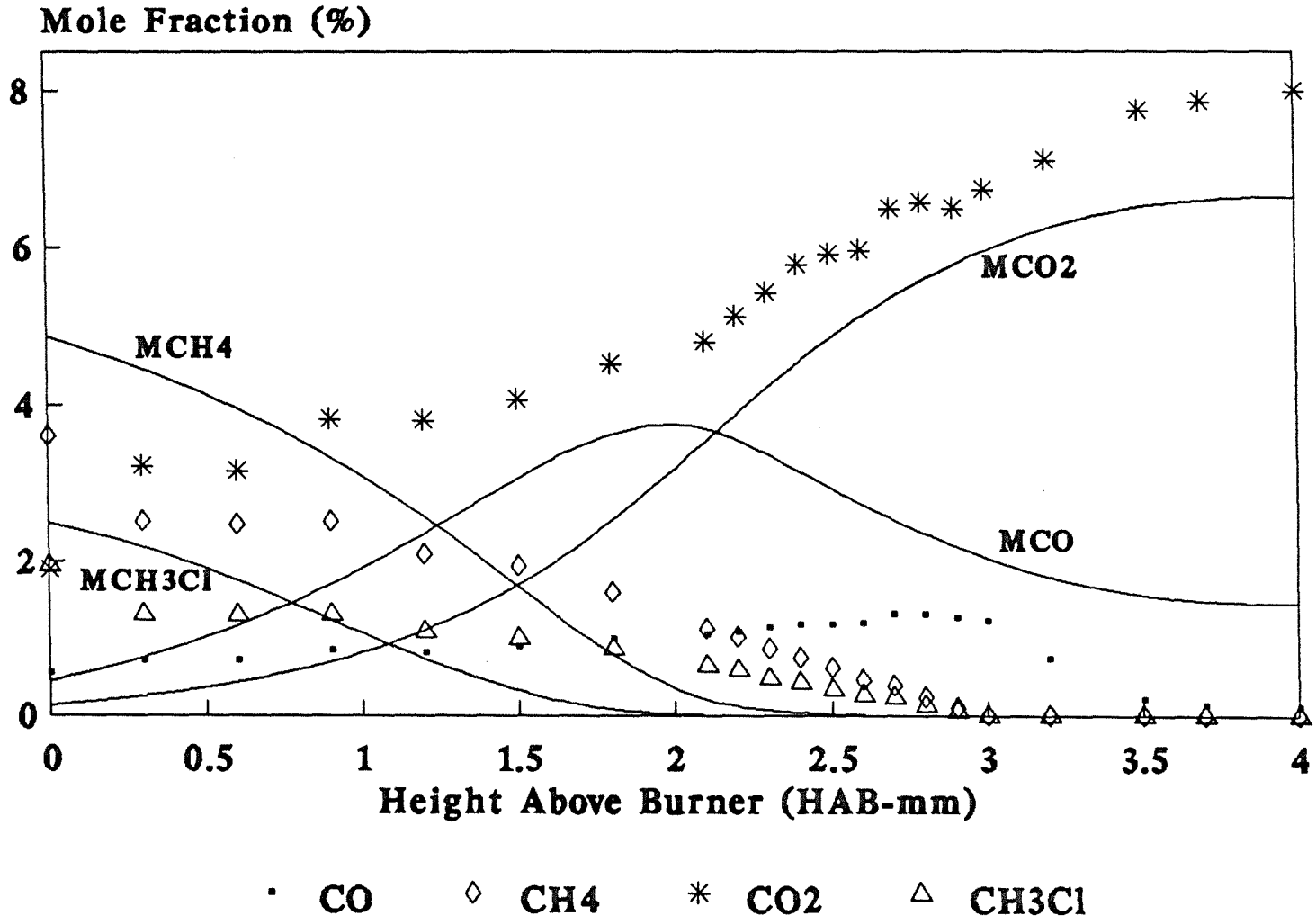

Figure 7 Comparison of Experimental & Model Results for ϕ=0.79, R=0.50

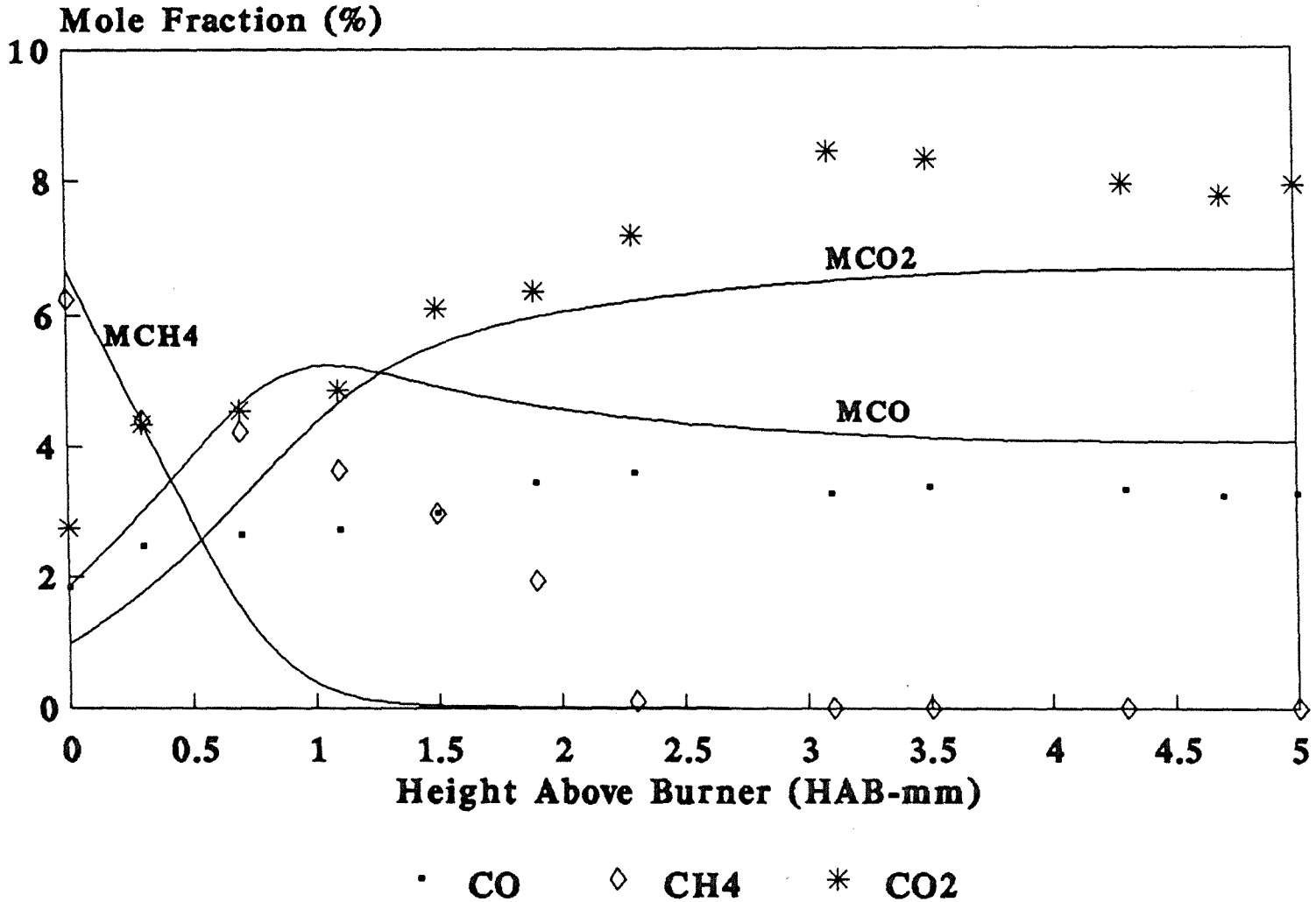

Figure 8 Comparison of Experimental & Model Results for ϕ=1.20, R=0

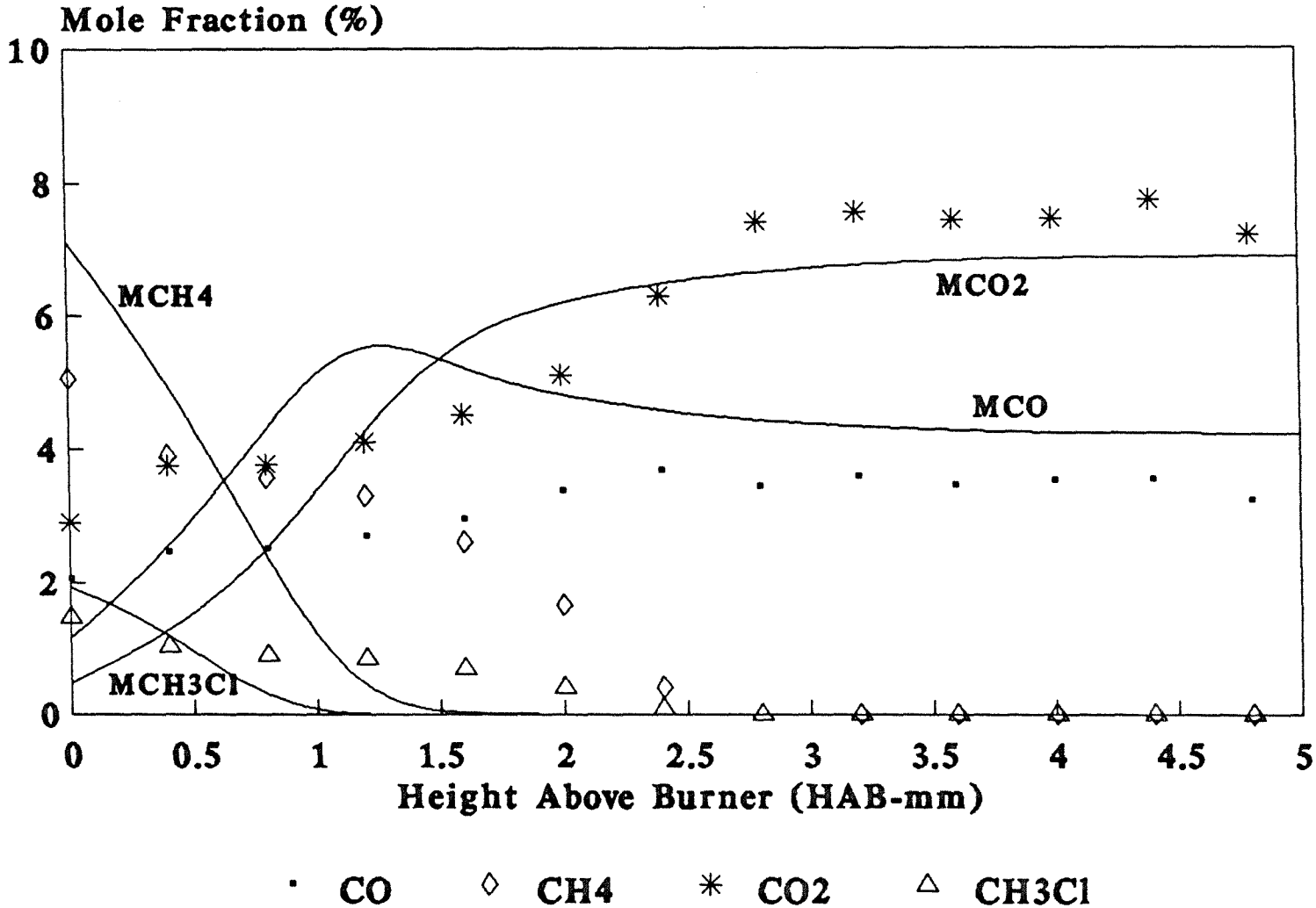

Figure 9 Comparison of Experimental & Model Results for ϕ=1.20, R=0.25

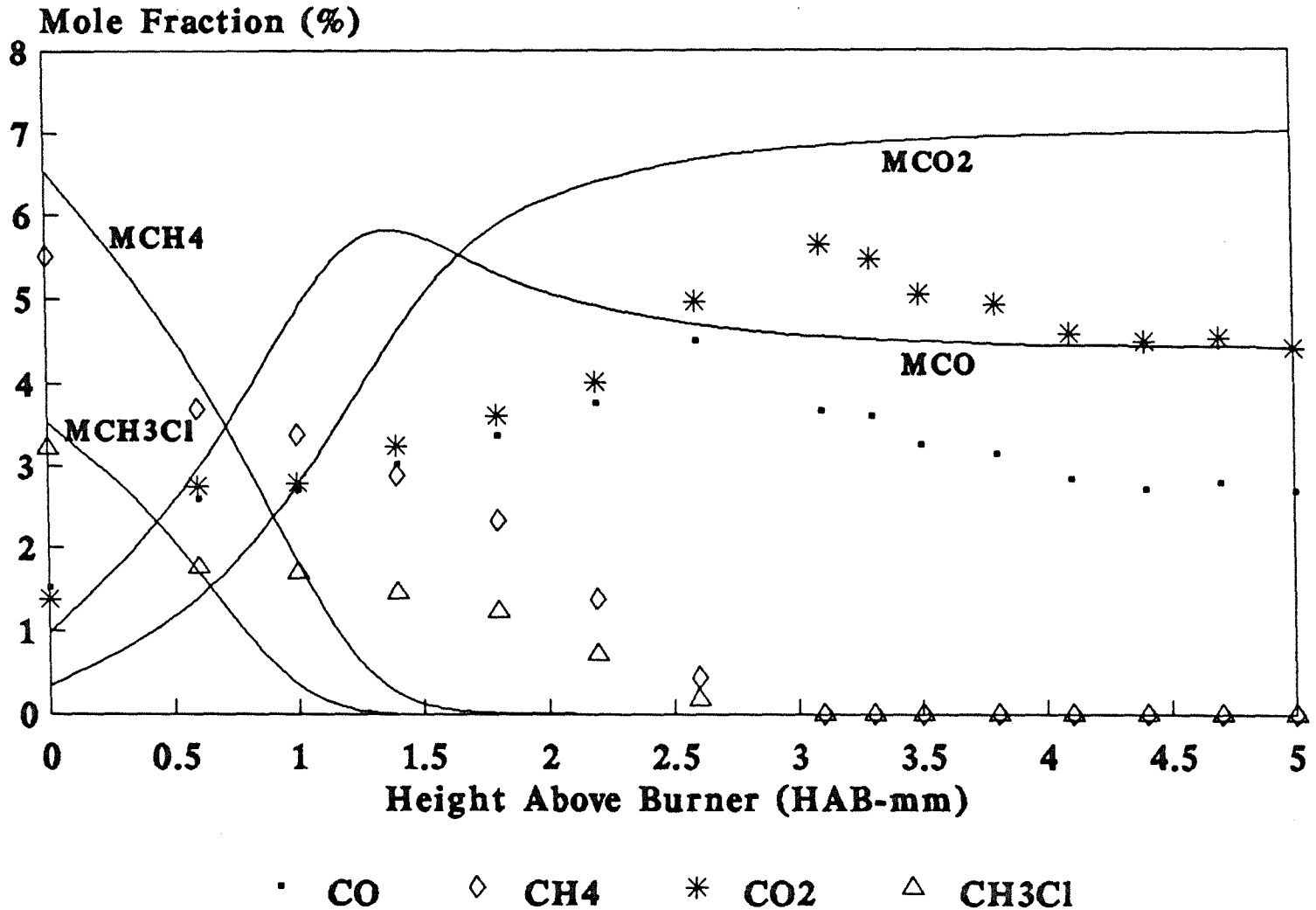

Figure 10 Comparison of Experimental & Model Results for ϕ=1.20, R=0.50

during the first stage of sampling at the probe tip and during their residence time in the probe (Pauwels, et al.,1990). Moreover, it is particularly difficult to accurately measure the temperature near the burner surface since the temperature gradients and radiation loss to the cooled burner surface are so large in this region. In the case of simulation, the uncertainties in the kinetics and transport data have significant impact on the computed species profile (Pauwels, et al.,1990).

Approaching higher HAB, the agreement improves. A global series-reaction feature is observed in these plots. The fuel CH_4 and CH_3Cl react with oxygen producing increasing amounts of CO, the intermediate, which reaches its peak and then declines as the result of conversion to the final product CO_2. It is also estimated that an uncertainty of ± 0.25 mm exists in the absolute position of the species concentration profiles.

The CO/CO_2 ratio is a good indicator of hydrocarbon combustion inhibition or efficiency, because the conversion of CO to CO_2 is a critical step in hydrocarbon flame stability and utilization. The experimental CO/CO_2 ratios versus HAB are shown in Figures 11 and 12.

Figure 11 includes three fuel lean cases at constant $\phi = 0.79$, and the curves show that increasing the CH_3Cl content results in higher CO/CO_2 ratios. Aside from the higher ratios with CH_3Cl present, all three curves have nearly the same shape. As observed, the curves have a marked drop around HAB of 2.5 mm to 3.0 mm. Finally, in the presence of excess oxygen, nearly all CO is consumed and the curves converge to the same CO/CO_2 ratio at high HAB.

Figure 12 includes three fuel rich cases at constant $\phi = 1.20$. The curves also show an increase in CO/CO_2 ratio with increasing CH_3Cl doping. But the increase in CO/CO_2 ratio in these fuel rich flames is higher

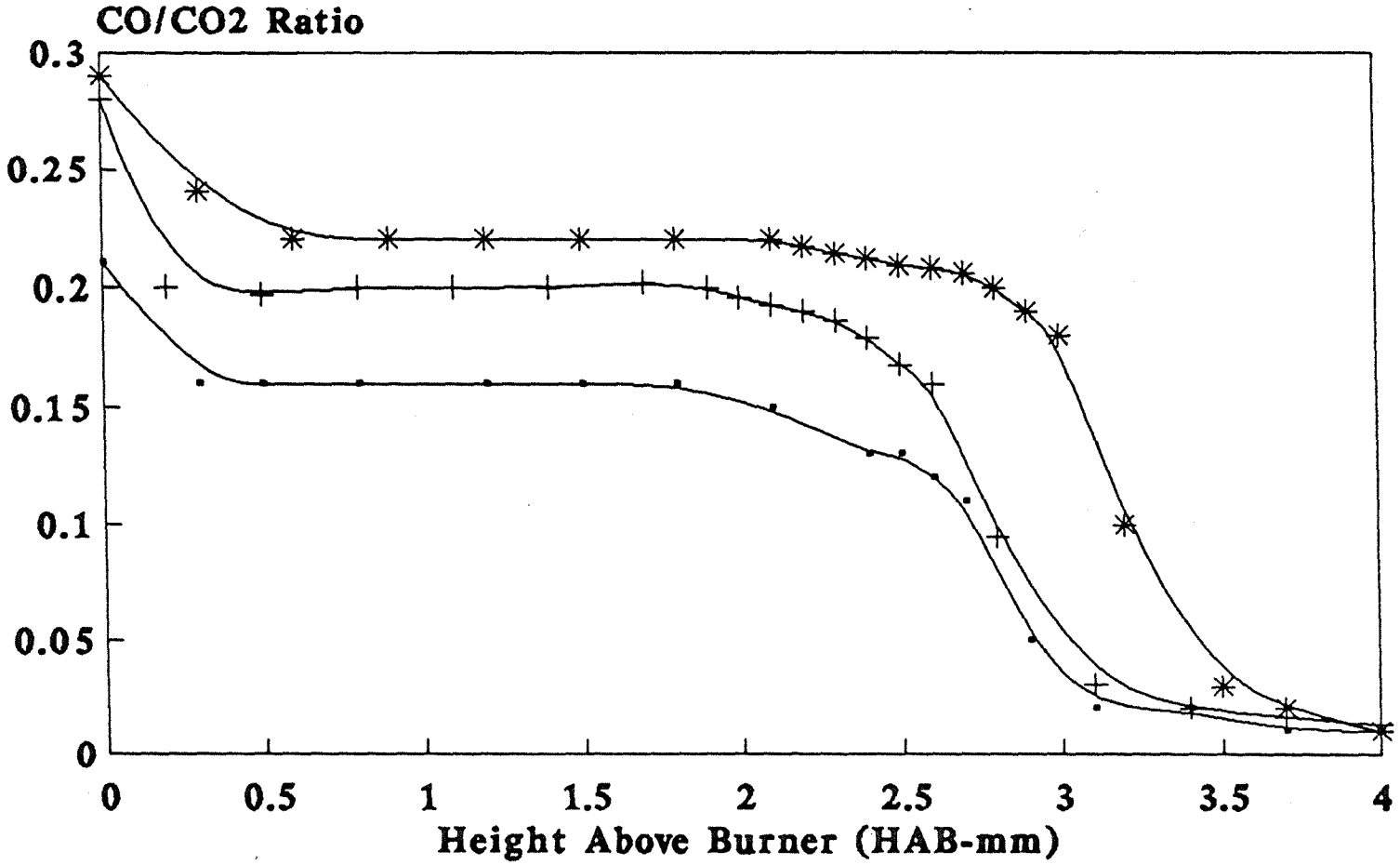

Figure 11 Experimental CO/CO2 Ratio Versus HAB for ϕ=0.79

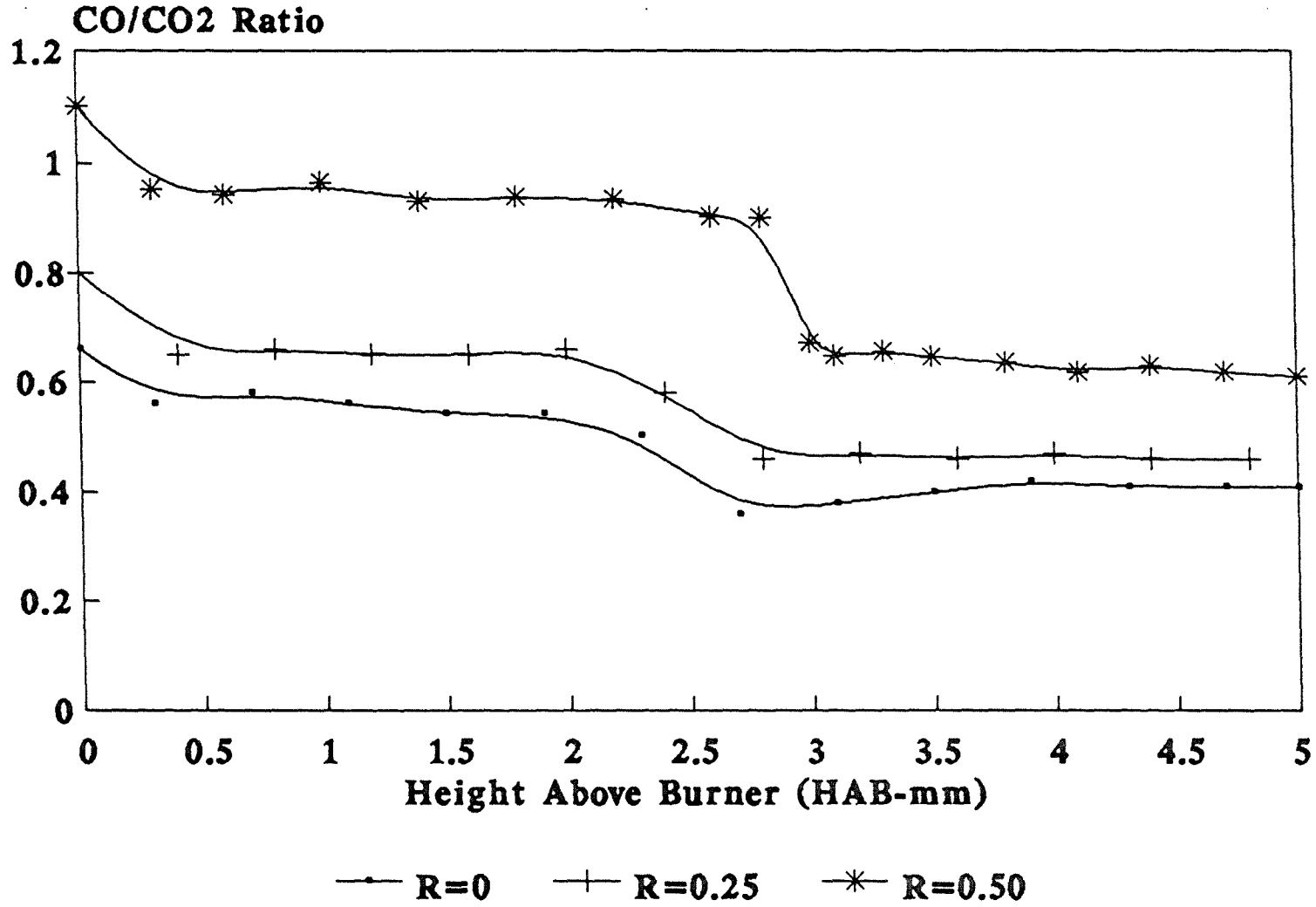

Figure 12 Experimental CO/CO2 Ratio Versus HAB for ϕ=1.20

than those in fuel lean cases, as is the absolute value of CO/CO_2 ratio. Similar to the fuel lean cases, all three curves have nearly the same shape and show a marked drop between HAB of 2.5 mm to 3.0 mm, where the fuel CH_4 and CH_3Cl are almost consumed completely (shown in Figure 5 through Figure 10). However, different from the fuel lean flames, there is still a considerable amount of CO existing in the fuel rich flames at high HAB because of the lack of oxygen.

Viewing Figures 11 and 12 together with Figures 5 to 10 clearly show that increasing the CH_3Cl loading at constant ϕ increases the CO/CO_2 ratio. This is strong evidence of flame inhibition by chlorinated hydrocarbons. Also, the lower CO/CO_2 ratios in fuel lean flames as compared to those in the fuel rich flames suggests that the presence of excess oxygen certainly helps the conversion of CO to CO_2 in hydrocarbon combustion.

5.2 Reaction Pathways From Rate-of-Production Analyses

Since the model predictions agree reasonably well with the experimental data, the rate-of-production (ROP) calculations can be performed with confidence. The ROP calculations give us the contributions of the forward and reverse reactions to the direct formation and consumption of a particular species at a specific height-above-burner (HAB). From analyses of ROP calculations, we are able to ascertain the major reaction pathways in the flames and better understand the chemistry of chlorocarbons in hydrocarbon combustion.

The most important pathways that occur in the mechanism are determined for both fuel lean (including R=0 and R=0.25) and fuel rich (including R=0 and R=0.25) flames at three HAB positions, which

correspond approximately to the locations of the preheat, flame front, and post-flame zone. Three positions are 0.4 mm, 1.2 mm, and 3.2 mm for fuel lean flames and 0.5 mm, 1.1 mm, and 3.5 mm for fuel rich flames. The results are illustrated in Figure 13 through Figure 24. The major species are displayed in the boxes, and the major attacking species beside the arrows. The thickness of the arrows signify the importance of the reactions predicted by the model. The thicker arrow means a higher rate for the reaction. Unconnected arrows on the diagram represent an accumulation of the same species collected from elsewhere. For example, the species CO is produced from CHO, as well as C_2H_2 and CH_2CO in Figure 13.

Reaction pathways for fuel lean flames are shown in Figure 13 through Figure 18. Figures 13 and 14 are the reaction pathway diagrams for the two fuel lean flames at HAB = 0.4 mm (in this preheat zone, T=1425 K for R=0 and T=1357 K for R=0.25). In both flames, H is abstracted from CH_4 by OH or HO_2 to form CH_3 radical. The CH_3 is then converted largely to CH_3O by reaction with HO_2, partly to C_2H_6 by combination with CH_3, and some to CH_2O by reaction with O atom. CH_3O thermally decomposes, and reacts with O_2 and CH_3 to produce CH_2O. The CH_2O then forms CHO via H abstraction by OH in the CH_4/air flame and by both Cl and OH in the CH_3Cl/CH_4/air flame. CHO reacts with O_2 to yield CO, which finally converts to CO_2 by the reaction with OH. Part of the CH_3O is directly converted to CO_2 by reaction with CO.

Reaction pathways for the C_2 branch are similar in both figures. The most notable difference is that Cl is an active participant, instead of OH, for several reactions in the chlorinated flame. C_2H_5 and C_2H_3 are formed primarily by Cl attacking C_2H_6 and C_2H_4 in Figure 14, but by OH attacking C_2H_6 and C_2H_4 in Figure 13.

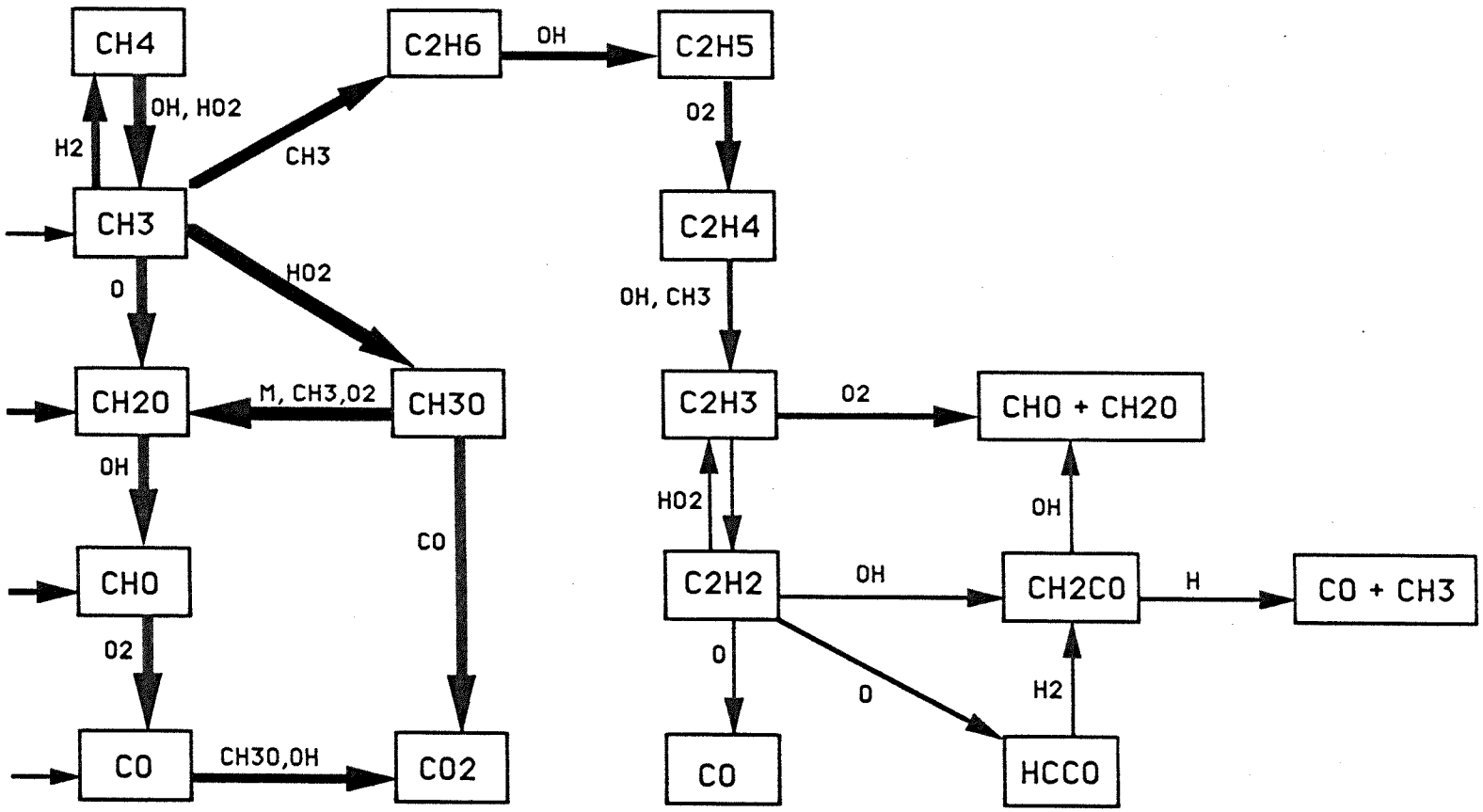

Figure 13 Reaction Pathways for Fuel Lean, R=0; HAB=0.4mm

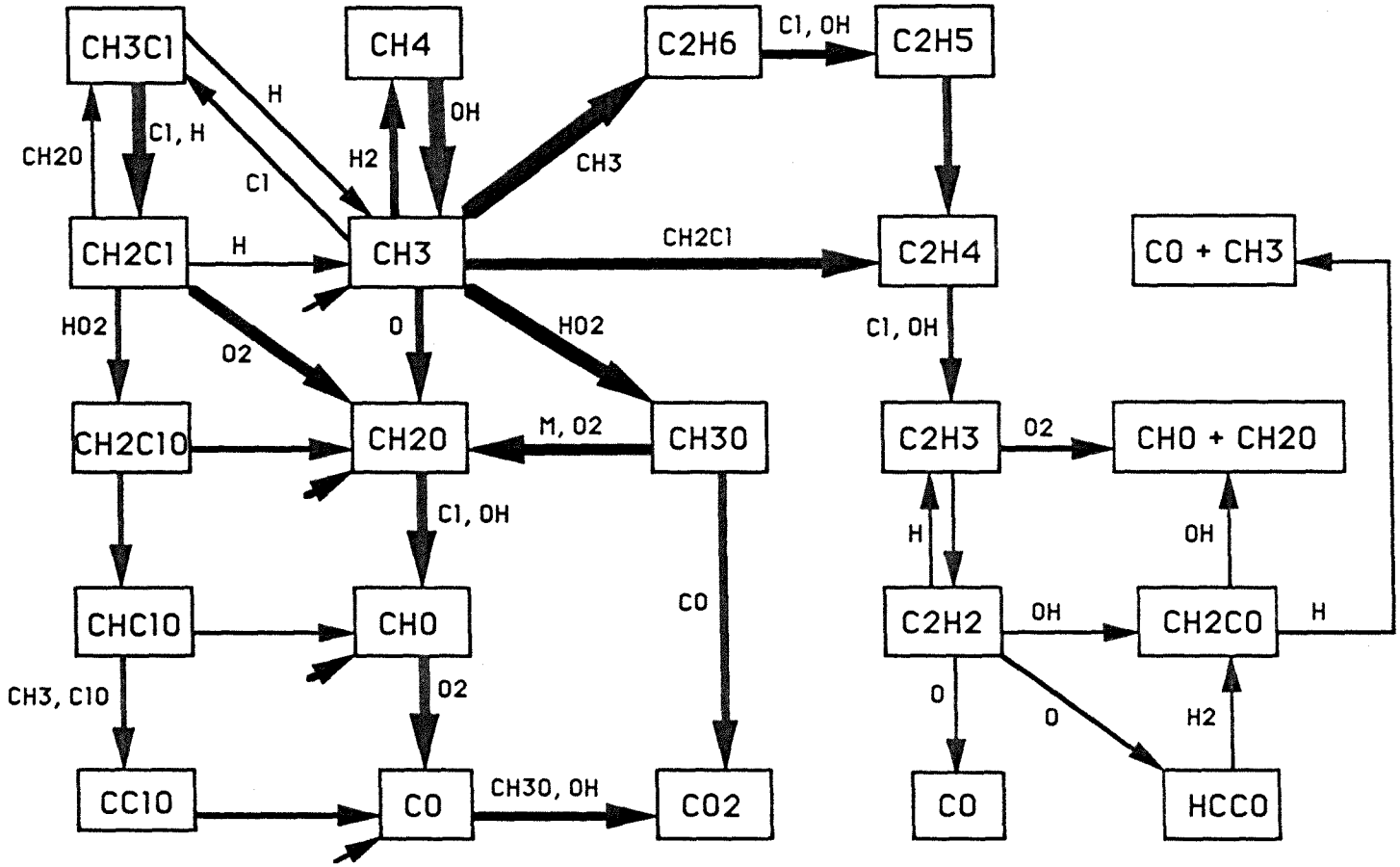

Figure 14 Reaction Pathways for Fuel Lean, R=0.25; HAB=0.4mm

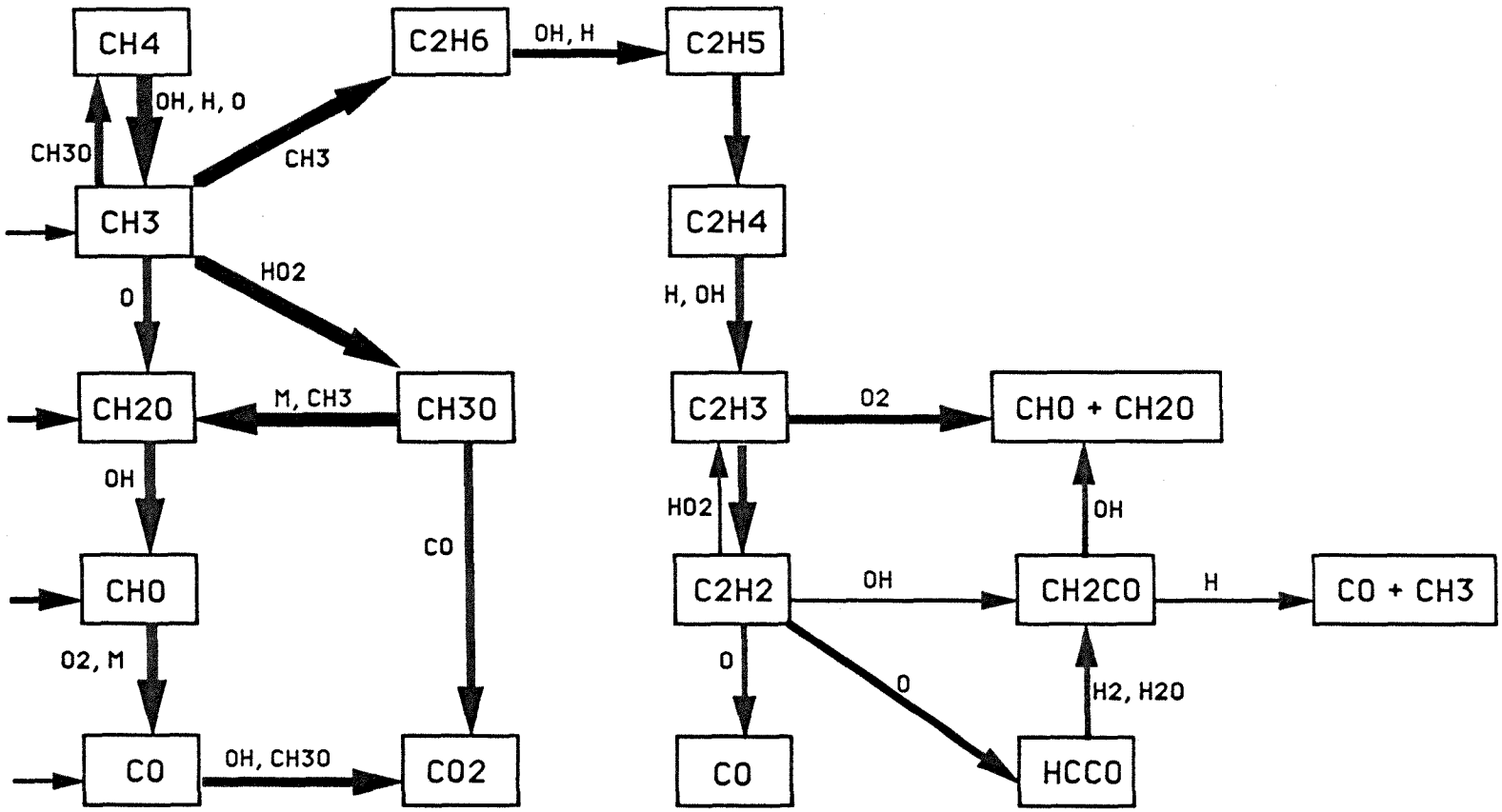

Figure 15 Reaction Pathways for Fuel Lean, R=0; HAB=1.2mm

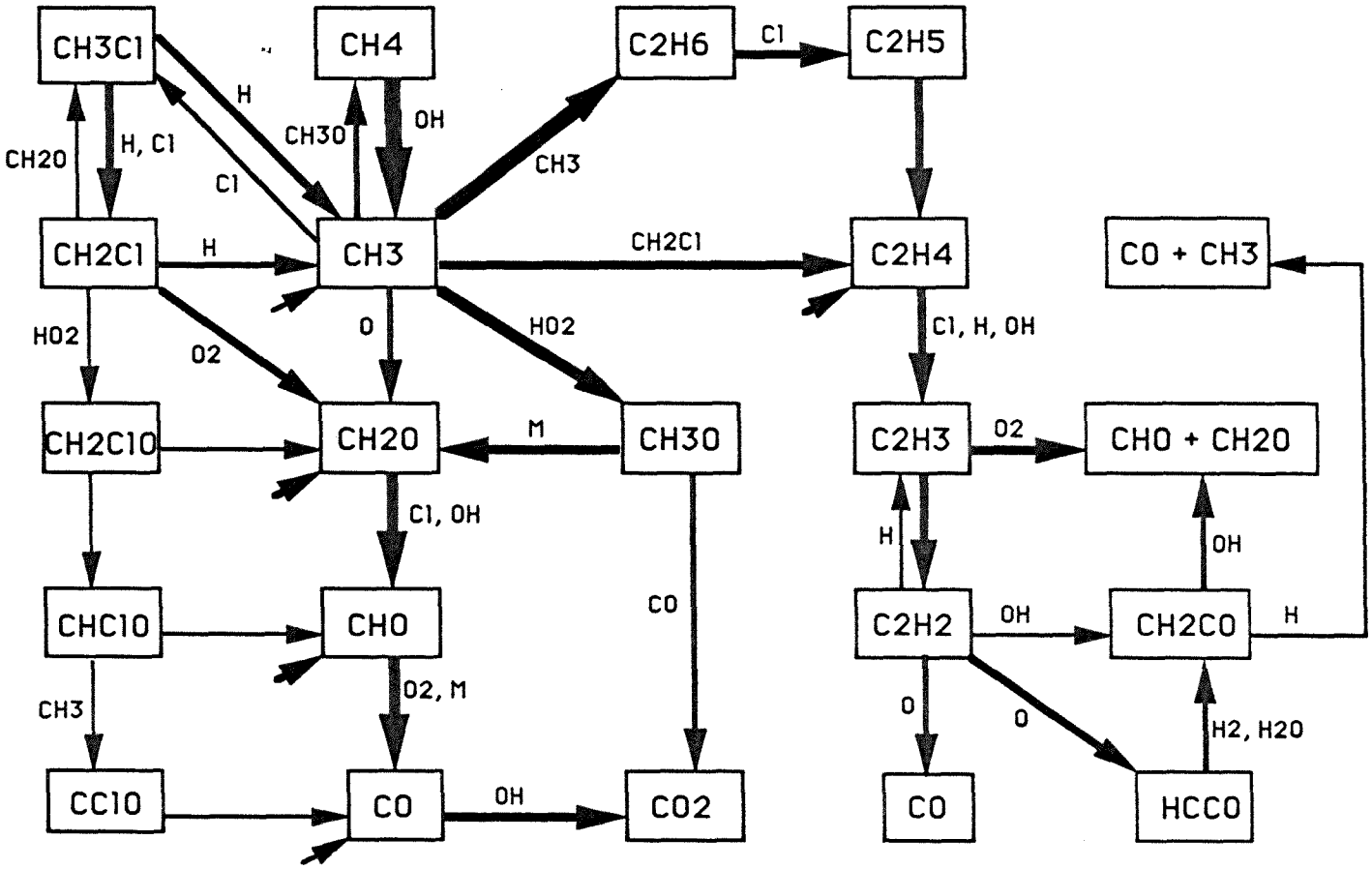

Figure 16 Reaction Pathways for Fuel Lean, R=0.25; HAB=1.2mm

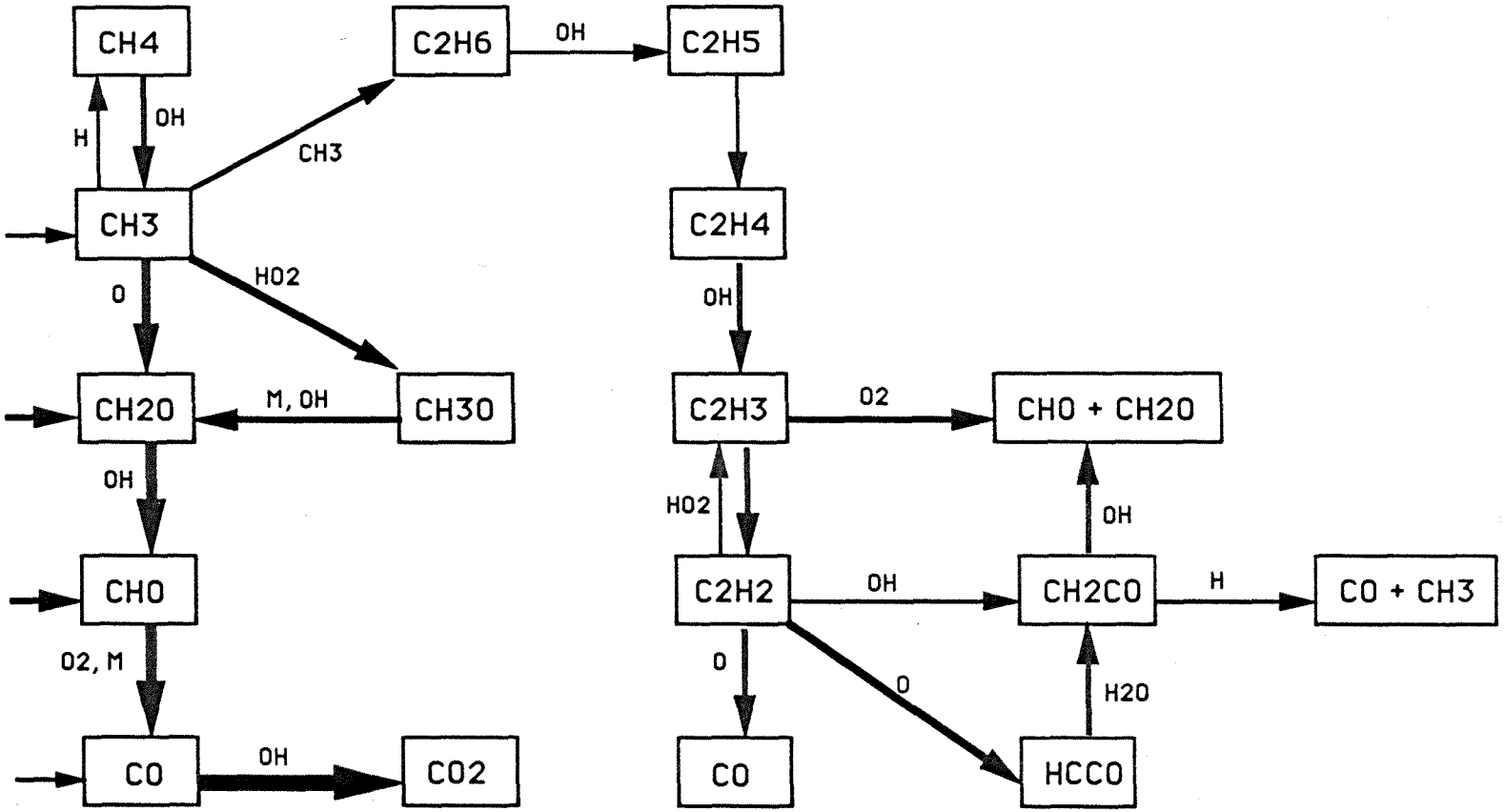

Figure 17 Reaction Pathways for Fuel Lean, R=0; HAB=3.2mm

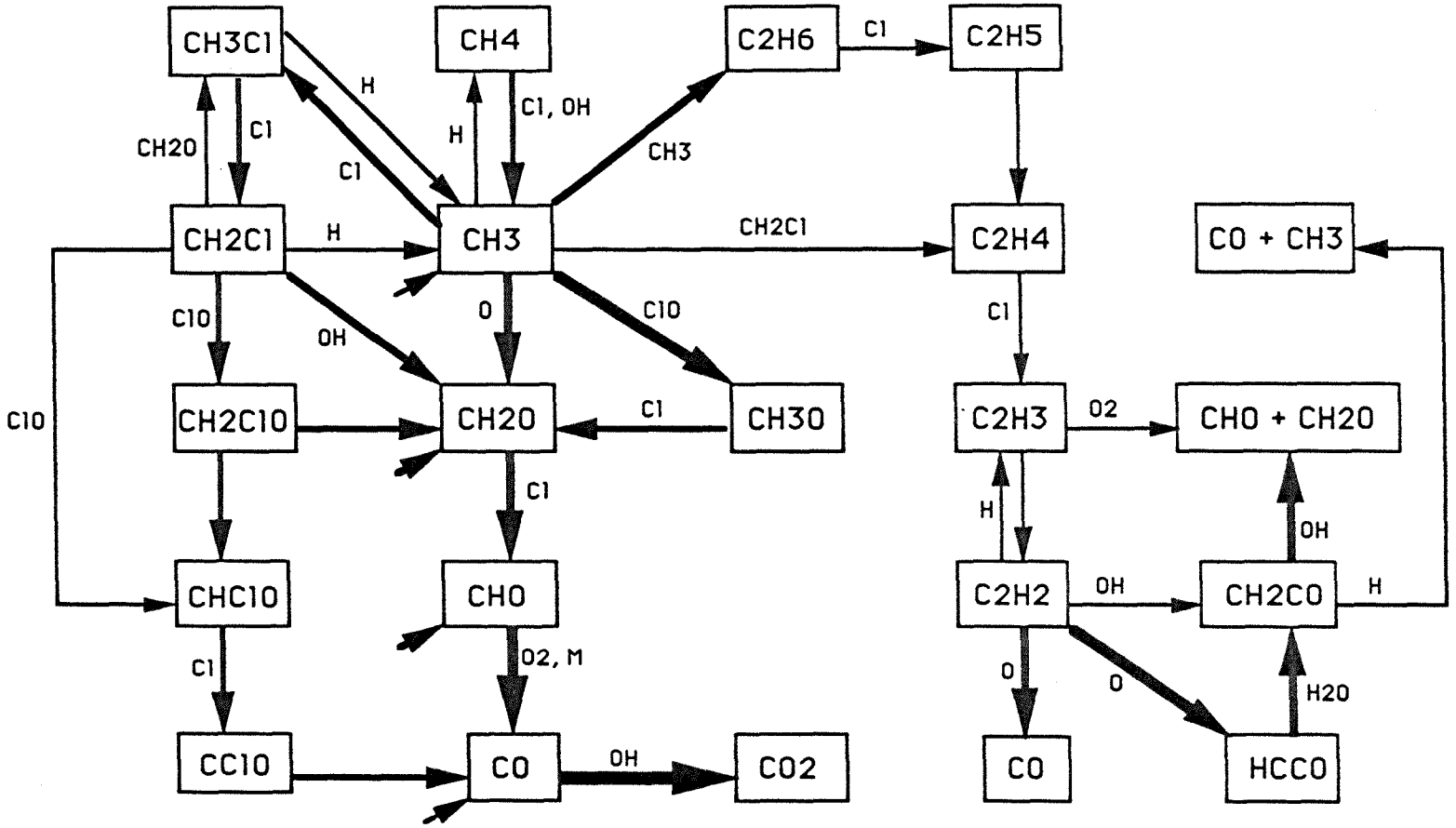

Figure 18 Reaction Pathways for Fuel Lean, R=0.25; HAB=3.2mm

The presence of CH_3Cl creates a long series of Cl-containing species. Initially H is abstracted to form CH_2Cl. From there, CH_2Cl takes four paths. In the major route it reacts with O_2 to form CH_2O. In minor routes, it reacts with CH_3 to form C_2H_4, with HO_2 to form CH_2ClO, and with H to form CH_3. Continuing the Cl series, CH_2ClO takes a path to produce CHClO, CClO, CO and finally CO_2. Besides CH_2ClO and CHClO also convert to CH_2O and CHO respectively.

The reaction pathways for the fuel lean flames at HAB=1.20 mm (flame front) are found in Figures 15 and 16 (T=1583 K for R=0 and T=1574 K for R=0.25). In Figures 15 and 16, there is a large portion of the CH_3 proceeding to C_2H_6. In Figure 16, Cl competes with H in several key reactions, while in Figure 15, OH competes with H in those reactions.

The reaction pathways for the fuel lean flames at HAB=3.2 mm (post-flame zone) are shown in Figures 17 and 18 (T=1525 K for R=0 and T=1541 K for R=0.25). In these figures we find a smaller portion of the CH_3 proceeding to C_2H_6. However, it is noted that C_2H_2 gains relative importance within C_2 branch, participating in several reaction steps leading to CO. In the CH_4/air flame, O is now most active in CH_3 conversion. In the CH_3Cl/CH_4/air flame, ClO is more active than O in CH_3 conversion. Furthermore, the Cl and ClO are dominant in many reactions at this HAB in the CH_3Cl-doped flame. More interesting, CH_2Cl is directly converted to CHClO by reaction with ClO.

Reaction pathways for fuel rich flames are shown in Figure 19 through Figure 24. Figures 19 and 20 illustrate the reaction pathways for fuel rich flames at HAB=0.5 mm which is in the preheat flame zone (T=1597 K for R=0 and T=1506 K for R=0.25). These two diagrams are

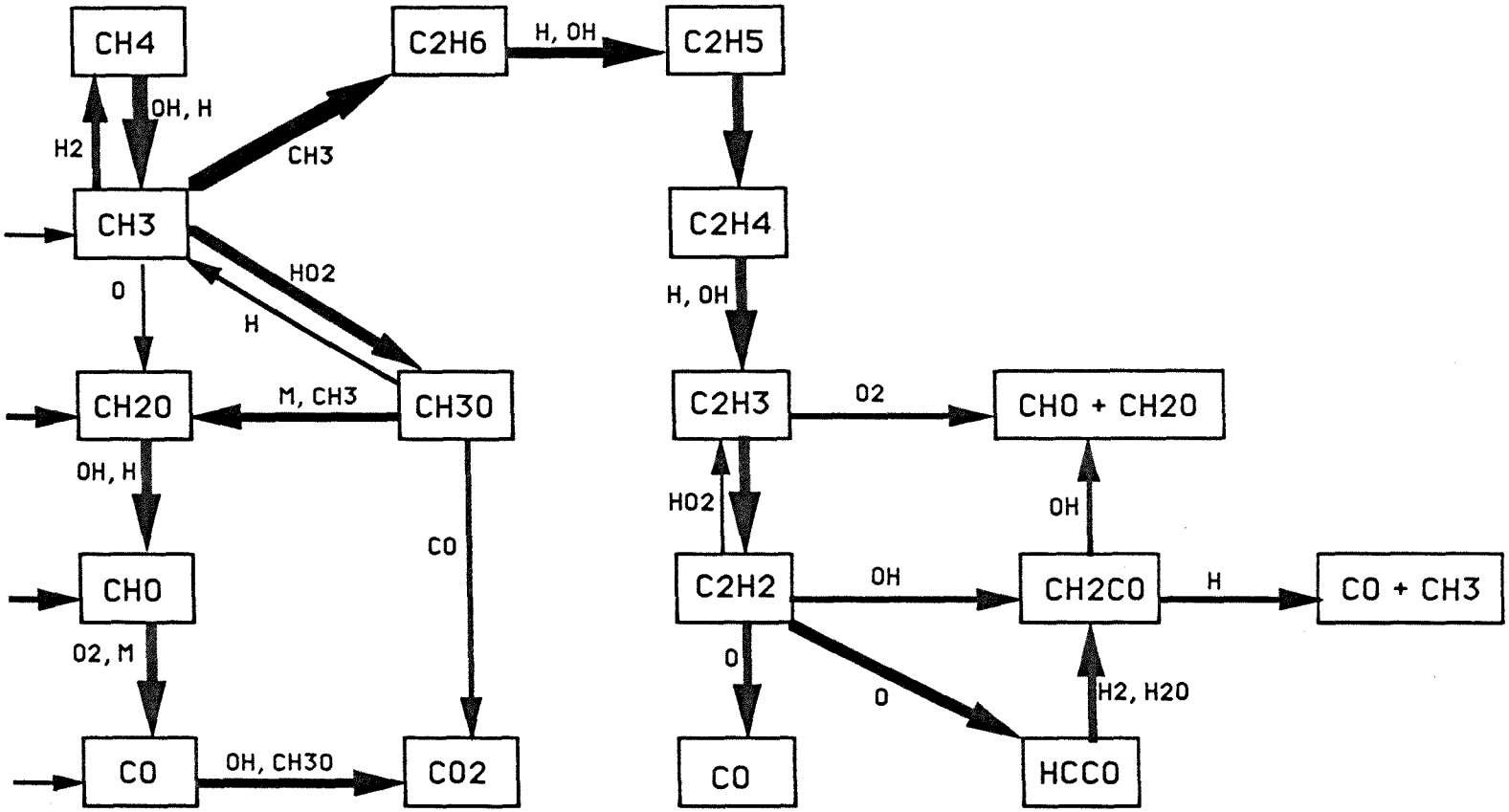

Figure 19 Reaction Pathways for Fuel Rich, R=0; HAB=0.5mm

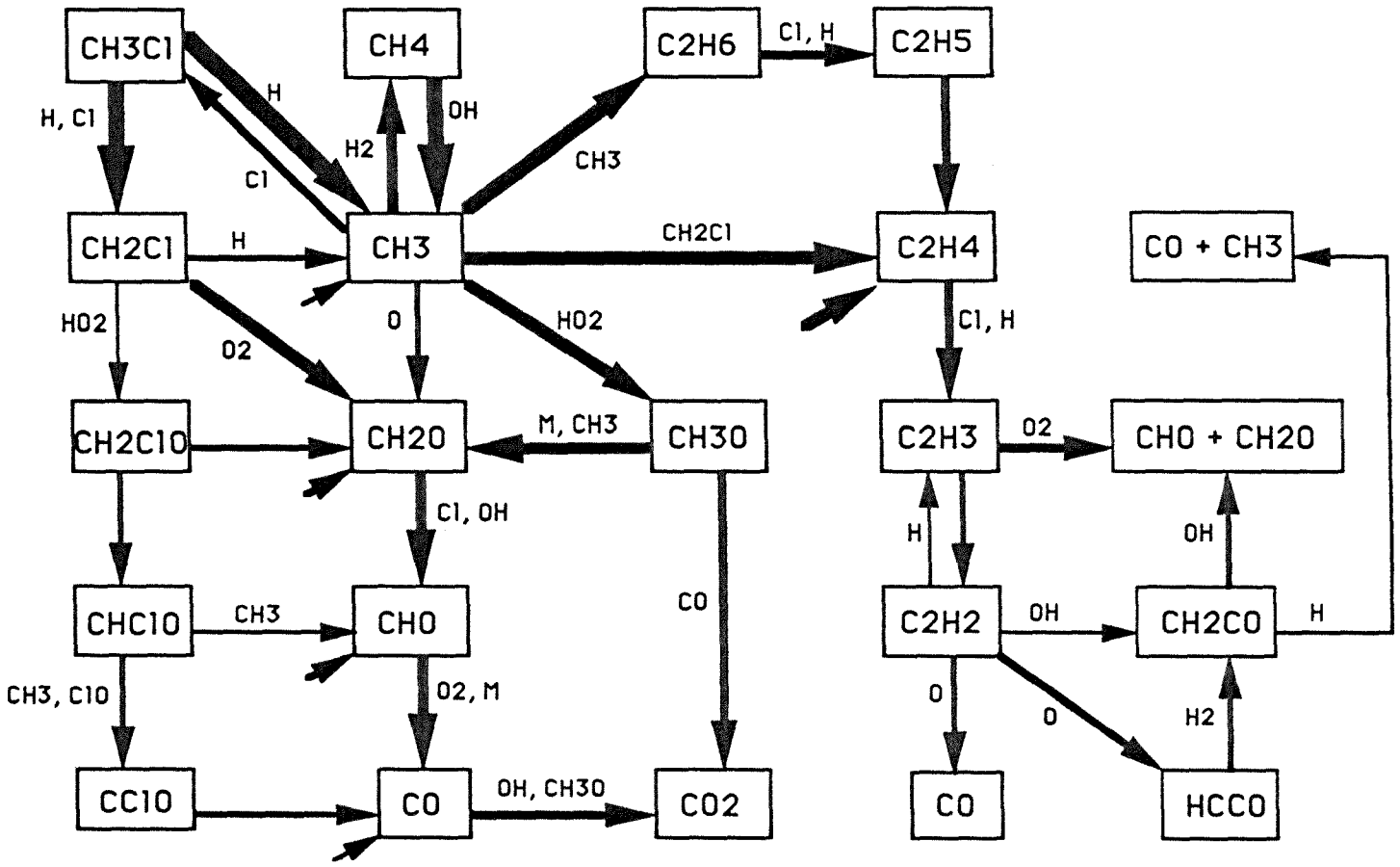

Figure 20 Reaction Pathways for Fuel Rich, R=0.25; HAB=0.5mm

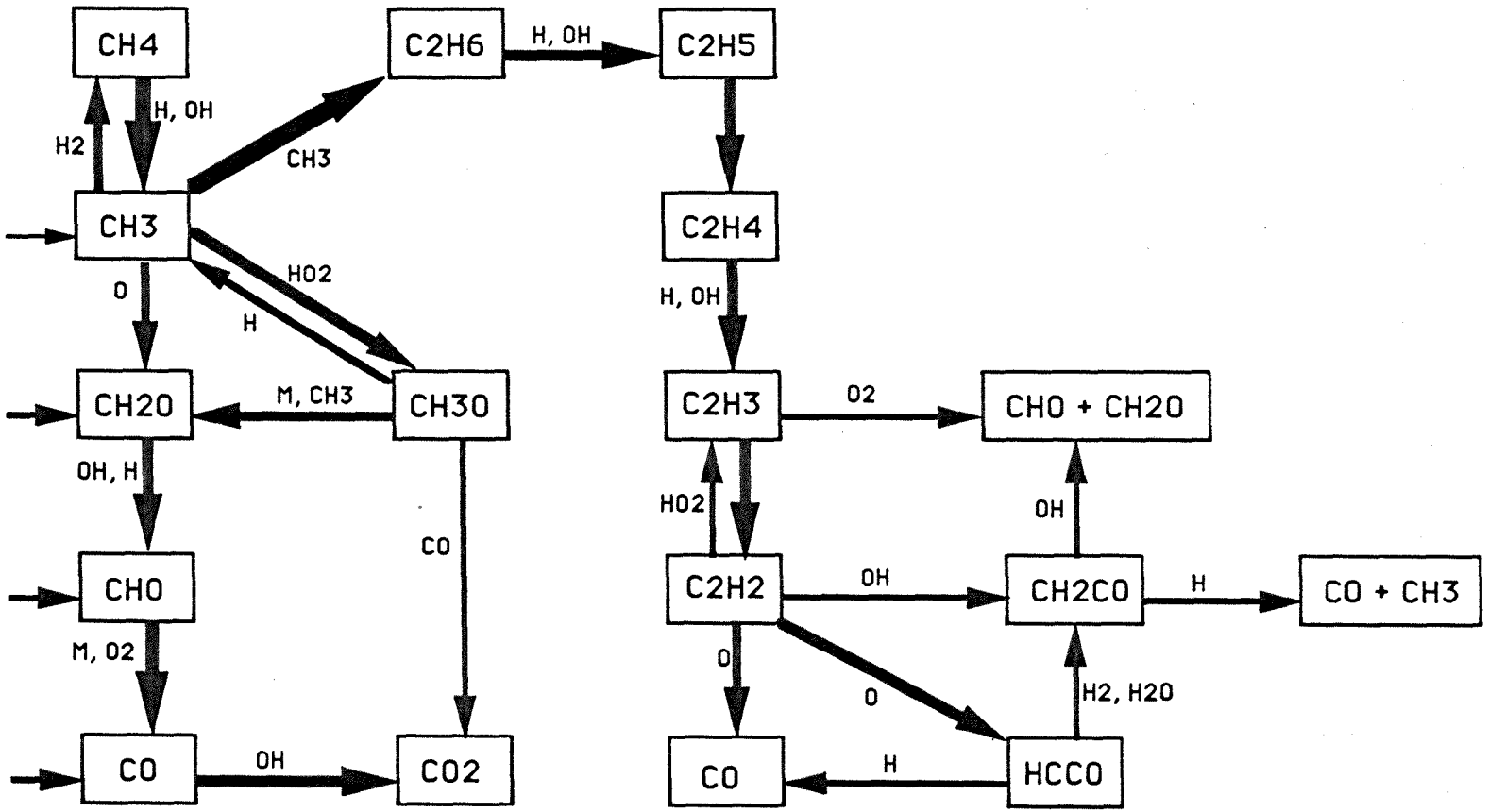

Figure 21 Reaction Pathways for Fuel Rich, R=0; HAB=1.1mm

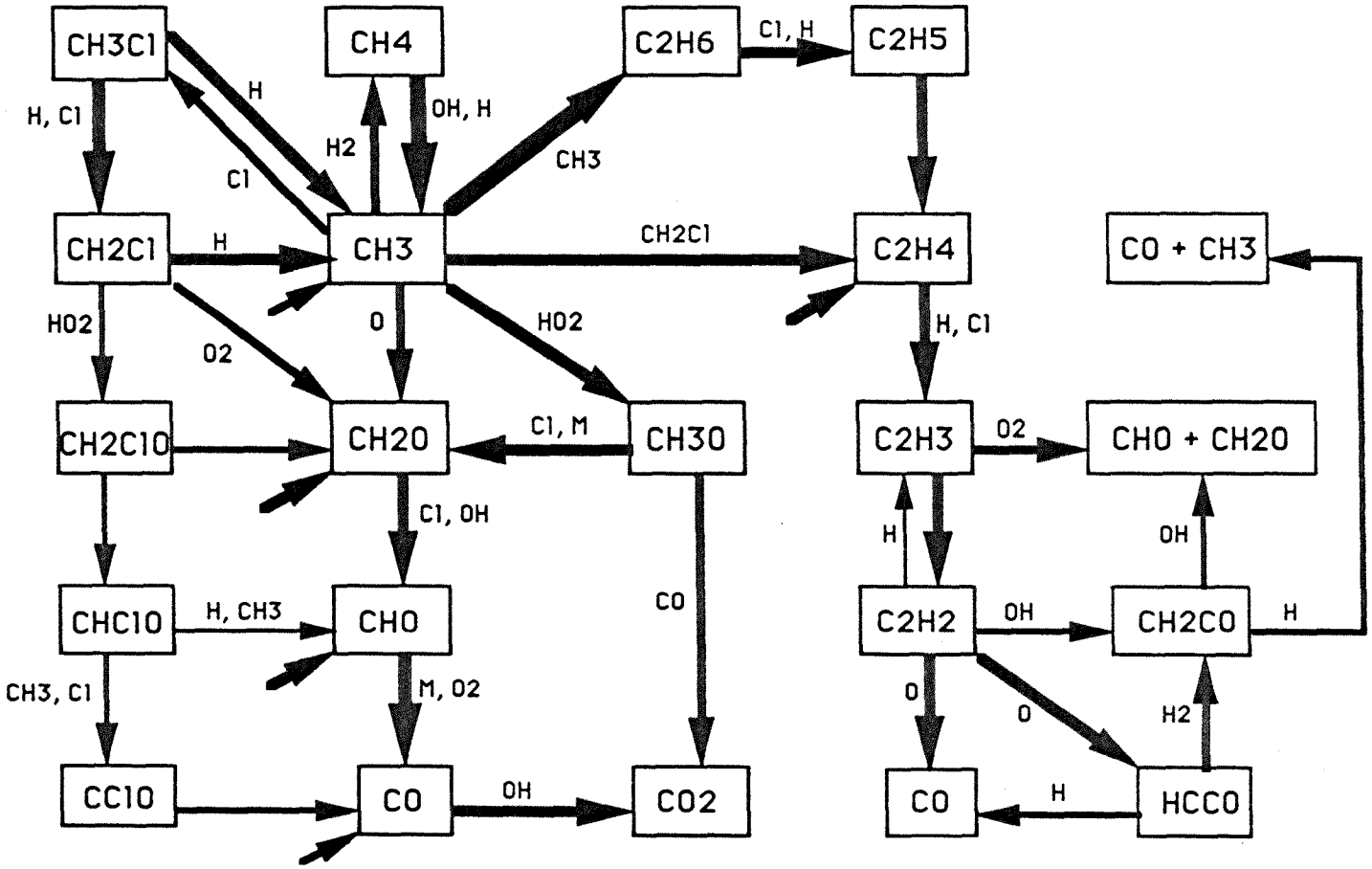

Figure 22 Reaction Pathways for Fuel Rich, R=0.25; HAB=1.1mm

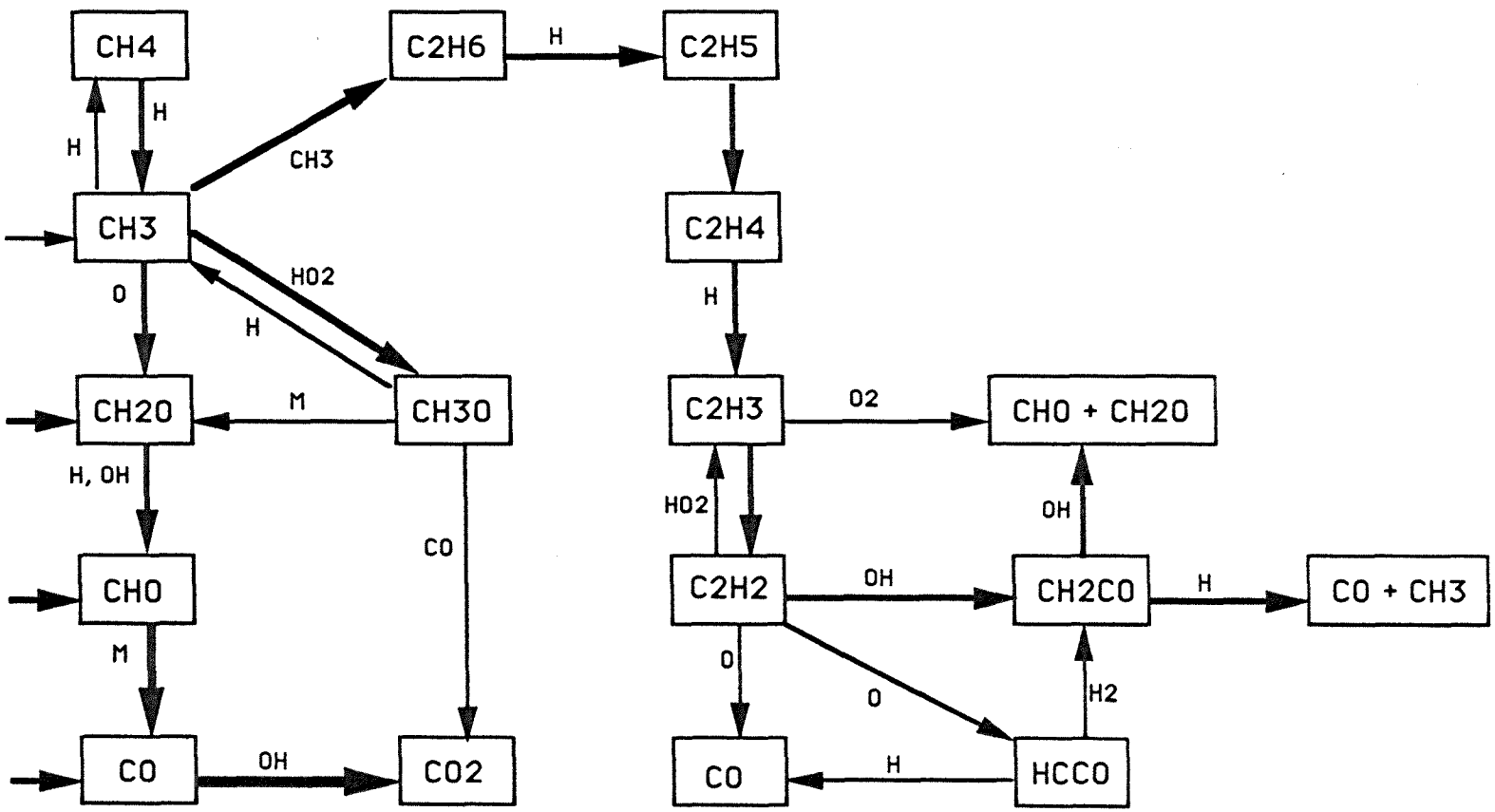

Figure 23 Reaction Pathways for Fuel Rich, R=0; HAB=3.5mm

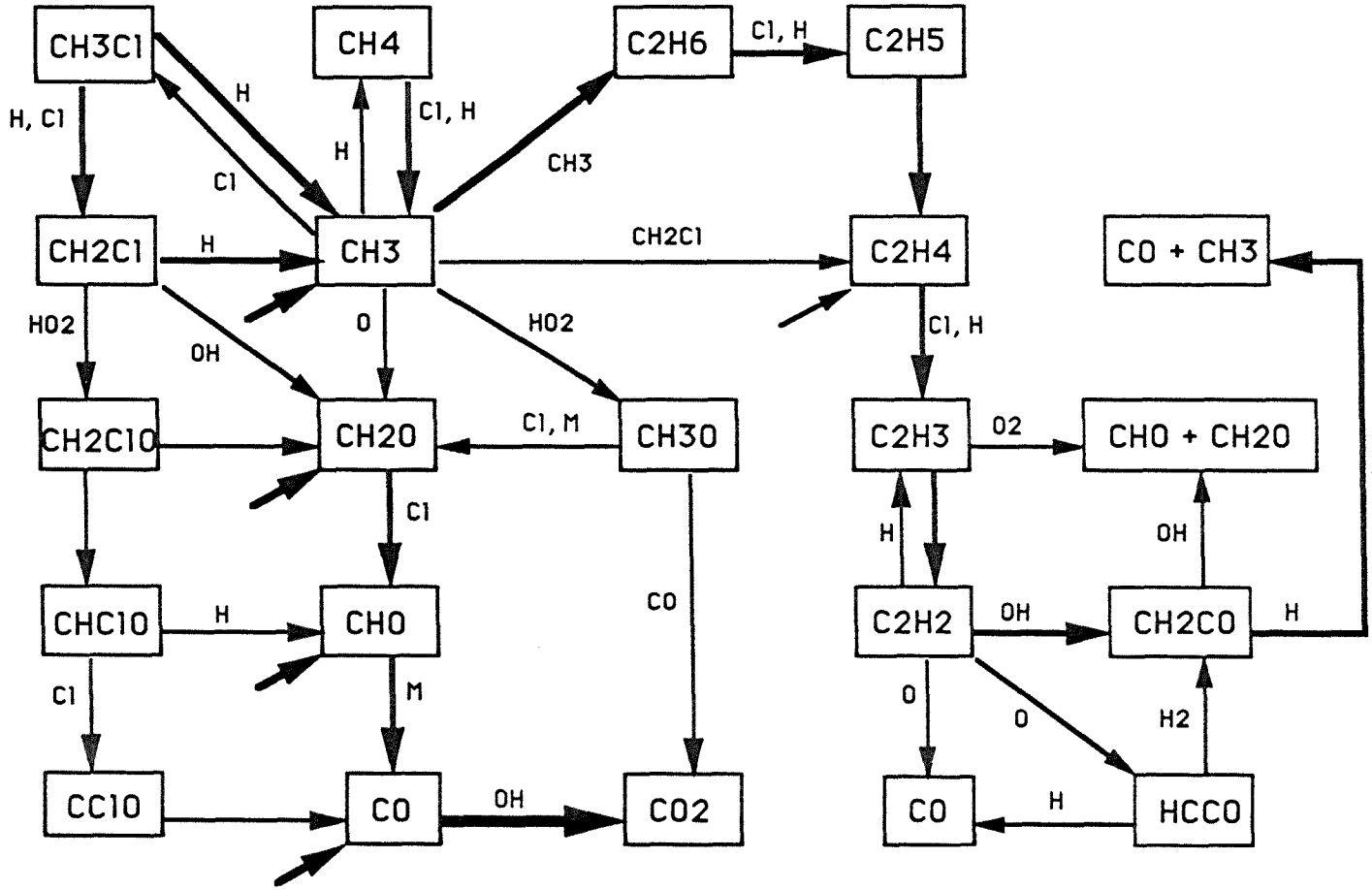

Figure 24 Reaction Pathways for Fuel Rich, R=0.25; HAB=3.5mm

similar to fuel lean cases in general. However, H plays an very important role in fuel rich flames; it either dominates or competes with OH and Cl in several key reactions. For instance, in Figure 20, H dominates in the reaction with CH_3Cl to form CH_2Cl, and competes with Cl in the reaction with C_2H_6 to form C_2H_5 and with C_2H_4 to form C_2H_3. Moreover, a large portion of CH_3Cl is converted to CH_3 by reaction with H. In Figure 19, it competes with OH in the reaction with CH_4 to produce CH_3 and dominates in the conversion of C_2H_6 to C_2H_4 and C_2H_4 to C_2H_3.

Figures 21 and 22 show the reaction pathways for fuel rich flames at HAB=1.1 mm. In this flame front zone (T=1676 K for R=0 and T=1697 K for R=0.25), H atom becomes more and more important. It becomes the dominating attacking species and also competes with other attacking species in more reactions. For example, in Figure 21, H becomes dominant in the conversion of CH_4 to CH_3, and a considerable portion of CH_3O converts back to CH_3 by H due to the high concentration of H. In Figure 22, it is noticed that H is a key species as well as Cl. H turns out to be dominant in the conversion of C_2H_4 to C_2H_3, and Cl turns out to be dominant in the conversion of CH_3O to CH_2O.

The reaction pathways for fuel rich flames at HAB=3.5 mm are found in Figures 23 and 24 (T=1592 K for R=0 and T=1642 K for R=0.25). In this post-flame zone, there is little or no oxygen left. OH radicals are less available for CH_4 conversion to CH_3, C_2H_6 to C_2H_4, and C_2H_4 to C_2H_3 in Figure 23. It is also true for the chlorinated flame (Figure 24) in the conversion of CH_4 to CH_3 and CH_2O to CHO. However, H atom still retains its importance in both flames. Cl is a major radical in the CH_3Cl flame.

5.3 Model Prediction of OH Radical

OH radical is required for the burnout of CO to CO_2, a key step in hydrocarbon combustion. Figure 25 presents the model predicted OH concentration profiles for three fuel lean flames (R=0, R=0.25, and R=0.50). It is obvious that the OH mole fraction decreases significantly when CH_3Cl is added. In order to find the reason for the lower OH level, the rate-of-production calculations are performed to obtain the major reactions of OH production and destruction.

Figures 26, 27, and 28 show the key reactions producing and consuming OH radicals in different HAB ranges. Although many reactions produce and consume OH, only the two most important reactions are presented, with their normalized contribution, in the particular HAB range. It is found that the exothermic, very critical reaction CO + OH = CO_2 + H, which is responsible for CO burnout, begins to be the primary OH consumer at 1.4 mm in Figure 26, at 2.5 mm in Figure 27, and 2.7 mm in Figure 28. This indicates the burnout of CO to CO_2 is delayed in CH_3Cl doping flames. It is also noted that the fast, exothermic reaction OH + HCl = Cl + H_2O either dominates or competes with other reactions to consume OH over the large HAB range (1.6 mm to 4.0 mm in Figure 27 and 1.0 mm to 4.0 mm in Figure 28). The relative rates of OH consumption via reaction OH + HCl = Cl + H_2O versus reaction CO + OH = CO_2 + H are 36% versus 26% in 2.0 - 2.4 mm HAB range in the R=0.25 case and 47% versus 28% in 2.1 - 2.6 mm HAB range in the R=0.50 case. This suggests that the reaction OH + HCl = Cl + H_2O is a major consumer of OH, limiting its availability for CO conversion. Consequently, the reduction of OH mole fraction shown in Figure 25 is due to the presence of CH_3Cl. This

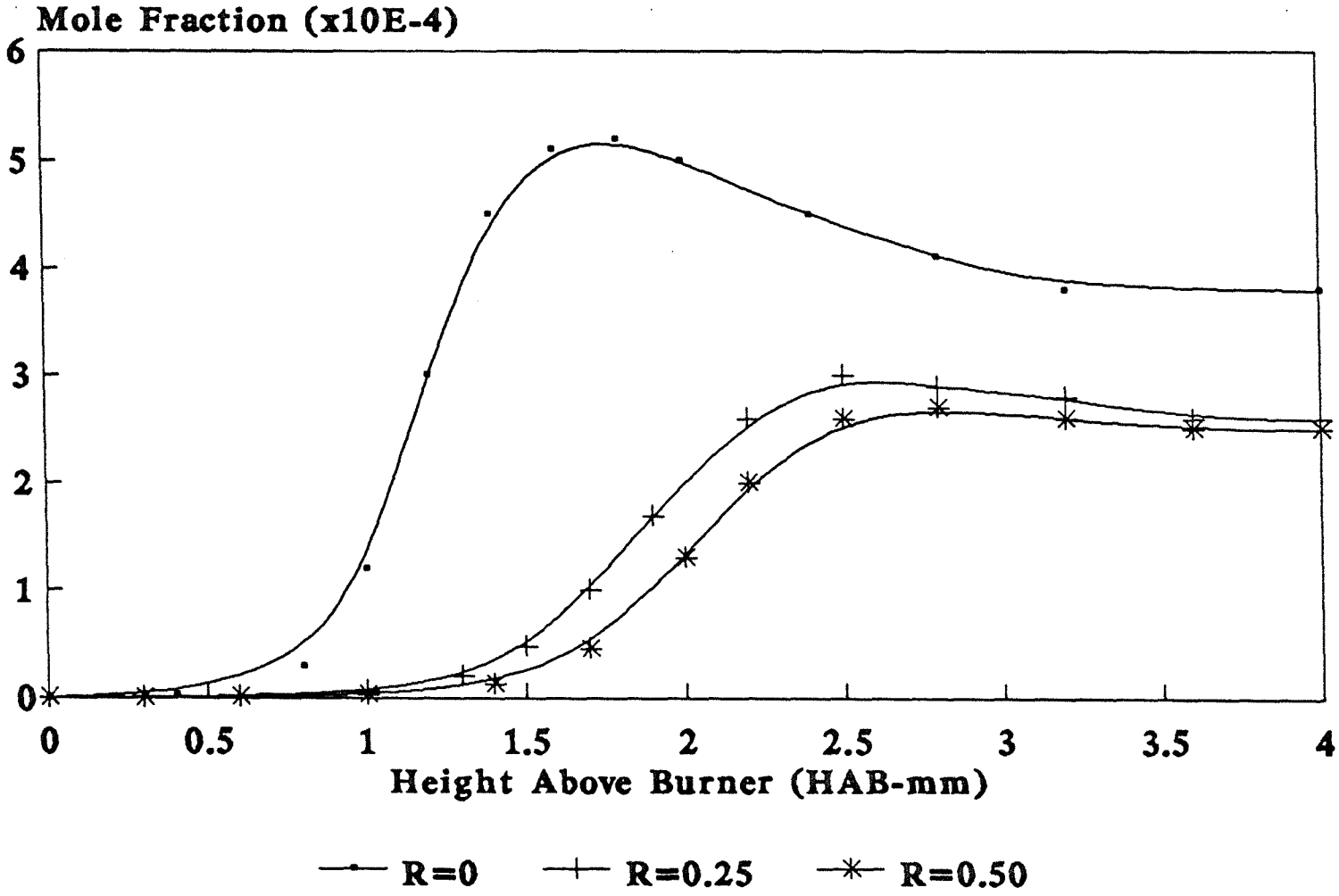

Figure 25 Model Predicted OH Concentration Profile for ϕ=0.79

	Production of OH		Destruction of OH		
(0 - 0.4 mm)	$CH_3 + HO_2 = CH_3O + OH$ $H_2O_2 + M = 2OH + M$	(53%) (35%)	$CH_4 + OH = CH_3 + H_2O$ $CH_2O + OH = CHO + H_2O$	(57%) (18%)	(0 - 1.1 mm)
(0.6 - 0.7 mm)	$H + O_2 = O + OH$ $CH_4 + O = CH_3 + OH$	(35%) (19%)	$CH_2O + OH = CHO + H_2O$ $CH_4 + OH = CH_3 + H_2O$	(26%) (21%)	(1.2 - 1.3 mm)
(0.8 - 1.05 mm)	$H + O_2 = O + OH$ $CH_3 + HO_2 = CH_3O + OH$	(34%) (17%)	$CO + OH = CO_2 + H$ $CH_2O + OH = CHO + H_2O$	(23%) (22%)	(1.4 mm)
(1.1 - 1.25 mm)	$H + O_2 = O + OH$ $H + HO_2 = 2OH$	(30%) (27%)	$CO + OH = CO_2 + H$ $H + H_2O = H_2 + OH$	(36%) (21%)	(1.5 - 1.8 mm)
(1.3 - 1.5 mm)	$H + HO_2 = 2OH$ $H + O_2 = O + OH$	(32%) (28%)	$CO + OH = CO_2 + H$ $OH + HO_2 = H_2O + O_2$	(63%) (26%)	(2.0 - 4.0 mm)
(1.6 mm)	$O + H_2O = 2OH$ $H + HO_2 = 2OH$	(32%) (28%)			
(1.8 - 4.0 mm)	$O + H_2O = 2OH$ $H + O_2 = O + OH$	(53%) (29%)			

Figure 26 Key Production and Destruction Reactions of OH Radical for Fuel Lean, R=0

	Production of OH		Destruction of OH		
(0 mm)	CH3 + HO2 = CH3O + OH	(81%)	CH4 + OH = CH3 + H2O	(69%)	(0 - 0.2 mm)
	CH2Cl + HO2 = CH2ClO + OH	(14%)	CH3Cl + OH = CH2Cl + H2O	(10%)	
(0.1 - 0.2 mm)	CH3 + HO2 = CH3O + OH	(51%)	CH4 + OH = CH3 + H2O	(61%)	(0.3 - 1.5 mm)
	H2O2 + M = 2OH + M	(33%)	CH2O + OH = CHO + H2O	(10%)	
(0.3 - 0.4 mm)	H2O2 + M = 2OH + M	(44%)	CH4 + OH = CH3 + H2O	(22%)	(1.6 - 1.7 mm)
	CH3 + HO2 = CH3O + OH	(28%)	OH + HCl = Cl + H2O	(19%)	
(0.45 - 0.5 mm)	H2O2 + M = 2OH + M	(37%)	OH + HCl = Cl + H2O	(26%)	(1.8 - 1.9 mm)
	H + O2 = O + OH	(19%)	H + H2O = H2 + OH	(18%)	
(0.6 - 1.3 mm)	H + O2 = O + OH	(38%)	OH + HCl = Cl + H2O	(36%)	(2.0 - 2.4 mm)
	CH4 + O = CH3 + OH	(22%)	CO + OH = CO2 + H	(26%)	
(1.4 - 1.6 mm)	H + O2 = O + OH	(37%)	CO + OH = CO2 + H	(63%)	(2.5 - 4.0 mm)
	CH3 + HO2 = CH3O + OH	(14%)	OH + HCl = Cl + H2O	(23%)	
(1.7 - 2.0 mm)	H + O2 = O + OH	(30%)			
	H + O2 = 2OH	(22%)			
(2.1 - 2.2 mm)	H + O2 = O + OH	(28%)			
	O + H2O = 2OH	(24%)			
(2.3 - 4.0 mm)	O + H2O = 2OH	(40%)			
	H + O2 = O + OH	(28%)			

Figure 27 Key Production and Destruction Reactions of OH Radical for Fuel Lean, R=0.25

	Production of OH		Destruction of OH		
(0 - 0.2 mm)	CH3 + HO2 = CH3O + OH	(58%)	CH4 + OH = CH3 + H2O	(62%)	(0 - 0.8 mm)
	CH2Cl + HO2 = CH2ClO + OH	(29%)	CH3Cl + OH = CH2Cl + H2O	(11%)	
(0.3 - 0.45 mm)	H2O2 + M = 2OH + M	(46%)	CH4 + OH = CH3 + H2O	(40%)	(1.0 - 1.7 mm)
	CH3 + HO2 = CH3O + OH	(22%)	OH + HCl = Cl + H2O	(17%)	
(0.5 - 0.6 mm)	H2O2 + M = 2OH + M	(46%)	OH + HCl = Cl + H2O	(31%)	(1.8 - 1.9 mm)
	H + O2 = O + OH	(18%)	CH4 + OH = CH3 + H2O	(17%)	
(0.8 - 1.6 mm)	H + O2 = O + OH	(40%)	OH + HCl = Cl + H2O	(35%)	(2.0 mm)
	CH4 + O = CH3 + OH	(17%)	H + H2O = H2 + OH	(17%)	
(1.7 - 2.4 mm)	H + O2 = O + OH	(33%)	OH + HCl = Cl + H2O	(47%)	(2.1 - 2.6 mm)
	O + H2O = 2OH	(17%)	CO + OH = CO2 + H	(28%)	
(2.5 - 4.0 mm)	O + H2O = 2OH	(35%)	CO + OH = CO2 + H	(70%)	(2.7 - 4.0 mm)
	H + O2 = O + OH	(27%)	OH + HCl = Cl + H2O	(21%)	

Figure 28 Key Production and Destruction Reactions of OH Radical for Fuel Lean, R=0.50

strongly supports the inhibition hypothesis offered by Barat et al. (1990) and Ho et al. (1992).

It is observed that the endothermic reaction $O + H_2O = OH + OH$ (ΔH_R = +17.23 Kcal/mole) becomes important later (at higher HAB) in chlorinated flames. And the reaction seems to become less important as Cl content increases.

Figure 29 is a plot of model predicted OH concentration profiles for the fuel rich flames studied. These curves have a similar shape. But the CH_3Cl-containing curves are shifted toward higher HAB according to the content of CH_3Cl loading, and then they all converge to about the same mole fraction of $0.6x10^{-4}$ at high HAB. Contrary to the fuel lean flames in Figure 25, the higher the CH_3Cl concentration, the higher the OH peak concentration appears. Compare Figure 25 (fuel lean flames) and Figure 29 (fuel rich flames), for R=0 case, the OH peak concentration in fuel lean flame (about $5.0x10^{-4}$) is much higher than that in fuel rich flame (about $3.0x10^{-4}$). For R=0.25 and R=0.50 cases, the OH peak concentration in fuel lean flames (about $2.5x10^{-4}$) is much lower than that in fuel rich flames (about $4.0x10^{-4}$). In order to explain the above phenomenon, we also perform the ROP calculations to get the key production and destruction reaction OH for these flames. The results are shown in Figures 30, 31 and 32 (R=0, R=0.25, and R=0.50 respectively).

Similar to the fuel lean flames, it is observed that the reaction of CO burnout $CO + OH = CO_2 + H$ starts to be dominant at 1.375 mm in Figure 30, at 1.625 mm in Figure 31, and at 1.75 mm in Figure 32, which also means CO burnout is delayed according to the CH_3Cl loading. But contrary to the fuel lean cases, here H_2 instead of HCl, competes with CO to consume OH by the reaction $H + H_2O = H_2 + OH$ (in reverse direction).

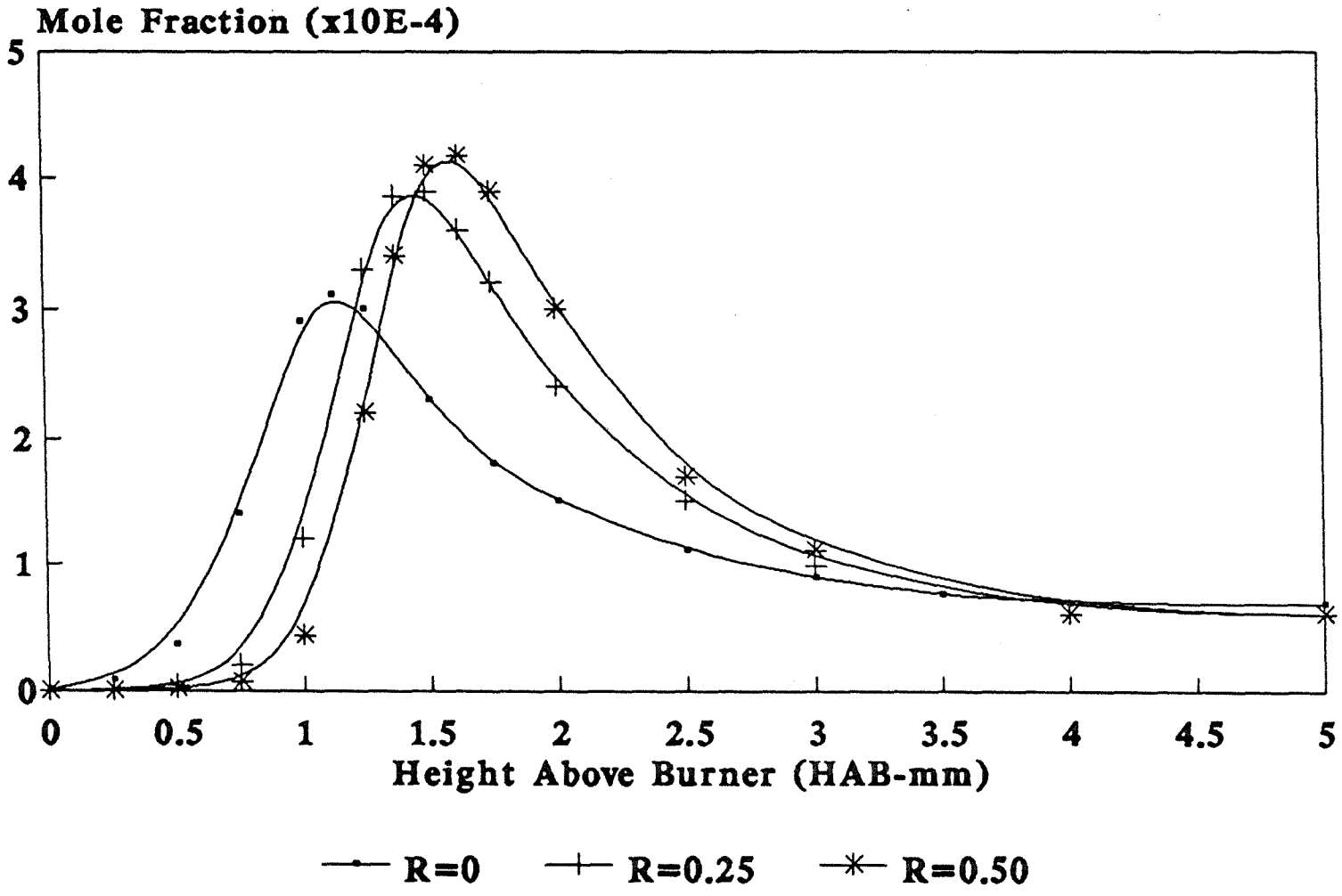

Figure 29 Model Predicted OH Concentration Profile for ϕ=1.20

	Production of OH		Destruction of OH		
(0 - 0.25 mm)	CH3 + HO2 = CH3O + OH H2O2 + M = 2OH + M	(70%) (21%)	CH4 + OH = CH3 + H2O CH2O + OH = CHO + H2O	(58%) (17%)	(0 mm)
(0.375 - 0.563 mm)	H + O2 = O + OH CH3 + HO2 = CH3O + OH	(34%) (17%)	CH4 + OH = CH3 + H2O H + H2O = H2 + OH	(56%) (22%)	(0.063 - 0.625 mm)
(0.625 - 0.75 mm)	H + O2 = O + OH H + HO2 = 2OH	(32%) (22%)	H + H2O = H2 + OH CH4 + OH = CH3 + H2O	(33%) (23%)	(0.688 - 0.813 mm)
(0.813 - 1.375 mm)	H + HO2 = 2OH H + O2 = O + OH	(41%) (25%)	H + H2O = H2 + OH CH2O + OH = CHO + H2O	(42%) (17%)	(0.875 - 1.0 mm)
(1.5 mm)	H + HO2 = 2OH O + H2O = 2OH	(50%) (20%)	H + H2O = H2 + OH CO + OH = CO2 + H	(47%) (21%)	(1.063 - 1.25 mm)
(1.75 mm)	H + HO2 = 2OH H + H2O = H2 + OH	(38%) (26%)	CO + OH = CO2 + H H + H2O = H2 + OH	(53%) (23%)	(1.375 - 1.5 mm)
(2.0 - 2.5 mm)	H + H2O = H2 + OH H + HO2 = 2OH	(81%) (10%)	CO + OH = CO2 + H CH2OH + H = CH3 + OH	(82%) (6%)	(1.75 - 2.25 mm)
(3.0 - 4.0 mm)	H + H2O = H2 + OH	(99%)	CO + OH = CO2 + H	(91%)	(2.5 - 4.0 mm)
(5.0 mm)	H + HO2 = 2OH	(90%)	H + H2O = H2 + OH CO + OH = CO2 + H	(50%) (46%)	(5.0 mm)

Figure 30 Key Production and Destruction Reactions of OH Radical for Fuel Rich, R=0

	Production of OH		Destruction of OH		
(0 - 0.375 mm)	$CH_3 + HO_2 = CH_3O + OH$	(69%)	$CH_4 + OH = CH_3 + H_2O$	(50%)	(0 mm)
	$CH_2Cl + HO_2 = CH_2ClO + OH$	(30%)	$CH_3Cl + OH = CH_2Cl + H_2O$	(14%)	
(0.438 mm)	$CH_3 + HO_2 = CH_3O + OH$	(37%)	$CH_4 + OH = CH_3 + H_2O$	(38%)	(0.125 - 0.281 mm)
	$H_2O_2 + M = 2OH + M$	(28%)	$OH + HCl = Cl + H_2O$	(16%)	
(0.5 mm)	$H_2O_2 + M = 2OH + M$	(29%)	$CH_4 + OH = CH_3 + H_2O$	(50%)	(0.313 - 0.875 mm)
	$H + O_2 = O + OH$	(26%)	$H + H_2O = H_2 + OH$	(23%)	
(0.625 - 0.875 mm)	$H + O_2 = O + OH$	(40%)	$H + H_2O = H_2 + OH$	(35%)	(1.0 - 1.125 mm)
	$CH_4 + O = CH_3 + OH$	(17%)	$CH_4 + OH = CH_3 + H_2O$	(17%)	
(1.0 - 1.188 mm)	$H + O_2 = O + OH$	(35%)	$H + H_2O = H_2 + OH$	(41%)	(1.188 mm)
	$H + HO_2 = 2OH$	(22%)	$OH + HCl = Cl + H_2O$	(14%)	
(1.25 - 2.0 mm)	$H + HO_2 = 2OH$	(36%)	$H + H_2O = H_2 + OH$	(45%)	(1.25 - 1.5 mm)
	$H + O_2 = O + OH$	(26%)	$CO + OH = CO_2 + H$	(21%)	
(2.5 - 4.0 mm)	$H + H_2O = H_2 + OH$	(69%)	$CO + OH = CO_2 + H$	(57%)	(1.625 - 1.75 mm)
	$OH + HCl = Cl + H_2O$	(17%)	$H + H_2O = H_2 + OH$	(23%)	
(5.0 mm)	$H + HO_2 = 2OH$	(45%)	$CO + OH = CO_2 + H$	(96%)	(2.0 - 4.0 mm)
	$H + O_2 = O + OH$	(37%)			
			$H + H_2O = H_2 + OH$	(44%)	(5.0 mm)
			$CO + OH = CO_2 + H$	(40%)	

Figure 31 Key Production and Destruction Reactions of OH Radical for Fuel Rich, R=0.25

	Production of OH		Destruction of OH		
(0 - 0.25 mm)	$CH_2Cl + HO_2 = CH_2ClO + OH$ $CH_3 + HO_2 = CH_3O + OH$	(51%) (48%)	$CH_4 + OH = CH_3 + H_2O$ $CH_3Cl + OH = CH_2Cl + H_2O$	(42%) (22%)	(0 - 0.188 mm)
(0.375 - 0.438 mm)	$H_2O_2 + M = 2OH + M$ $CH_3 + HO_2 = CH_3O + OH$	(42%) (19%)	$CH_4 + OH = CH_3 + H_2O$ $H + H_2O = H_2 + OH$	(48%) (20%)	(0.25 - 0.875 mm)
(0.5 mm)	$H_2O_2 + M = 2OH + M$ $H + O_2 = O + OH$	(38%) (16%)	$H + H_2O = H_2 + OH$ $CH_4 + OH = CH_3 + H_2O$	(31%) (19%)	(1.0 - 1.125 mm)
(0.625 mm)	$H + O_2 = O + OH$ $H_2O_2 + M = 2OH + M$	(29%) (19%)	$H + H_2O = H_2 + OH$ $OH + HCl = Cl + H_2O$	(40%) (21%)	(1.25 - 1.5 mm)
(0.75 - 1.0 mm)	$H + O_2 = O + OH$ $CH_4 + O = CH_3 + OH$	(42%) (16%)	$H + H_2O = H_2 + OH$ $CO + OH = CO_2 + H$	(39%) (29%)	(1.625 mm)
(1.125 - 1.375 mm)	$H + O_2 = O + OH$ $H + HO_2 = 2OH$	(35%) (23%)	$CO + OH = CO_2 + H$ $H + H_2O = H_2 + OH$	(42%) (32%)	(1.75 mm)
(1.5 - 2.0 mm)	$H + HO_2 = 2OH$ $H + O_2 = O + OH$	(32%) (27%)	$CO + OH = CO_2 + H$	(96%)	(2.0 - 4.0 mm)
(2.5 - 4.0 mm)	$H + H_2O = H_2 + OH$ $OH + HCl = Cl + H_2O$	(53%) (24%)	$CO + OH = CO_2 + H$ $H + H_2O = H_2 + OH$	(46%) (33%)	(5.0 mm)
(5.0 mm)	$H + O_2 = O + OH$ $H + HO_2 = 2OH$	(34%) (26%)			

Figure 32 Key Production and Destruction Reactions of OH Radical for Fuel Rich, R=0.50

And surprisingly, product H_2O causes the reaction OH + HCl = Cl + H_2O to proceed in reverse to produce OH in the CH_3Cl-doped flames. This may be the reason causing higher OH peak concentrations in the CH_3Cl-doped flames in Figure 29. Also it suggests that the inhibition of CO burnout to CO_2 is primary due to the high concentration of H_2 in fuel rich flames.

CHAPTER 6
CONCLUSION

This thesis has presented experimental and modeling results from premixed, atmospheric pressure, laminar, flat CH_4/air flames doped with CH_3Cl in both fuel lean and fuel rich regions.

The results show that a reasonable level of agreement exists between experimental and model predicted concentration profiles for the major species CO, CO_2, CH_4, and CH_3Cl. With a constant equivalence ratio in the fuel lean flames, the experimental CO/CO_2 ratios increase as the CH_3Cl doping increases over almost the entire HAB range of study. However, the ratios converge to about the same value at high HAB. With a constant equivalence ratio in the fuel rich flames, the CO/CO_2 ratios are also observed to be higher with increasing CH_3Cl content over the entire HAB range. Furthermore, there is a significant increase in the absolute value of CO/CO_2 ratio at each position compared to the fuel lean flames.

The major reaction pathways responsible for the destruction of the fuels, and the formation and destruction of the intermediates at various positions in the flame are discussed. In the fuel lean flames, the Cl atom is very active in several reactions involving abstraction of H from species such as CH_2O, C_2H_6, and C_2H_4. The product HCl depletes OH rapidly and reduces the OH available for CO burnout ($OH + CO = CO_2 + H$), thus inhibiting the conversion of CO to CO_2. In fuel rich flames, the H_2 instead of HCl, is found to consume OH, also limiting the CO burnout. Furthermore, the product H_2O can react with Cl to form OH, which indicates the Cl is still a key radical in fuel rich CH_3Cl-containing flames.

APPENDIX

A. Flowmeter Calibration

This appendix consists of the calibration data and calibration curves for Air, CH_4, CH_3Cl, and N_2 gas flowmeters.

Table 3 Calibration Data for Gas Flowmeters

	Air	CH_4	CH_3Cl (large tube)	CH_3Cl (small tube)	N_2 (Shroud)
Reading	(ml/min)*	(ml/min)*	(ml/min)*	(ml/min)*	(ml/min)*
10	1600	436	216	70	957
20	3570	625	303	97	1533
30	5380	825	382	125	2104
40	7283	1024	463	156	2628
50	9087	1206	540	198	3119
60	11055	1393	612	224	3617
70	12830	1579	684	265	4060
80	14685	1752	767	295	4568
90	16545	1920	843	332	5093
100	18290	2078	910	359	5486
110	19955	2244	977	385	5839
120	21545	2415	1058	421	6196
130	23150	2578	1125	458	6602
140	24790	2734	1183	493	7087
150	26180	2891	1265	530	7558

* Rotameters are calibrated at T = 25 ^{0}C and P = 20 psig.

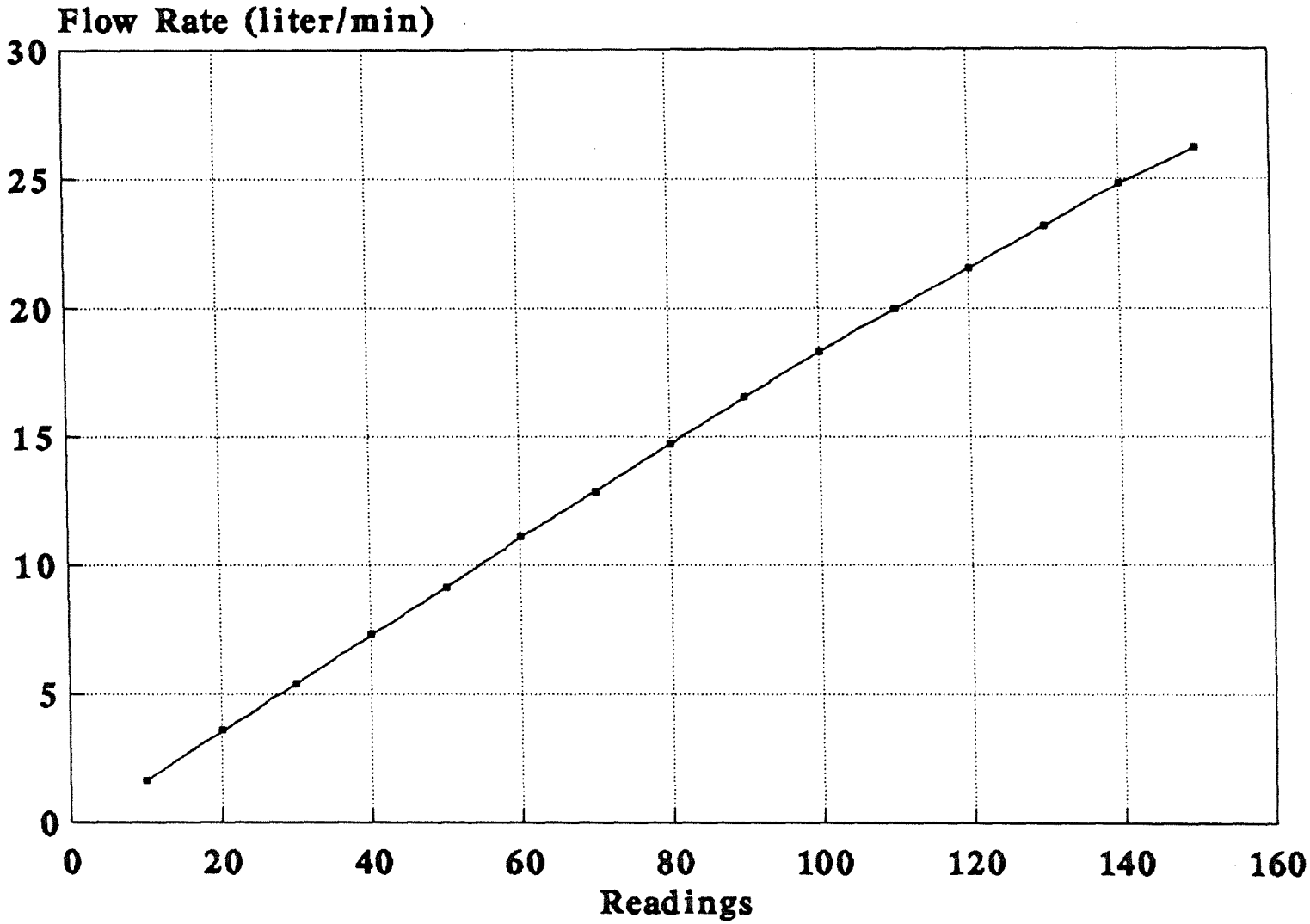

Figure 33 Calibration Curve for Air Flowmeter

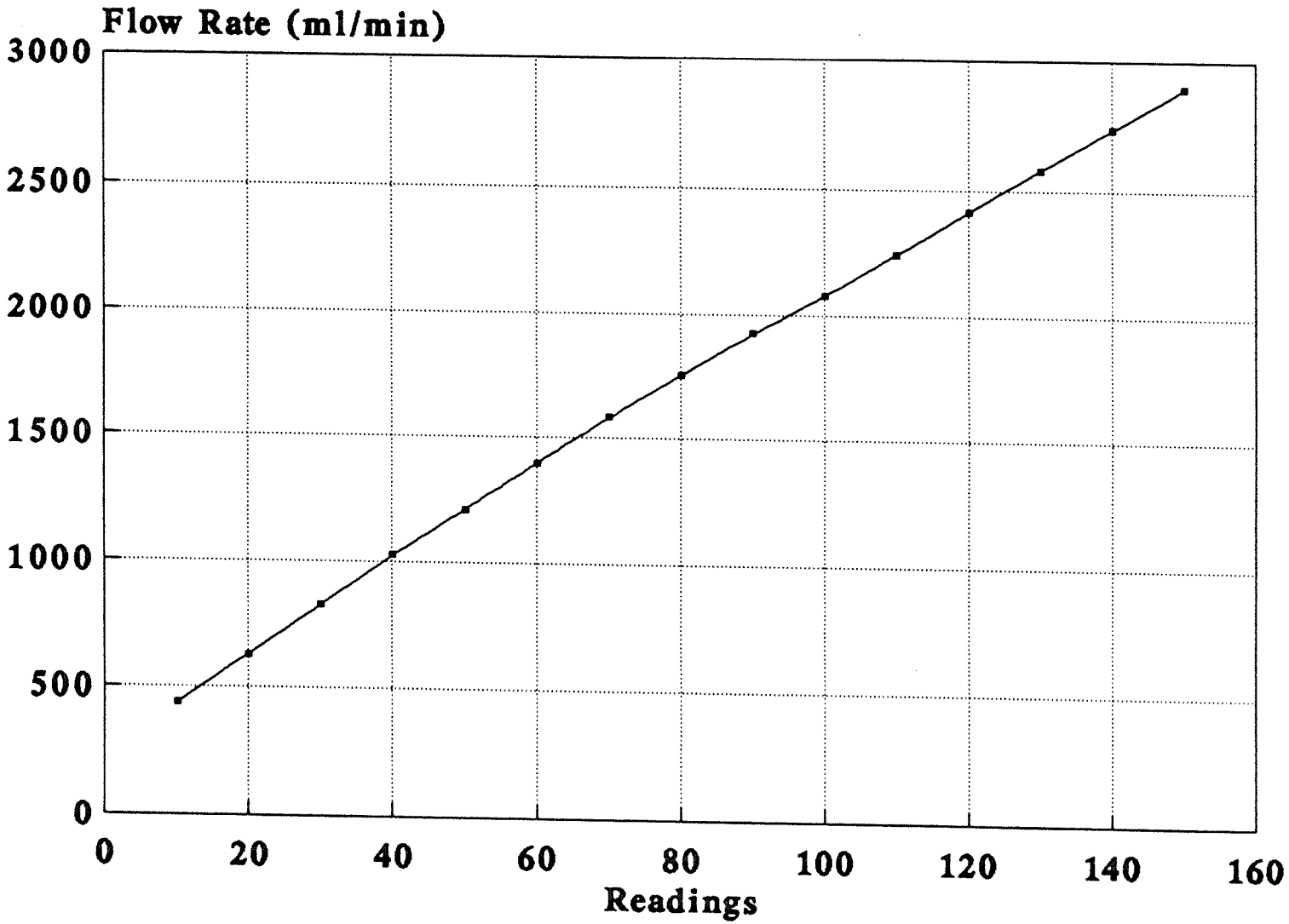

Figure 34 Calibration Curve for CH4 Flowmeter

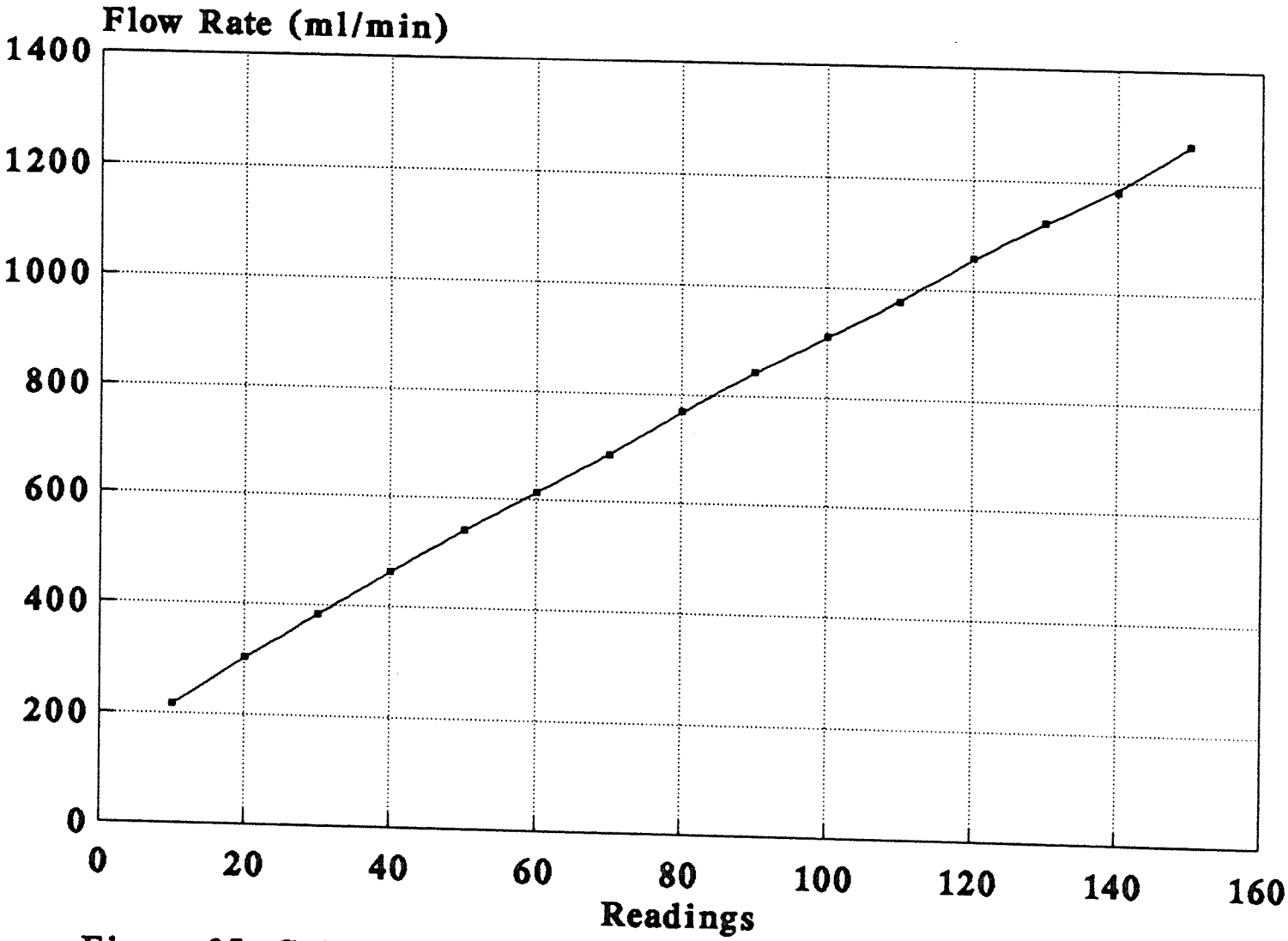

Figure 35 Calibration Curve for CH3Cl Flowmeter (large tube)

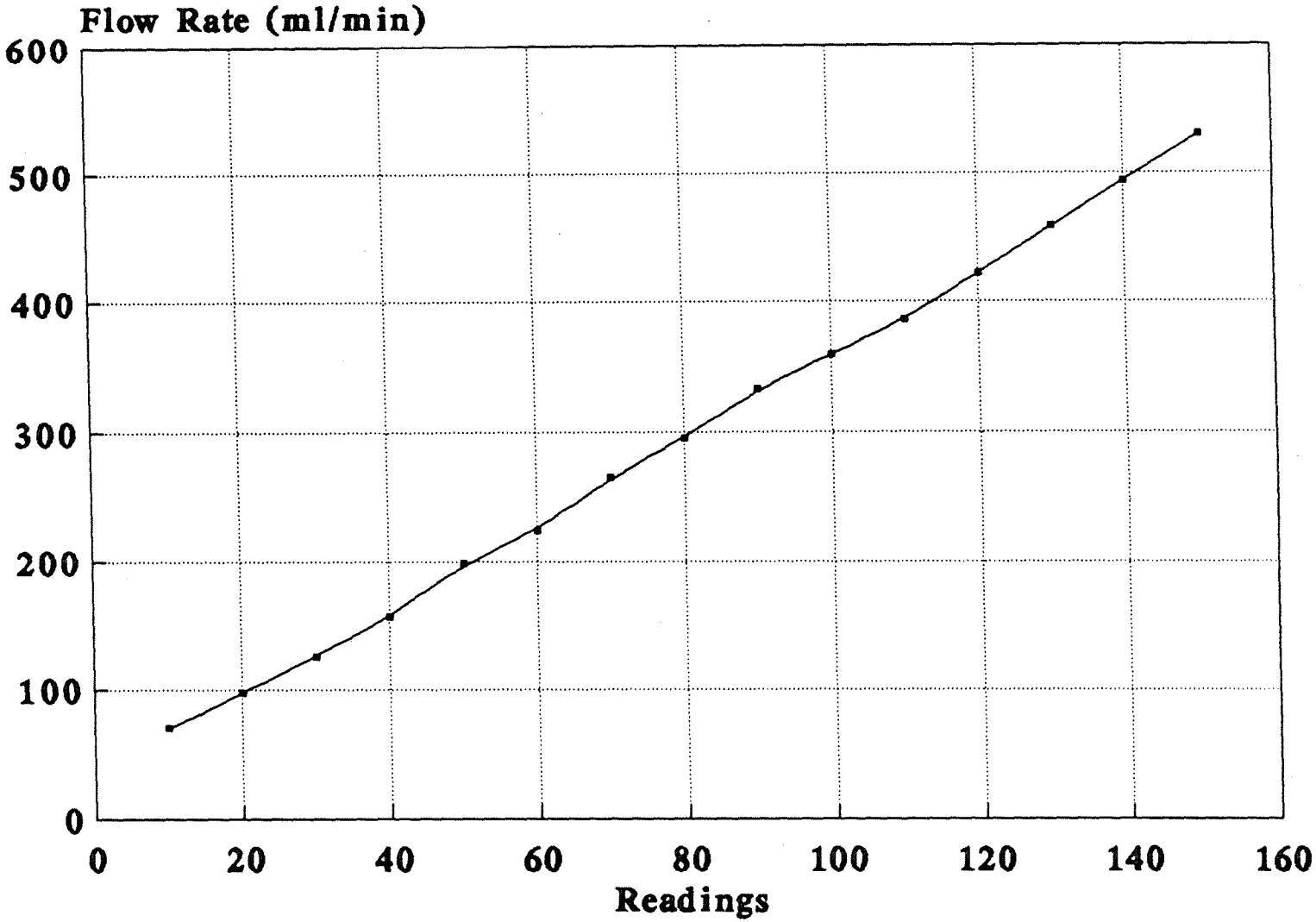

Figure 36 Calibration Curve for CH3Cl Flowmeter (small tube)

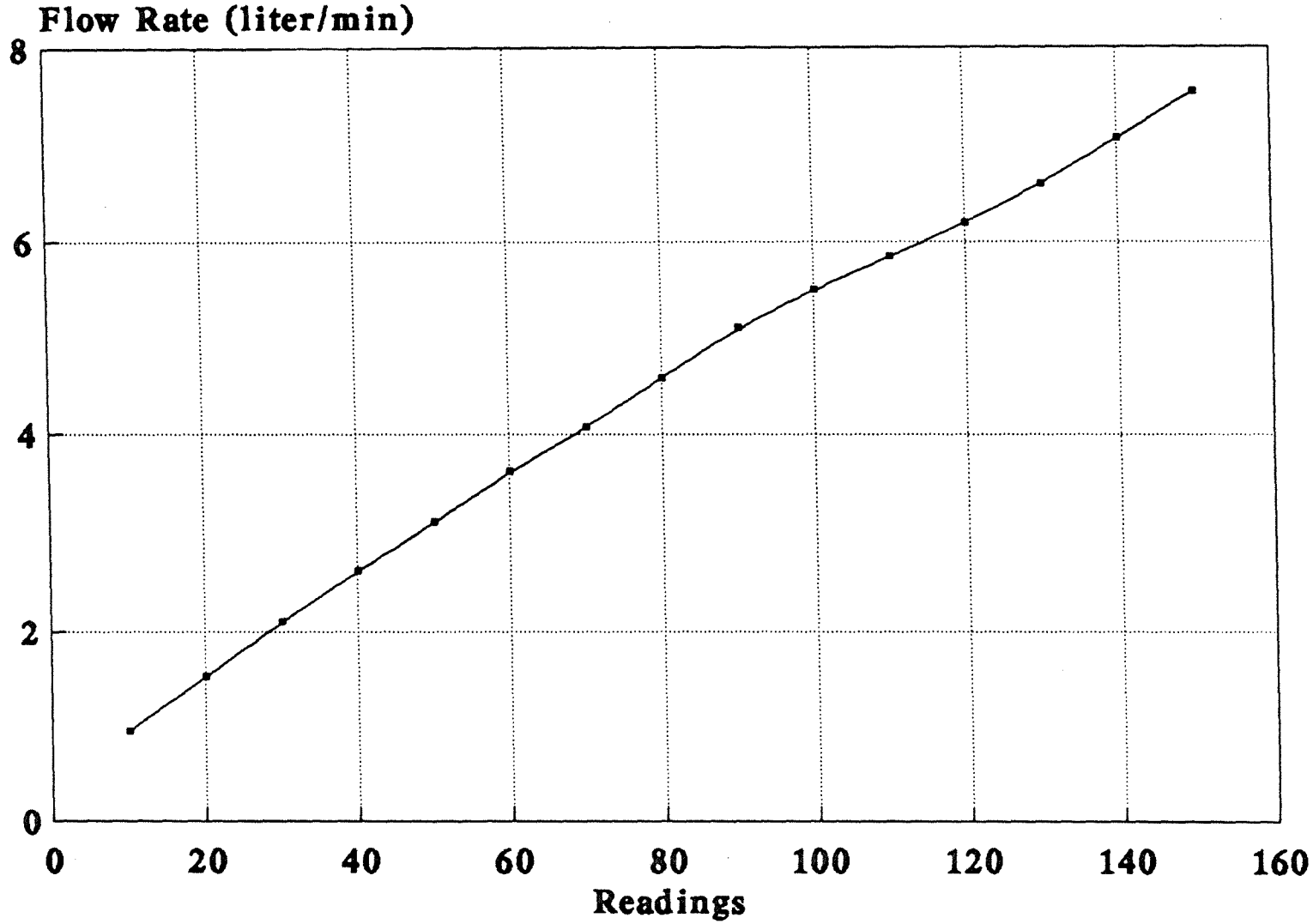

Figure 37 Calibration Curve for N2 (shroud gas) Flowmeter

B. Detailed Gas Sampling Procedures

To perform gas sampling, the following operating steps including the GC system setup, flame establishment, and GC analysis should be followed to get quick and good results.

1 Set up GC system

1.1) Make sure there is no leakage in GC system by evacuating the system, closing all valves, and watching the pressure reading on the gauge C. If the pressure doesn't drop, it means there is no leakage.

1.2) Turn on the temperature controllers for the transfer line and the catalytic converter, set temperature at 100 ^{0}C for the transfer line and at 300 ^{0}C for the converter.

1.3) Open the nitrogen and hydrogen cylinders. Check all the operating pressures for GC according to the Table 1.

1.4) Turn on the GC power and program the GC. Ignite two FID detectors.

1.5) Turn on the integrators. Set up the parameters as shown in Figure 40.

1.6) Wait for "READY" indicator on the GC.

2 Set up the gas flow rate and locate the quartz micro-probe

2.1) Switch on the hydrocarbon detector.

2.2) Switch on the water pump. Make sure the HCl scrubber water pump valves (refer to Figure 1: valves E and F are on the hood, valve G is plastic) for HCl fume trap are open.

2.3) Adjust water flow with the inlet valve F on the hood until cavitation disappears.

2.4) Put the quartz probe in the center of the burner and put a piece of paper on the burner surface, raise the burner until the probe orifice touches the paper and pull the paper out carefully.

2.5) Open the cooling water for the burner (pressure gage at 40 psig). Open the water for the probe.

2.6) Open the methane, methyl chloride (if it is needed) cylinders and the air inlet valve. Set the flow rate of each gas according to the flame initial feed conditions (Table 2) and check the pressure gages. The pressure for each gas should be 20 psig.

3 Flame gas sampling by GC

3.1) When GC system is ready, turn on the vacuum pump.

3.2) Open the control valve D (on the gas flow control panel in Figure 1) for premixed fuel and air. Light the burner flame.

3.3) Adjust the water flow for the probe to avoid the water boiling;

3.4) Adjust the six-port sampling valve loop pressure to 5 inHg by controlling rotameter A.

3.5) Switch two six-port valves from collection position to injection position at the same time, then quickly start the GC program and the integrators; now the GC is running and the integrators are recording the data.

3.6) Switch the six-port valves back to the collection position after at least 5 minutes.

3.7) Collect and record the data from the integrators when the GC run's are finished.

3.8) Move the burner to another HAB for next gas sampling.

3.9) Repeat step 3.4) to 3.8) until HAB reaches the desired final value, for instance, HAB = 4.0 mm.

4 After completion of flame gas sampling

4.1) Stop the flame by turning off the fuel and air (turn off valve D).

4.2) Turn off the scrubber water, then switch off the water pump.

4.3) Switch off the vacuum pump, then remove the probe from the burner surface.

4.4) Clean the burner surface with acetone and then let the air flow through the burner and dry it up.

4.5) Increase the GC column temperature to 199 ^{0}C so that any large hydrocarbon molecules remaining in the column will be elute.

4.6) Close the hydrogen line when FID is not needed.

4.7) Let the flame sample transfer line cool down. Fill the line with little acetone and let the nitrogen flow through the line from one end, and collect the dirty acetone from the other end of the line.

4.8) Turn off GC main power before closing the nitrogen.

McKENNA PRODUCTS, INC.

Powder Metallurgy

P. O. BOX 331 PITTSBURG, CALIFORNIA 94565

(415) 432-3113
(415) 689-3680

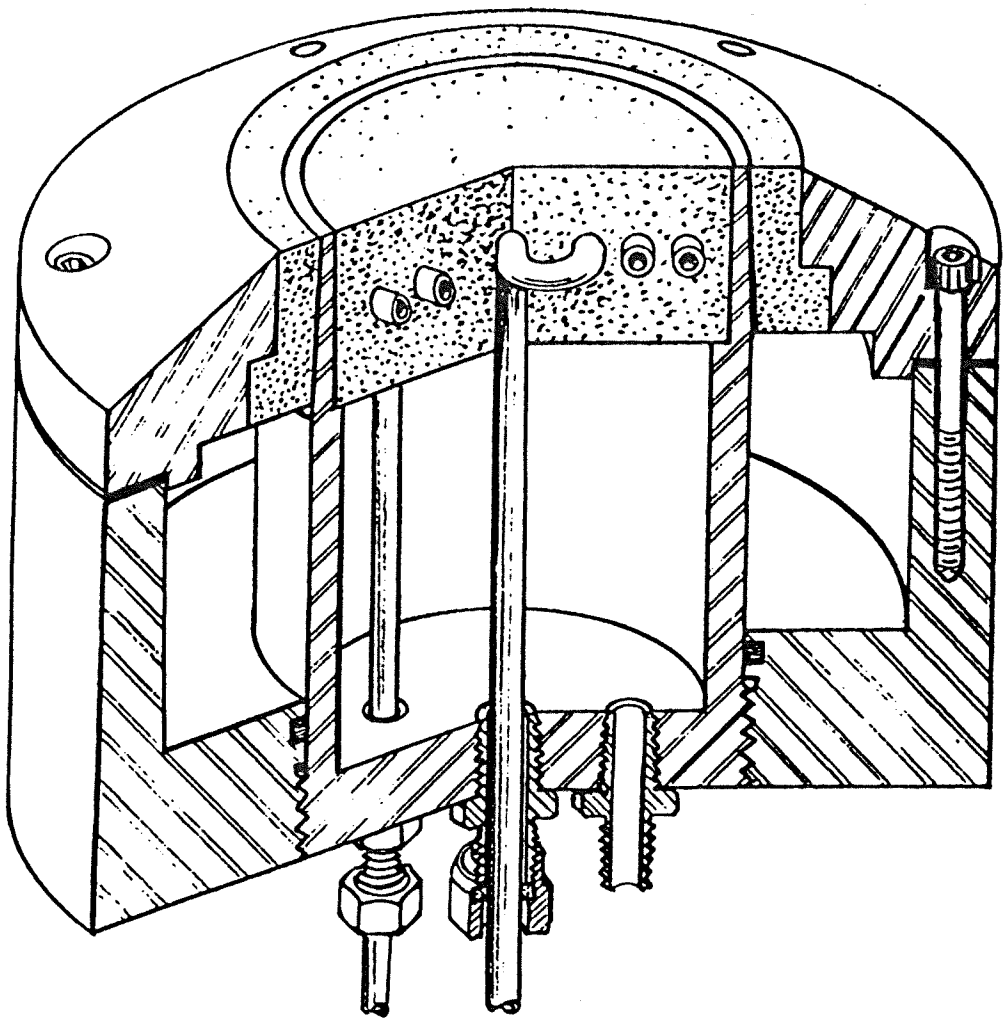

Figure 38 Flat Flame Burner

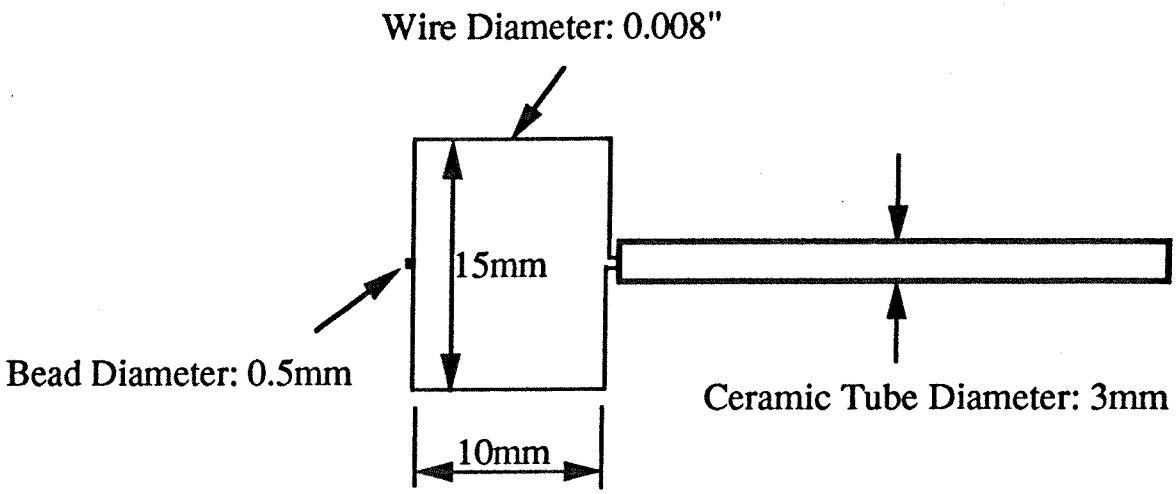

Figure 39 Sketch of Thermocouple

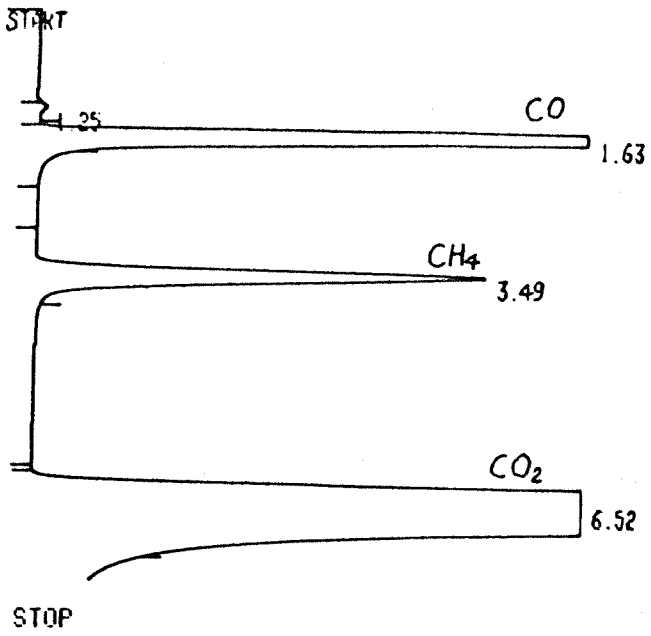

RUN # 59 JUN/04/92 12:41:23

AREA%

RT	AREA	TYPE	AR/HT	AREA%
1.25	456	PB	0.106	0.035
1.63	184860	PB	0.106	14.319
3.49	37136	PB	0.189	2.876
6.52	1068600	PB	0.316	82.770

TOTAL AREA= 1291100
MUL FACTOR= 1.0000E+00

LIST: LIST
PEAK CAPACITY: 1159

ZERO = 0,-0.6
ATT 2↑ = 1
CHT SP = 1.0
PK WD = 0.11
THRSH = -1
AR REJ = 0

Figure 40 Sample Output From Integrator A

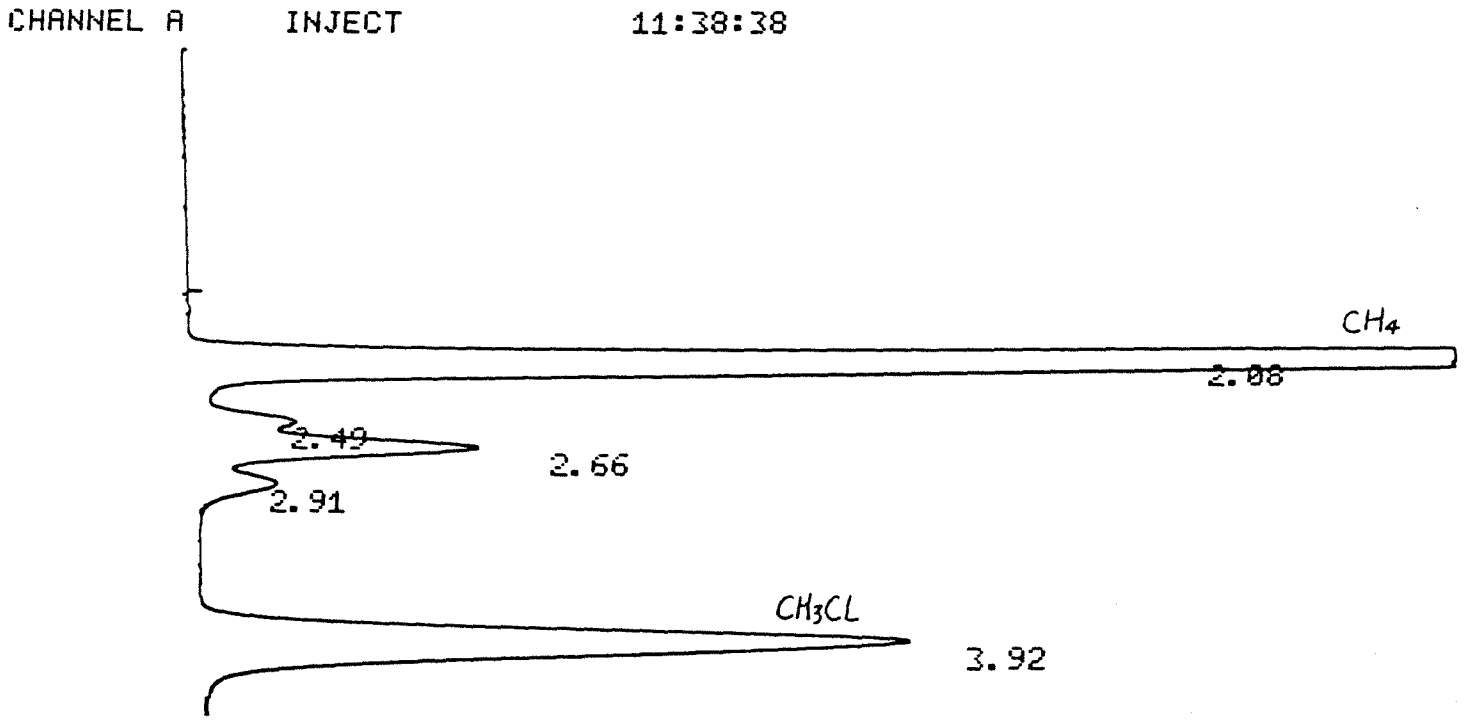

11:38:38 CH= "A" PS= 1.

FILE 1. METHOD 0. RUN 28 INDEX 28

PEAK#	AREA%	RT	AREA BC
1	70.433	2.08	38045 01
2	1.518	2.49	820 02
3	5.778	2.66	3121 02
4	1.516	2.91	819 03
5	20.755	3.92	11211 01
TOTAL	100.		54016

Figure 41 Sample Output From Integrator B

C. Chemical Reaction Mechanism

Table 4 Mechanism

Reaction*	A	n	E
C2H6+CH3=C2H5+CH4	2.7E-01	4.00	8280.
CH3+C2H5=CH4+C2H4	5.5E+11	0.00	0.
CH2CL2 = CHCL + HCL	8.73E37	-7.68	86730.
CH2CL2 = CH2CL + CL	7.40E40	-7.87	84990.
CH3CL = CH3 + CL	1.26E37	-6.91	90540.
CH3CL = CH2S + HCL	8.52E27	-5.13	109640.
CH2CL2 + H = CH2CL + HCL	7.00E13	0.00	7100.
CHCL2 + H2 = CH2CL2 + H	4.63E12	0.00	15295.
CH2CL + H2 = CH3CL + H	3.90E12	0.00	14059.
CH2CL2 + CL = CHCL2 + HCL	2.79E13	0.00	2940.
CH3CL + H = CH3 + HCL	6.64E13	0.00	7620.
CH4 = CH3 + H	1.03E33	-5.58	111810.
CH4 + H = CH3 + H2	1.55E14	0.00	11000.
CH4 + CL = CH3 + HCL	3.09E13	0.00	3600.
CH3CL + CL = CH2CL + HCL	3.16E13	0.00	3300.
CH2CL2 + CH3 = CH4 + CHCL2	6.76E10	0.00	7200.
CH2CL2 + CH3 = CH3CL + CH2CL	1.40E11	0.00	4900.
CH3CL + CH3 = CH4 + CH2CL	3.30E11	0.00	9400.
CHCL2 + CHCL2 = C2H2CL4	9.08E45	-10.56	13170.
CHCL2 + CHCL2 = C2H2CL3 + CL	1.36E30	-5.23	14180.
CHCL2 + CHCL2 = C2HCL3 + HCL	6.72E35	-7.11	13210.
CH2CL + CH2CL = C2H4CL2	7.84E45	-10.21	13150.
CH2CL + CH2CL = CH2CLCH2 + CL	9.34E29	-4.94	14070.
CH2CL + CH2CL = C2H3CL + HCL	3.75E35	-6.73	13160.
CH2CL + CHCL2 = C2H3CL3	5.02E48	-11.10	14760.
CH2CL + CHCL2 = CH2CCL2 + HCL	1.62E37	-7.53	14940.
CH2CL + CHCL2 = CHCLCHCL + HCL	9.31E38	-7.78	14860.
CH2CL + CH3 = C2H5CL	3.27E40	-8.49	10590.
CH2CL + CH3 = C2H4 + HCL	3.50E28	-4.49	9180.
CH2CL + CH3 = C2H5 + CL	9.27E19	-2.07	10130.
CHCL2 + CH3 = CH3CHCL2	2.28E41	-8.68	11620.
CHCL2 + CH3 = C2H3CL + HCL	1.35E30	-4.96	11550.
CHCL2 + CH3 = CH3CHCL + CL	2.74E25	-3.45	12810.
CH2CL + H = CH3CL	3.04E25	-4.47	3490.
CH2CL + H = CH2S + HCL	9.48E04	1.91	2600.
CH2CL + H = CH3 + CL	5.12E14	-0.22	310.
CHCL2 + H = CH2CL2	4.81E26	-4.82	3810.
CHCL2 + H = CH2CL + CL	1.25E14	-0.03	570.
C2H3CL + H = CH2CLCH2	5.01E23	-4.21	8470.
C2H3CL + H = C2H4 + CL	1.55E13	-0.02	5840.
C2H3CL + H = C2H3 + HCL	1.20E12	0.00	15000.
C2HCL3 + H = CH2CLCCL2	1.51E23	-4.18	7520.
C2HCL3 + H = C2H2CL3	2.87E22	-4.09	10890.
C2HCL3 + H = CH2CCL2 + CL	1.45E13	-0.01	5830.
C2HCL3 + H = CHCLCHCL + CL	7.37E12	-0.01	9220.
C2H3CL3 = CHCLCHCL + HCL	1.39E20	-2.03	60450.

Table 4 Mechanism (continued)

Reaction	A	n	E
C2H3CL3 = CH2CCL2 + HCL	3.13E19	-2.02	60330.
CH3CHCL2 = C2H3CL + HCL	2.94E21	-2.37	59460.
CH3CHCL2 = CH3CHCL + CL	3.17E42	-8.10	92670.
C2H2CL4 = C2HCL3 + HCL	8.62E21	-2.57	51870.
C2H4CL2 = C2H3CL + HCL	6.76E19	-1.93	58710.
C2H5CL = C2H4 + HCL	7.81E19	-2.00	60660.
C2H5CL = C2H5 + CL	2.35E43	-8.50	96980.
C2H5CL + CL = HCL + CH3CHCL	3.55E13	0.00	1500.
C2H5CL + CL = HCL + CH2CLCH2	1.12E13	0.00	1500.
C2H5CL + H = HCL + C2H5	1.00E14	0.00	7900.
C2H3CL = C2H2 + HCL	1.62E28	-4.29	75780.
C2H3CL = C2H3 + CL	1.71E38	-7.13	96370.
C2H6 = C2H5 + H	6.22E47	-9.76	111250.
C2H6 = CH3 + CH3	5.34E54	-11.12	112210.
C2H4 = C2H2 + H2 (DISSOC,WAR)	8.52E43	-8.32	121240.
C2H4 = C2H3 + H (DISSOC,DEAN)	8.53E30	-5.87	118240.
CH2CCL2 + H = C2H3CL+ CL	7.21E12	0.00	7510.
CHCLCHCL + H = C2H3CL + CL	3.44E13	-0.03	5890.
C2H6 + H = C2H5 + H2	6.61E13	0.00	3600.
C2H6 + CL = C2H5 + HCL	4.37E13	0.00	100.
C2H6 + O = C2H5 + OH	2.51E13	0.00	6400.
C2H6 + OH = C2H5 + H2O	8.85E09	1.04	1810.
C2H5 = C2H4 + H (DISSOC,DEAN)	1.83E39	-7.75	52820.
C2H5 + H = CH3 + CH3 (QRRK)	1.35E22	-2.17	7000.
C2H5 + O = CH2O + CH3	1.00E13	0.00	0.
C2H5 + O2 = C2H4 + HO2	2.00E12	0.00	4992.
C2H5 + HO2 = C2H4 + H2O2 (TSA)	3.01E11	0.00	0.
C2H4 + OH = C2H3 + H2O (TSA)	1.58E04	2.75	4173.
C2H4 + CH3 = CH4 + C2H3 (WAR)	4.20E11	0.00	11113.
C2H4 + O2 = C2H3 + HO2 (TSA)	4.22E13	0.00	57623.
C2H4 + H = C2H3 + H2	6.92E14	0.00	14500.
C2H4 + CL = C2H3 + HCL (BENSON88)	2.39E13	0.00	2600.
C2H3 = C2H2 + H (DISSOC,DEAN)	6.24E29	-5.29	46500.
C2H3 + O2 = C2H2 + HO2 (TSA)	1.21E11	0.00	0.
C2H3 + O2 = CHO + CH2O (GUTMAN84)	3.97E12	0.00	-250.
C2H2 + CL = C2H + HCL (BENSON84)	1.58E14	0.00	16900.
C2H2 + O2 = C2H + HO2 (TSA)	1.21E13	0.00	74520.
C2H2 + O = CO + CH2 (WAR)	4.10E08	1.50	1700.
C2H2 + O = HCCO + H (MILLER)	1.02E07	2.00	1900.
C2H2 + OH = C2H + H2O (TSA)	1.45E04	2.68	12040.
C2H2 + OH = CH2CO + H	5.91E11	0.00	2170.
C2H + O2 = CO + CHO (T)	2.41E12	0.00	0.
C2H + H2 = C2H2 + H (T)	1.15E13	0.00	2880.
C2H + CH4 = C2H2 + CH3 (T)	1.81E12	0.00	500.
C2H + OH = CH2 + CO (T)	1.81E13	0.00	0.
C2H + OH = C2H2 + O (T)	1.81E13	0.00	0.
HCCO + H = CH2S + CO (WAR)	3.00E13	0.00	0.
CH2CO + O = CH2 + CO2 (MILLER)	1.74E12	0.00	1350.
CH2CO + H = HCCO + H2 (MILLER)	5.00E13	0.00	8000.

Table 4 Mechanism (continued)

Reaction	A	n	E
CH2CO + O = HCCO + OH (MILLER)	1.00E13	0.00	8000.
CH2CO + OH = HCCO + H2O (MILLER)	7.50E12	0.00	2000.
CH2CO + M = CH2 + CO + M	3.00E15	0.00	75980.
CH2CO + OH = CHO + CH2O	2.80E13	0.00	0.
CH2CO + H = CH3 + CO (NIST)	1.50E04	2.83	672.8
CH2S + M = CH2 + M (MILLER)	1.00E13	0.00	0.
CH2S + O2 = CO + H2O	2.41E11	0.00	0.
CH2S + CH4 = C2H5 + H	9.43E12	-0.13	6620.
CH2S + CH4 = CH3 + CH3	3.45E22	-2.48	7460.
CH2S + CH4 = C2H6	5.78E46	-10.31	12830.
CH2S + CH3CL = C2H5CL	7.85E31	-6.15	5830.
CH2S + CH3CL = C2H4 + HCL	1.60E18	-1.47	2710.
CH2S + CH3CL = C2H5 + CL	3.09E07	1.70	520.
CH2S + H2 = CH4	3.82E25	-4.47	3770.
CH2S + H2 = CH3 + H	1.27E14	-0.08	130.
CH2 + CH4 = CH3 + CH3	1.82E05	0.00	0.
CH2 + CH3CL = CH3 + CH2CL	9.10E04	0.00	0.
CH2 + H2 = CH3 + H	3.01E09	0.00	0.
CH2 + H2O = CH3 + OH	9.64E07	0.00	0.
CH4 + O2 = CH3 + HO2 (TSA)	4.04E13	0.00	56910.
CH4 + O = CH3 + OH (TSA)	1.02E09	1.50	8600.
CH4 + OH = CH3 + H2O (TSA)	1.93E05	2.40	2110.
CH4 + HO2 = CH3 + H2O2	2.00E13	0.00	18000.
CH3 + O2 = CH2O + OH	3.59E09	-0.14	10150.
CH3 + O2 = CH3O + O	2.88E15	-1.15	30850.
CH3 + O = CH2O + H	7.00E13	0.00	0.
CH3 + OH = CH3O + H	3.87E12	-0.19	13741.
CH3 + HO2= CH3O + OH	2.00E13	0.00	0.
CH3O + O2 = CH2O + HO2	6.62E10	0.00	2600.
CH3O + M = CH2O + H + M	1.00E14	0.00	25100.
CH3O + CO = CO2 + CH3	1.57E13	0.00	11800.
CH3O + HO2 = CH2O + H2O2	3.01E11	0.00	0.
CH3O + CH3 = CH4 + CH2O	2.41E13	0.00	0.
CH3O + O = OH + CH2O	6.03E12	0.00	0.
CH3O + OH = H2O + CH2O	1.81E13	0.00	0.
CH3O + H = CH2O + H2	1.99E13	0.00	0.
CH3O + CH2 = CH3 + CH2O	1.81E13	0.00	0.
CH3O + C2H5 = C2H6 + CH2O	2.41E13	0.00	0.
CH3O + CLO = HOCL + CH2O	2.41E13	0.00	0.
CH3O + CL = HCL + CH2O	4.0E14	0.00	0.
CH2O + CLO = CHO + HOCL	5.50E03	2.81	5860.
CH2O + C2H5 = CHO + C2H6	5.50E03	2.81	5860.
CH2O + CH3 = CH4 + CHO (WAR)	1.00E11	0.00	6090.
CH2O + H = CHO + H2 (WAR)	2.50E13	0.00	3990.
CH2O + O = CHO + OH	3.50E13	0.00	3510.
CH2O + OH= CHO + H2O	3.00E13	0.00	1190.
CH2O + HO2= CHO+ H2O2	1.00E12	0.00	8000.
CH2O + CL = CHO + HCL	5.00E13	0.00	500.
CH2O + M = CHO + H + M	5.00E16	0.00	76200.

Table 4 Mechanism (continued)

Reaction	A	n	E
CH2O + O2 = CHO + HO2 (TANG)	2.05E13	0.00	38945.
CHO + M = H + CO + M (WARNATZ)	2.50E14	0.00	16790.
CHO + H = CO + H2	2.00E14	0.00	0.
CHO + O2 = CO + HO2 (T)	5.12E13	0.00	1690.
CHO + O = CO + OH (T)	3.01E13	0.00	0.
CHO + O = H + CO2 (T)	3.01E13	0.00	0.
CHO + OH = CO + H2O (T)	3.01E13	0.00	0.
CO + OH = CO2 + H	4.40E06	1.50	-741.
CO + HO2=CO2+OH	5.80E13	0.00	22934.
CO + O2 = CO2 +O	2.50E12	0.00	47800.
CO + O + M = CO2 + M (TSA)	6.17E14	0.00	3000.
H + O2 = O + OH	1.69E17	-0.90	17390.
H+O2 = HO2 (WAR)	7.00E17	-0.80	0.
O + H2 = H + OH	1.08E04	2.80	5920.
O + H2O = OH + OH	1.5E10	1.14	17240.
H + H2O = H2 + OH	4.6E08	1.60	18560.
H + OH + M =H2O + M	7.5E23	-2.60	0.
O2 + M = O + O + M	1.20E14	0.00	107552.
H + O + M = OH + M	2.29E14	0.00	3900.
H + HO2=OH + OH	1.69E14	0.00	870.
H + HO2 = H2 + O2	6.62E13	0.00	2130.
O + HO2 = OH + O2	2.00E13	0.00	0.
OH + HO2 = H2O + O2	2.00E13	0.00	0.
OH + H2O2 = HO2 + H2O (T)	1.75E12	0.00	320.
O + H2O2 = HO2 + OH (T)	9.63E06	2.00	3970.
H + H2O2 = H2 + HO2 (T)	4.82E13	0.00	7950.
H + H2O2 = OH + H2O (T)	2.41E13	0.00	3970.
O2 + H2O2 = HO2 + HO2 (T)	5.42E13	0.00	39740.
H2O2 + M = OH + OH + M (T)	1.29E33	-4.86	53250.
O + HCL = OH + CL	5.24E12	0.00	6400.
OH + HCL = CL + H2O	2.45E12	0.00	1100.
H2 + M = H + H + M	4.57E19	-1.40	104390.
CL + CL + M = CL2 + M	2.34E14	0.00	-1800.
H + CL + M = HCL + M	1.00E17	0.00	0.
H + HCL = H2 + CL	2.30E13	0.00	3500.
CL + HO2= HCL + O2	1.08E13	0.00	-338.
CL + HO2 = CLO + OH	2.47E13	0.00	894.
CLO + CO = CL + CO2	6.03E11	0.00	17400.
CHCLO + H = CHO + HCL	8.33E13	0.00	7400.
CHCLO + H = CH2O + CL	6.99E14	-0.58	6360.
CH3 + CLO = CH3O + CL	3.33E11	0.46	30.
CH3 + CLO = CH2O + HCL	3.47E18	-1.80	2070.
CH2CL2 + O2 = CHCL2 + HO2	1.35E13	0.00	51800.
CH2CL2 + HO2 = CHCL2 + H2O2	6.67E12	0.00	18270.
CH2CL2 + OH = CHCL2 + H2O	2.83E12	0.00	2090.
CH2CL2 + O = CHCL2 + OH	6.00E12	0.00	5760.
CH2CL + O2 = CH2CLOO	2.73E33	-7.50	4440.
CH2CL + O2 = CH2O + CLO	1.91E14	-1.27	3810.
CH2CL + O2 = CHCLO +OH	4.00E13	0.00	34000.

Table 4 Mechanism (continued)

Reaction	A	n	E
CH2CL + O = CH2CLO (QRRK)	1.29E15	-1.98	1100.
CH2CL + O = CH2O + CL (QRRK)	5.59E13	-0.13	710.
CH2CL + OH = CH2O + HCL (QRRK)	1.24E22	-2.72	3860.
CH2CL + OH = CH2OH + CL (QRRK)	2.00E12	0.29	3270.
CH2CL + HO2 = CH2CLO + OH	1.00E13	0.00	0.
CH2CLO = CHCLO + H	1.83E27	-5.13	21170.
CH2CLO = CH2O + CL	4.53E31	-6.41	22560.
CHCLO = CHO + CL	8.86E29	-5.15	92920.
CHCLO = CO + HCL	1.10E30	-5.19	92960.
CH2CL + CLO = CH2CLO + CL	4.15E12	0.07	1110.
CH2CL + CLO = CHCLO + HCL	4.13E19	-2.22	2360.
CH2CL + CH2O = CH3CL + CHO	2.00E11	0.00	6000.
CH3CL + O2 = CH2CL + HO2	2.02E13	0.00	54000.
CH3CL + O = CH2CL + OH	1.70E13	0.00	7300.
CH3CL + OH = CH2CL + H2O	2.45E12	0.00	2700.
CH3CL + HO2 = CH2CL + H2O2	1.00E13	0.00	21660.
H2O2 + CL = HCL + HO2 (DEMORE)	6.62E12	0.00	1950.
CLO + CH4 = CH3 + HOCL (NIST)	6.03E11	0.00	15000.
CLO + CH3CL = CH2CL + HOCL	3.03E11	0.00	10700.
CLO + H2 = HOCL + H	6.03E11	0.00	14100.
OH + HOCL = H2O + CLO (DEMO)	1.81E12	0.00	990.
H + HOCL = HCL + OH (CH3CL)	9.55E13	0.00	7620.
CL + HOCL = CL2 + OH (DEM)	1.81E12	0.00	260.
CL + HOCL = HCL + CLO	7.28E12	0.00	100.
O + HOCL = OH + CLO (DEM)	6.03E12	0.00	4370.
HOCL = CL + OH	1.76E20	-3.01	56720.
HOCL = H + CLO	8.12E14	-2.09	93690.
O + CL2 = CL + CLO (BAU)	2.51E12	0.00	2720.
H + CL2 = HCL + CL (BAU)	8.59E13	0.00	1170.
C2H3 + CL2 = C2H3CL + CL (TIM)	5.25E12	0.00	-480.
CHCLO + OH = CCLO + H2O	7.5E12	0.00	1200.
CHCLO + O = CCLO + OH	8.8E12	0.00	3500.
CHCLO + O2 = CCLO + HO2	4.5E12	0.00	41800.
CHCLO + CL = CCLO + HCL	1.25E13	0.00	500.
CHCLO + CH3 = CCLO + CH4	2.5E13	0.00	6000.
CHCLO + CH3 = CHO + CH3CL	1.5E13	0.00	8800.
CHCLO + CLO = CCLO + HOCL	1.1E13	0.00	500.
CCLO = CO + CL	1.3E14	0.00	8000.
CCLO + OH = CO + HOCL	3.3E12	0.00	0.
CCLO + O2 = CO2 + CLO	1.0E13	0.00	0.
CCLO + CL = CO + CL2	4.0E14	0.00	800.
COCL2 + M = CCLO + CL + M	1.2E16	0.00	75500.
COCL2 + OH = CCLO + HOCL	1.0E13	0.00	23300.
COCL2 + O = CCLO + CLO	2.0E13	0.00	17000.
COCL2 + H = CCLO + HCL	5.0E13	0.00	6300.
COCL2 + CL = CCLO + CL2	3.2E14	0.00	23500.
COCL2 + CH3 = CCLO + CH3CL	1.9E13	0.00	12900.
CHCL3 = CHCL2 + CL	5.7E12	0.00	67700.
CHCL3 = CCL2 + HCL	5.2E12	0.00	51500.

Table 4 Mechanism (continued)

Reaction	A	n	E
CHCL3 + OH = H2O + CCL3	3.3E12	0.00	2300.
CHCL3 + O2 = HO2 + CCL3	1.0E13	0.00	47200.
CHCL3 + HO2 = H2O2 + CCL3	4.5E10	0.00	14200.
CHCL3 + H = HCL + CHCL2	3.6E12	0.00	6200.
CHCL3 + O = OH + CCL3	3.00E12	0.00	4900.
CHCL3 + CH3 = CH3CL + CHCL2	2.4E13	0.00	12000.
CHCL3 + CL = HCL + CCL3	1.6E13	0.00	3300.
CCL3 + H2 = CHCL3 + H (NIST)	5.01E12	0.00	14300.
CCL3 + CH4 = CHCL3 + CH3 (NIST)	5.00E12	0.00	14900.
CCL2 + O2 = COCL2 + O	5.78E10	0.00	4100.
CHCLCHCL = C2HCL + HCL	7.26E13	0.00	69100.
CH2CCL2 = C2HCL + HCL	1.45E14	0.00	69220.
C2HCL3 = C2CL2 + HCL	7.26E13	0.00	74440.
C2HCL + H = HCL + C2H (GREG)	1.00E13	0.00	17030.
C2HCL + H = C2H2 + CL (GREG)	2.00E13	0.00	2100.
CCL3 + CH3 = C2H3CL3	9.54E46	-10.66	11740.
CCL3 + CH3 = CH2CCL2 + HCL	1.62E30	-5.33	8640.
CCL3 + CH3 = CH3CCL2 + CL	3.98E22	-2.63	7090.
CCL3 + CH2CL = C2H2CL4	4.01E45	-10.15	10670.
CCL3 + CH2CL = C2HCL3 + HCL	4.74E30	-5.08	8810.
CCL3 + CH2CL = C2H2CL3 + CL	5.90E23	-2.84	8960.
CHCL + CHCL = CHCLCHCL (C2H5X2)	4.00E12	0.00	0.
CHCL + O2 = CHCLO + O (CH3+O2)	1.50E13	0.00	2860.
CHCL + O = CHCLO (EST)	1.00E13	0.00	0.
CHCL + O2 = CO + HOCL (0.5CH2	1.20E11	0.00	0.
CH2OH + H = CH3 + OH (MILLER)	1.00E14	0.00	0.
CH2OH + M = CH2O + H + M (MILLER)	1.00E14	0.00	25000.
CH2OH + H = CH2O + H2 (MILLER)	2.00E13	0.00	0.
CH2OH + OH = CH2O + H2O (MILLER)	1.00E13	0.00	0.
CH2OH + O = CH2O + OH (MILLER)	1.00E13	0.00	0.
CH2OH + O2 = CH2O + HO2 (MILLER)	1.48E13	0.00	1500.
CH2OH + CL = CH2O + HCL (BBB)	8.11E15	-0.75	900.
CH2 + O2 = CH2O + O	1.00E14	0.00	3700.
C2H4 + O = CH3 + CHO	2.70E30	-4.54	39490.
C2H4 + OH = CH3 + CH2O	1.29E11	0.00	9080.
C2H4 + OH = CH3CHO + H	3.21E11	0.00	9800.
C2H2 + OH = CH3 + CO	2.63E12	0.00	750.

* The forward rate coefficients are in the modified Arrhenius form: $k_f = AT^n\exp(E/RT)$. Units are in K, mole, cal, cc, sec.

D. Sample Input File for Fuel Lean, R=0 Flame

```
/   flame configuration, burner stabilized with
specified temperature
BURN
MOLE
TGIV
/ENRG
/   in the event of a Newton failure, take 100
timesteps of 1.E-6
TIME    100  1.00E-5
/   begin on a uniform mesh of 6 points
NPTS      6
/      definition of the computational interval
XEND  0.40
XCEN  0.25
WMIX  0.10
/   pressure and inlet mass flow rate
PRES  1.0 (atmospheres)
FLRT  1.02E-02 (g/cm**2-sec)
/   adaptive mesh criteria
GRAD  0.3
CURV  0.8
/   unreacted mole fractions
MOLE
REAC    O2    0.1939
REAC    N2    0.7293
REAC    CH4   0.0768
/   estimated products
PROD    N2    0.7293
PROD    CO2   0.0768
PROD    H2O   0.1536
PROD    O2    0.0403
/   estimated intermediate mole fractions
INTM    CO          1.0E-02
INTM    C2H2        1.0E-02
INTM    C2H4        3.0E-03
INTM    CH3         1.0E-05
INTM    CH2         1.0E-08
INTM    CH2S        1.0E-11
INTM    C2H3        1.0E-08
INTM    C2H         1.0E-12
INTM    C2H5        1.0E-09
INTM    C2H6        1.0E-06
INTM    CH2CO       5.0E-06
INTM    HCCO        1.0E-08
INTM    OH          1.0E-03
INTM    H           5.0E-03
INTM    O           1.0E-04
INTM    HO2         1.0E-04
INTM    H2O2        3.0E-04
INTM    CH3O        1.0E-08
```

```
/   tolerances for the Newton iteration
ATOL  1.E-09
RTOL  1.E-4
/   tolerances for the time step Newton iteration
ATIM  1.E-5
RTIM  1.E-5
/   print control
PRNT    1
/      given temperature profile
TEMP      0.0    1009.0
TEMP      0.025  1313.0
TEMP      0.05   1500.0
TEMP      0.075  1559.0
TEMP      0.085  1571.0
TEMP      0.095  1580.0
TEMP      0.105  1585.0
TEMP      0.11   1586.0
TEMP      0.115  1585.0
TEMP      0.125  1581.0
TEMP      0.15   1560.0
TEMP      0.175  1550.0
TEMP      0.20   1543.0
TEMP      0.25   1533.0
TEMP      0.30   1527.0
TEMP      0.35   1521.0
TEMP      0.40   1515.0
/TRANSPORT OPTION TAKING THERMAL DIFFUSION
TDIF
/read the solution from restart file
/RSTR
/ASEN
/CNTN
END
```

E. Sample Output of Rate-of-Production Calculation

```
##################################################################

NORMALIZED & ABSOLUTE RATE-OF-PRODUCTION COEFF. FOR MESH #1

12. OH                                  NORMALIZED     ABSOLUTE
                                                    (MOLES/CC-SEC)

    54.CH4+OH=CH3+H2O                   -7.89E-01     (-1.55E-06)

    60.CH3+HO2=CH3O+OH                   9.56E-01     ( 1.73E-06)

    75.CH2O+OH=CHO+H2O                  -1.04E-01     (-2.05E-07)

         NET RATE-OF-PRODUCTION (MOLES/CC-SEC)  =  1.81E-06
         NET RATE-OF-CONSUMPTION (MOLES/CC-SEC) =  1.97E-06
##################################################################

NORMALIZED & ABSOLUTE RATE-OF-PRODUCTION COEFF. FOR MESH #2

12. OH                                  NORMALIZED     ABSOLUTE
                                                    (MOLES/CC-SEC)

    54.CH4+OH=CH3+H2O                   -7.80E-01     (-1.87E-06)

    60.CH3+HO2=CH3O+OH                   8.08E-01     ( 1.89E-06)

    75.CH2O+OH=CHO+H2O                  -1.02E-01     (-2.45E-07)

    106.H2O2+M=2OH+M                     1.54E-01     ( 3.61E-07)

         NET RATE-OF-PRODUCTION (MOLES/CC-SEC)  =  2.34E-06
         NET RATE-OF-CONSUMPTION (MOLES/CC-SEC) =  2.40E-06
##################################################################

NORMALIZED & ABSOLUTE RATE-OF-PRODUCTION COEFF. FOR MESH #3

12. OH                                  NORMALIZED     ABSOLUTE
                                                    (MOLES/CC-SEC)

    54.CH4+OH=CH3+H2O                   -7.67E-01     (-4.03E-06)

    60.CH3+HO2=CH3O+OH                   5.27E-01     ( 2.72E-06)

    75.CH2O+OH=CHO+H2O                  -1.01E-01     (-5.33E-07)

    106.H2O2+M=2OH+M                     3.46E-01     ( 1.79E-06)

         NET RATE-OF-PRODUCTION (MOLES/CC-SEC)  =  5.17E-06
         NET RATE-OF-CONSUMPTION (MOLES/CC-SEC) =  5.26E-06
##################################################################
```

F. Thermodynamic Data Base

Table 5 Thermodynamic Bata Base

SPECIES	HF(298)	S(298)	CP300	CP400	CP500	CP600	CP800	CP1000	CP1500
AR	0.00	36.98	4.97	4.97	4.97	4.97	4.97	4.97	4.97
N2	0.00	45.77	6.86	7.06	7.17	7.25	7.45	7.83	8.27
C(S)	0.00	21.83	2.06	2.86	3.50	4.02	4.73	5.16	5.65
C	170.88	38.31	4.98	4.97	4.97	4.97	4.97	4.97	4.97
CL	28.90	39.50	5.20	5.34	5.40	5.41	5.35	5.30	5.24
H2	0.00	31.21	6.90	6.95	6.99	7.02	7.10	7.21	7.72
H	52.10	27.36	4.97	4.97	4.97	4.97	4.97	4.97	4.97
CH	142.00	43.72	6.97	6.97	7.03	7.12	7.41	7.77	8.74
HCL	-22.07	44.64	6.96	6.95	6.99	7.07	7.29	7.56	8.10
CL2	0.00	53.30	8.10	8.38	8.59	8.74	8.91	8.99	9.10
CH2	92.35	46.32	8.28	8.62	8.99	9.37	10.15	10.88	12.22
CH2S	101.44	44.15	8.28	8.62	8.99	9.37	10.15	10.88	12.22
CH3	35.12	46.38	9.26	10.05	10.81	11.54	12.90	14.09	16.26
CH4	-17.90	44.48	8.51	9.77	11.10	12.44	15.00	17.20	20.61
C2H	132.00	49.58	8.88	9.61	10.22	10.73	11.54	12.16	13.32
C2H2	54.19	48.01	10.60	11.97	13.08	13.97	15.31	16.29	18.31
C2H3	67.10	56.20	10.89	12.47	13.87	15.11	17.15	18.73	21.34
C2H4	12.54	52.39	10.28	12.73	14.91	16.84	20.02	22.45	26.21
C2H5	28.36	57.90	12.26	14.81	17.13	19.24	22.85	25.74	30.54
C2H6	-20.24	54.85	12.58	15.77	18.68	21.31	25.80	29.33	34.91
C3H2	106.65	117.98	12.96	15.17	16.93	18.31	20.28	21.57	23.85
C3H3	77.26	89.99	14.05	16.34	18.27	19.89	22.40	24.23	27.23
C*C*C	45.92	58.30	14.19	17.19	19.77	21.97	25.45	28.01	32.04
C3H7	23.99	69.07	16.85	21.45	25.39	28.75	34.09	38.05	44.58
C#CC	44.32	59.30	14.57	17.30	19.68	21.75	25.11	27.68	31.85
C3H3	83.33	56.99	14.06	16.34	18.25	19.86	22.35	24.17	27.21
CCCC	-30.15	74.12	23.31	29.74	35.36	40.26	48.22	54.21	63.67
CHCL	71.00	56.17	8.80	9.45	10.13	10.81	12.11	13.22	14.78
CH2CL	26.10	59.60	9.32	10.18	11.14	12.14	14.10	15.83	18.31
CCL2	52.10	49.00	11.09	11.91	12.52	12.98	13.61	14.09	15.41
CHCL2	23.50	67.40	13.11	13.90	14.68	15.44	16.83	17.98	19.80
CCL3	19.00	71.01	15.25	16.58	17.53	18.19	18.88	19.14	19.56
CCL4	-22.90	74.20	19.91	21.70	22.96	23.81	24.67	24.95	25.51
CH3CL	-19.59	56.01	9.77	11.58	13.20	14.63	17.02	18.87	21.80
CH2CL2	-22.80	64.59	12.26	14.23	15.88	17.26	19.36	20.81	22.90
CHCL3	-24.20	70.66	15.77	17.78	19.31	20.46	21.96	22.82	24.21
C2HCL	46.90	58.10	13.17	14.29	15.18	15.88	16.88	17.55	18.80
C2CL2	50.10	65.00	15.71	16.71	17.48	18.07	18.86	19.32	20.05
C2H3CL	5.00	63.09	12.33	15.31	17.73	19.67	22.47	24.26	26.88
CH2CCL2	0.62	69.25	15.81	18.43	20.56	22.26	24.68	26.19	28.21
CHCLCHCL	1.15	69.25	15.81	18.43	20.56	22.26	24.68	26.19	28.21
CH2CCL	60.40	64.46	11.39	14.08	16.35	18.26	21.23	23.38	26.87
C2H2CL	60.40	64.46	11.39	14.08	16.35	18.26	21.23	23.38	26.87

Table 5 Thermodynamic Data Base (continued)

SPECIES	HF(298)	S(298)	CP300	CP400	CP400	CP500	CP600	CP1000	CP1500
CCL2CH	58.20	68.88	17.52	20.13	22.16	23.70	25.74	26.90	28.60
C2HCL2	58.20	68.88	17.52	20.13	22.16	23.70	25.74	26.90	28.60
C2HCL3	-1.40	77.63	19.22	21.82	23.75	25.14	26.80	27.60	28.98
CH2CLCH2	20.78	68.50	14.00	17.38	20.13	22.37	25.81	28.42	33.43
CH2CH2CL	20.78	68.50	14.00	17.38	20.13	22.37	25.81	28.42	33.43
C2H4CL	17.51	67.31	14.10	17.19	19.79	21.98	25.42	27.99	32.50
CH3CHCL	17.51	67.31	14.10	17.19	19.79	21.98	25.42	27.99	32.50
CH3CCL2	10.50	73.60	17.28	20.32	22.86	24.95	28.09	30.18	33.09
CHCL2CH2	16.40	74.30	17.36	20.38	22.90	24.98	28.12	30.22	33.08
CH2CLCHCL	11.49	75.80	16.81	19.99	22.56	24.63	27.67	29.75	33.21
C2H3CL2	11.49	74.30	17.28	20.32	22.84	24.93	28.05	30.16	33.09
CH2CLCCL2	7.05	83.20	20.21	23.27	25.68	27.55	30.14	31.77	34.50
CCL3CH2	11.90	82.90	20.21	23.27	25.68	27.55	30.14	31.77	34.50
C2H2CL3	8.50	83.10	20.21	23.27	25.68	27.55	30.14	31.77	34.50
C2H5CL	-26.83	66.03	15.06	18.62	21.67	24.28	28.43	31.47	36.27
CH3CHCL2	-30.60	72.89	18.29	21.87	24.81	27.23	30.87	33.44	37.80
C2H4CL2	-31.01	73.78	18.99	22.14	24.74	26.90	30.32	33.06	38.79
CH2CLCH2CL	-31.01	73.78	18.99	22.14	24.74	26.90	30.32	33.06	38.79
CH3CCL3	-34.60	78.60	22.52	25.79	28.45	30.59	33.70	35.73	38.91
C2H3CL3	-34.60	78.60	22.52	25.79	28.45	30.59	33.70	35.73	38.91
C2H2CL4	-36.00	86.01	25.23	28.66	31.32	33.35	36.05	37.59	39.82
C2HCL4	5.80	87.90	23.50	26.50	28.76	30.42	32.52	33.68	35.70
C2HCL5	-34.00	91.00	28.42	31.85	34.44	36.33	38.61	39.62	40.51
C2CL6	-33.80	95.10	32.63	35.82	38.12	39.69	41.35	41.89	42.52
C2CL5	7.50	92.20	27.59	30.24	32.22	33.66	35.37	36.12	36.87
C2CL3	56.50	79.03	20.99	23.40	25.21	26.52	28.09	28.80	29.70
C2CL4	-3.40	81.46	22.75	24.99	26.68	27.92	29.39	30.00	30.52
CH2CLCHCL2	-36.10	81.50	21.01	24.72	27.67	29.99	33.25	35.36	38.91
CLO	24.20	54.10	7.50	7.91	8.21	8.43	8.69	8.81	9.00
CL2O	21.00	64.00	11.41	12.21	12.76	13.12	13.46	13.55	13.81
CLO2	25.00	61.50	9.99	10.97	11.72	12.27	12.97	13.32	13.80
HOCL	-17.80	56.50	8.91	9.56	10.08	10.50	11.13	11.58	12.40
COCL2	-52.60	67.80	13.81	15.21	16.26	17.03	17.97	18.45	19.21
CHCLO	-39.30	61.80	11.12	12.46	13.55	14.42	15.70	16.58	18.11
O	59.55	38.47	5.23	5.14	5.08	5.04	5.01	5.01	4.98
O2	0.00	49.01	7.02	7.23	7.44	7.65	8.04	8.35	8.73
OH	9.49	43.88	7.16	7.08	7.05	7.05	7.15	7.33	7.87
H2O	-57.80	45.10	8.02	8.19	8.41	8.66	9.24	9.85	11.23
HO2	3.50	54.73	8.37	8.95	9.48	9.96	10.78	11.43	12.47
H2O2	-32.53	55.66	10.42	11.46	12.35	13.10	14.30	15.21	16.85
CO	-26.42	47.21	6.96	7.02	7.13	7.27	7.61	7.94	8.41
CHO	10.40	53.66	8.27	8.76	9.27	9.78	10.73	11.51	12.55
CLO	24.20	54.10	7.50	7.91	8.21	8.43	8.69	8.81	9.00
CL2O	21.00	64.00	11.41	12.21	12.76	13.12	13.46	13.55	13.81
OCLO	25.00	61.50	9.99	10.97	11.72	12.27	12.97	13.32	13.80
HOCL	-17.80	56.50	8.91	9.56	10.08	10.50	11.13	11.58	12.40

Table 5 Thermodynamic Data Base (continued)

SPECIES	HF(298)	S(298)	CP300	CP400	CP500	CP600	CP800	CP1000	CP1500
COCL2	-52.60	67.80	13.81	15.21	16.26	17.03	17.97	18.45	19.21
CHCLO	-39.30	61.80	11.12	12.46	13.55	14.42	15.70	16.58	18.11
CO2	-94.05	51.07	8.90	9.85	10.65	11.31	12.30	12.97	13.93
CH2O	-27.70	52.26	8.45	9.46	10.49	11.49	13.34	14.86	16.95
CH3O	3.90	53.25	9.01	10.66	12.22	13.69	16.28	18.38	21.56
CH2CO	-14.60	57.79	12.98	15.17	16.92	18.32	20.31	21.61	23.80
CH3OH	-48.06	57.28	10.48	12.48	14.34	16.05	19.00	21.35	24.96
CH3CHO	-39.69	63.20	13.22	15.76	18.16	20.38	24.17	27.00	30.60
C3O2	-22.38	116.09	16.08	17.85	19.29	20.47	22.18	23.31	24.93
CCC	-24.79	64.62	17.63	22.62	27.00	30.84	37.12	41.87	49.27
CC.C	22.30	69.24	15.74	20.09	23.93	27.32	32.93	37.25	44.27
C3H4	44.35	59.39	14.56	17.31	19.69	21.75	25.08	27.62	31.85
C4H4	62.84	98.86	17.64	21.15	24.11	26.59	30.43	33.20	37.66
C*CC*C	34.97	123.08	18.80	22.79	26.41	29.66	35.14	39.32	45.44
CCC*C	-0.13	83.45	20.50	26.02	30.82	34.99	41.76	46.89	55.09
C5	234.00	138.26	14.71	17.08	18.93	20.36	22.29	23.43	25.06
C6H	233.20	167.88	21.67	25.06	27.61	29.50	31.87	33.18	35.59
C6H2	162.61	133.69	21.43	25.61	28.84	31.31	34.63	36.71	40.66
CC6H6	19.82	64.32	19.70	26.83	32.78	37.71	45.13	50.17	57.30
C*CC*CC*C	37.95	79.13	28.11	31.88	36.35	41.12	50.44	58.04	66.37
C6H9	50.85	87.74	27.73	31.95	36.89	42.16	52.43	60.88	70.58
CC6H7	56.05	44.94	27.42	31.08	35.43	40.09	49.16	56.53	64.27
CC6H8	25.86	46.76	23.26	27.71	33.10	38.91	50.19	59.16	67.10
CC6H9	41.36	76.65	25.45	30.12	35.64	41.54	53.03	62.40	72.70
C8H	287.40	217.28	26.39	31.32	35.05	37.80	41.26	43.13	46.28
C8H2	216.83	209.94	28.66	34.13	38.21	41.18	44.85	46.84	50.67
CC6H5C6H5	37.90	106.45	35.80	48.46	59.22	68.22	81.57	89.76	96.71
CCL	103.29	53.64	7.72	8.04	8.28	8.46	8.69	8.81	8.98
C2CL	125.99	59.33	11.51	11.99	12.43	12.82	13.50	14.04	15.01
C2HCL2	58.63	70.65	17.52	20.13	22.16	23.70	25.74	26.90	28.60
C2H2CL2	1.14	69.25	15.81	18.43	20.56	22.26	24.68	26.19	28.21
PHCL2	7.11	81.45	27.82	34.49	40.04	44.56	50.91	54.38	56.12
CC6H5CL	12.35	74.78	23.26	30.49	36.50	41.30	47.90	52.45	82.71
PHPHCL	38.39	113.80	39.89	52.56	63.18	71.78	83.82	92.04	140.19
PHCLPHCL	38.88	121.14	44.05	56.59	66.97	75.24	86.48	94.03	144.89
CH2CLO	2.16	63.27	11.23	13.27	15.01	16.47	18.72	20.28	22.41
CH2CLOO	3.50	73.11	15.77	16.86	18.20	19.66	22.52	24.85	27.05
CH2OOCL	10.00	78.60	17.47	20.02	22.20	24.05	26.92	28.92	31.68
CH2OH	-5.90	59.61	9.72	11.21	12.58	13.84	15.98	17.61	19.80
CCLO	-4.00	63.50	10.80	11.28	11.68	12.02	12.53	12.88	13.40
HCCO	42.58	60.62	11.79	13.51	14.73	15.61	16.96	18.21	19.36

Unit: Hf, Kcal/mole; S and Cp, cal/mole-K.

G. Transport Data Base

The transport data base used in the model is listed in Table 6. Six columns in the table are, in order:

1. The species name.
2. An index indicating whether the molecule has a monatomic, linear or nonlinear geometrical configuration. If the index is 0, the molecule is a single atom. If the index is 1, the molecule is linear, and if it is 2, the molecule is nonlinear.
3. The Lennard-Jones potential well depth ε/k_B in Kelvins.
4. The Lennard-Jones collision diameter σ in Angstroms.
5. The dipole moment μ in Debye. Note: a Debye is 10^{-18} $cm^{3/2}erg^{1/2}$.
6. The polarizability α in cubic Angstroms.
7. The rotational relaxation collision number Z_{rot} at 298K.

Table 6 Transport Data Base

AR	0	93.300	3.542	0.000	1.640	1.0
He	0	10.220	2.551	0.000	0.200	1.0
N2	1	97.530	3.621	0.000	1.760	4.000
H2	1	59.700	2.827	0.000	0.800	280.0
O2	1	106.700	3.467	0.000	1.600	1.0
H	0	145.000	2.05	0.000	0.670	1.0
O	0	80.000	2.75	0.000	0.800	1.0
C	0	84.000	3.500	0.000	0.830	1.0
CL	0	151.000	3.339	0.000	2.300	1.0
OH	1	480.000	2.750	1.660	1.290	1.0
H2O	2	809.100	2.641	1.800	1.490	4.0
HO2	2	220.150	3.458	1.510	1.780	1.0
H2O2	2	289.300	4.196	2.200	2.180	3.8
HCL	1	344.700	3.339	1.100	2.640	1.0
CH	1	480.000	2.750	0.30	1.430	1.0
CO	1	91.700	3.690	0.110	1.950	1.8
HCO	1	340.400	4.284	2.550	2.590	1.0
CHO	1	340.400	4.284	2.550	2.590	1.0
CL2	1	316.000	4.217	0.200	4.600	1.0
CLO	1	211.350	3.842	1.700	2.990	1.0
CL2O	2	370.870	4.387	2.070	5.290	1.0
OCLO	2	418.000	4.165	0.780	3.680	1.0
HOCL	2	453.970	3.968	1.930	3.390	1.0
COCL2	1	376.000	4.700	1.100	6.790	1.0
CHCLO	2	361.000	4.340	1.500	4.890	1.0
CO2	1	195.200	3.941	0.000	2.610	2.1
HCHO	1	334.600	4.304	2.300	2.990	2.0
CH2O	1	334.600	4.304	2.300	2.990	2.0
CH2S	1	144.000	3.745	0.000	1.830	1.0
CH2(1)	1	144.000	3.745	0.000	1.830	1.0
CH2	1	144.000	3.745	0.000	1.830	1.0
CH3	2	151.000	3.745	0.000	2.230	1.0
CH4	2	148.600	3.758	0.000	2.600	13.0
C2H	1	253.940	4.000	1.100	3.240	1.0
C2H2	1	231.800	4.033	0.000	3.640	1.0
C2H3	1	227.770	4.102	0.700	3.040	1.0
C2H4	1	224.700	4.163	0.000	3.440	1.0
C2H5	2	246.840	4.320	0.370	4.060	1.0
C2H6	2	215.700	4.443	0.000	4.460	1.0
CHCL	1	224.700	4.163	1.570	3.730	1.0
CCL	1	227.770	4.102	1.870	3.030	1.0
CCL2	1	348.000	4.644	0.000	5.630	1.0
CCL3	2	444.360	5.031	0.000	7.930	1.0
CHCL2	2	420.850	4.694	1.570	6.030	1.0
CH2CL	2	340.280	4.305	0.800	3.830	1.0
CH3O	2	453.970	3.968	1.500	2.920	1.0
CH3O2	2	418.000	4.165	1.500	3.610	1.0
CH3CL	2	350.000	4.182	1.900	4.230	1.0
CH2CL2	2	356.300	4.898	1.800	6.430	1.0
CHCL3	2	340.200	5.389	1.100	8.330	1.0
CCL4	2	322.700	5.947	0.000	10.530	1.0
CLC#C.	1	332.620	4.335	1.540	5.140	1.0
C2CL	1	332.620	4.335	0.440	5.140	1.0

Table 6 Transport Data Base (continued)

C2HCL	1	332.620	4.335	0.440	5.540	1.0
CLC#CH	1	332.620	4.335	0.440	5.540	1.0
CLC#CCL	1	442.700	4.958	0.000	7.440	1.0
C2CL2	1	442.700	4.958	0.000	7.440	1.0
CHCLCH	1	345.170	4.738	1.500	5.740	1.0
CHCLC.H	1	345.170	4.738	1.500	5.740	1.0
CH2CCL	1	345.170	4.738	1.500	5.740	1.0
CHCLCCL	1	426.190	5.140	0.900	7.640	1.0
CCL2CH	1	412.180	5.013	1.340	7.640	1.0
C2CL3	1	473.360	5.247	0.900	9.540	1.0
C2H3CL	1	349.000	4.644	1.500	6.140	1.0
CH2CCL2	1	412.180	5.013	1.340	8.040	1.0
CHCLCHCL	1	426.190	5.140	0.900	8.040	1.0
C2HCL3	1	472.500	5.316	0.900	9.940	1.0
C2CL4	1	514.900	5.640	0.000	11.840	1.0
C2H4CL	2	379.290	4.816	2.000	5.960	1.0
CH3CHCL	2	379.290	4.816	2.000	5.960	1.0
CH3C.HCL	2	379.290	4.816	2.000	5.960	1.0
CH2CLCH2	2	379.290	4.816	2.000	5.960	1.0
CH2CLC.H2	2	379.290	4.816	2.000	5.960	1.0
CH2CLCHCL	2	471.190	5.116	1.800	7.860	1.0
CH3CCL2	2	435.910	5.103	2.000	7.860	1.0
CHCL2CH2	2	435.910	5.103	2.000	7.860	1.0
CH2CLCCL2	2	498.910	5.379	1.700	9.760	1.0
CCL3CH2	2	451.390	5.447	1.780	9.760	1.0
C2H2CL3	2	498.910	5.379	1.700	9.760	1.0
CCL3CHCL	2	515.870	5.761	0.900	11.660	1.0
CHCL2CCL2	2	525.050	5.872	1.320	11.660	1.0
C2HCL4	2	525.050	5.872	1.320	11.66	1.0
C2CL5	2	556.000	6.142	0.910	13.560	1.0
C2H5CL	2	300.000	4.898	2.000	6.360	1.0
CH3CHCL2	2	435.900	5.102	2.000	8.260	1.0
C2H4CL2	2	471.200	5.116	1.800	8.260	1.0
C2H3CL3	2	498.900	5.397	1.700	10.160	1.0
CH3CCL3	2	454.000	5.406	1.770	10.160	1.0
C2H2CL4	2	540.700	5.868	1.320	12.060	1.0
CH2CLCCL3	2	520.600	5.841	1.390	12.060	1.0
C2HCL5	2	556.000	6.142	0.920	13.960	1.0
C2CL6	2	581.780	6.457	0.000	15.860	1.0
HCOOH	2	460.570	4.010	1.500	2.880	1.0
CH3OH	2	381.800	3.626	1.700	3.320	1.0
CH2CLOH	2	535.000	4.610	1.800	5.220	1.0
CH2CLO	2	535.00	4.610	1.800	4.820	1.0
CH2CLO.	2	535.00	4.610	1.800	4.820	1.0
CH2OH	2	453.970	4.268	1.700	2.920	1.0
CH2CLOOH	2	598.000	4.900	1.800	5.910	1.0
CH2CLOO	2	598.000	4.900	1.800	5.510	1.0
CH2OOCL	2	400.800	4.880	0.0	5.510	1.0
CLOO	2	418.000	4.165	0.530	3.680	1.0
CH3OOCL	2	400.800	4.880	0.0	5.910	1.0
CH3OCL	2	329.600	4.587	1.850	5.220	1.0
C2H5OH	2	362.600	4.530	1.700	5.150	1.0
C2H5OCL	2	364.010	5.044	1.940	7.050	1.0

Table 6 Transport Data Base (continued)

C.H2CH2OCL	2	364.010	5.044	1.940	6.650	1.0
C2H4OCL	2	364.010	5.044	1.940	6.650	1.0
CH2CLCH2OH	2	481.500	5.042	1.780	7.050	1.0
CH2CLCH2O	2	481.500	5.042	1.780	6.650	1.0
CCLO	1	388.530	4.730	1.800	4.490	1.0
COCL	1	388.530	4.730	1.80	4.490	1.0
HOOCL	2	418.000	4.165	0.530	4.080	1.0
CH2OCL	2	329.600	4.587	1.850	4.820	1.0
HCCOH	2	150.000	2.500	1.400	4.330	1.000
C3H2	1	333.350	4.410	0.0	4.820	1.0
C3H3	1	331.880	4.511	0.100	5.220	1.0
C*C*C	1	331.880	4.511	0.200	5.620	1.0
C3H6	2	248.900	4.807	0.400	6.110	1.0
C3H8	2	237.100	5.118	0.000	6.290	1.0
C3H7	2	237.100	5.118	0.000	5.890	1.0
C3H4	2	333.350	4.521	0.700	5.770	1.0
C#CC	1	333.350	4.521	0.700	5.770	1.0
C3H5	2	248.900	4.807	0.400	5.710	1.0
C4H10	2	531.400	4.687	0.000	8.120	1.0
C4H2	1	357.000	5.180	0.000	0.000	1.000
C4H3	1	357.000	5.180	0.000	0.000	1.000
C4H4	1	357.000	5.180	0.000	0.000	1.000
CHCL2O	2	452.160	4.878	1.690	6.520	1.0
CH2OOH	2	418.030	4.165	0.0	3.410	1.0
CHCO	1	314.010	4.232	1.400	3.930	1.0
HCCO	1	314.010	4.232	1.400	3.930	1.0
HCCO.	1	314.010	4.232	1.400	3.930	1.0
CH2CO	1	314.010	4.232	1.400	4.330	1.0
CH3CO	2	388.530	4.730	2.500	4.420	1.0
CHCL2OH	2	452.160	4.878	1.010	6.230	1.0
CHCLOH	2	465.050	4.664	1.800	4.620	1.0
CHCL2OO	2	540.660	4.966	0.0	7.210	1.0
CHCLOOCL	2	446.240	5.118	0.0	7.210	1.0
CHCL2OOH	2	540.660	4.966	0.0	7.610	1.0
CCL2OH	2	452.160	4.878	1.690	6.520	1.0
CCL3OH	2	555.690	5.085	1.440	8.820	1.0
CCL2OOH	2	540.660	4.966	0.0	7.210	1.0
CCL2OO	2	540.660	4.966	0.0	6.810	1.0
COCL2O	2	480.520	4.789	0.0	6.810	1.0
CCL3OO	2	584.450	5.170	1.800	9.110	1.0
CCL2OOCL	2	492.130	5.345	0.0	9.110	1.0
CCL3O	2	555.690	5.085	1.440	8.420	1.0
CCL3OOH	2	584.450	5.170	1.800	9.510	1.0
CH2CHCLOH	2	452.160	4.878	1.690	6.250	1.0
CH2CHOH	2	440.330	4.641	0.0	4.970	1.0
CH2CHO	2	388.530	4.730	2.500	4.220	1.0
CH3CHCLO	2	452.160	4.878	1.690	6.250	1.0
CH3CHO	2	388.530	4.730	2.500	4.620	1.0
CH2OHCHCL	2	529.960	4.878	1.770	6.250	1.0
CH2CLCHO	2	493.040	4.861	1.990	6.520	1.0
CH2CHCLO	2	452.160	4.878	1.690	5.850	1.0
CH2OCHCL	2	421.310	4.844	2.000	5.850	1.0
CH2CCL2OH	2	546.300	5.181	1.440	8.150	1.0

Table 6 Transport Data Base (continued)

CH2CCLOH	2	487.570	4.865	1.640	6.870	1.0
CH3CCL2O	2	546.300	5.181	1.440	8.150	1.0
CH3CCLO	2	431.660	4.793	2.710	6.520	1.0
CH2OHCCL2	2	546.300	5.181	1.640	8.150	1.0
CHCL2CH2O	2	546.300	5.181	1.640	8.150	1.0
CHCL2CHO	2	472.870	5.231	2.360	8.420	1.0
CH2CCL2O	2	546.300	5.181	1.440	7.750	1.0
CH2OCCL2	2	471.260	5.000	0.0	7.750	1.0
CHCLCCL2OH	2	483.350	5.429	1.660	10.050	1.0
CHCLCCLOH	2	544.940	5.090	0.0	8.770	1.0
CH2CLCCL2O	2	483.350	5.429	1.660	10.050	1.0
CHCLOHCCL2	2	547.390	5.429	0.0	10.050	1.0
CCL2CHOH	2	544.920	5.090	1.640	8.770	1.0
CHCL2CHCLO	2	547.390	5.429	0.0	10.050	1.0
CHCLCCL2O	2	547.390	5.429	0.0	9.650	1.0
CCL2CCL2OH	2	626.410	5.577	0.0	11.950	1.0
CCL2CCLOH	2	591.960	5.297	0.0	10.670	1.0
CCL2CCLO	2	591.960	5.297	0.0	10.270	1.0
CCL2CO	2	419.970	4.614	0.0	8.130	1.0
CHCL2CCL2O	2	626.410	5.577	0.0	11.950	1.0
CCL2CCL2O	2	626.410	5.577	0.0	11.550	1.0
CH2CCLOO	2	516.210	4.957	0.0	7.160	1.00
CH2CCLO	2	431.660	4.793	2.710	6.470	1.00
CH2OCCLO	2	565.240	4.965	0.0	6.140	1.00
C2H2OH	2	224.700	4.162	0.000	0.000	1.000
C3H2	2	209.000	4.100	0.000	0.000	1.000
C3H3	1	252.000	4.760	0.000	0.000	1.000
C3H4	1	252.000	4.760	0.000	0.000	1.000
C3H6	2	266.800	4.982	0.000	0.000	1.000
C3H7	2	266.800	4.982	0.000	0.000	1.000
I*C3H7	2	266.800	4.982	0.000	0.000	1.000
N*C3H7	2	266.800	4.982	0.000	0.000	1.000
C3H8	2	266.800	4.982	0.000	0.000	1.000
C4H	1	357.000	5.180	0.000	0.000	1.000
C4H2OH	2	224.700	4.162	0.000	0.000	1.000
C4H8	2	357.000	5.176	0.000	0.000	1.000
C4H9	2	357.000	5.176	0.000	0.000	1.000
S*C4H9	2	357.000	5.176	0.000	0.000	1.000
C4H9	2	357.000	5.176	0.000	0.000	1.000
I*C4H9	2	357.000	5.176	0.000	0.000	1.000
CH3CHO	2	436.000	3.970	0.000	0.000	2.000
CH3CO	2	436.000	3.970	0.000	0.000	2.000
CH2CHO	2	436.000	3.970	0.000	0.000	2.000
CH3O2	2	417.000	3.690	1.700	0.000	2.000
CH4O	2	417.000	3.690	1.700	0.000	2.000
HE	0	10.200	2.576	0.000	0.000	0.000
C2HO	2	150.000	2.500	0.000	0.000	1.000
C	0	84.00	3.5	0.00	0.00	0.0
C*C*C	2	252.00	4.760	0.000	0.000	0.000
C#CC	2	252.000	4.760	0.000	0.000	0.000
C4H2O	2	357.00	5.180	0.000	0.000	0.000
C2H5O	2	450.00	4.36	0.00	0.00	1.0

WORK CITED

1. Barat, R.B., Sarofim, A.F., Longwell, J.P., and Bozzelli, J.W." Inhibition of a Fuel Lean Ethlene/Air Flame in a Jet Stirred Combustor by Methyl Chloride: Experimental and Mechanistic Analyses." *Combust. Sci. and Tech.*, 74 (1990): 361-378

2. Biordi, J.C., Lazzara, C.P., and Papp, J.F. "Flame-Structure Studies of CF3Br-Inhibited Methane Flames." *14th Symposium (International) on Combustion*, The Combust. Institute, (1973) p.367

3. Bradley, D., and Matthews, K.J. "Measurement of High Gass Temperatures with Fine Wire Thermocouple." *Journal of Mech. Eng. Sci.*, 10 (1968): 299

4. Bradley, D., Dixon-Lewis, G., Habik, S., Kwa, L.K., and El-sherif, S. "Laminar Flame Structure and Burning Velocities of Premixed Methanol-Air." *Combustion and Flame*, 85 (1991): 105-120

5. Cundy, V.A., Morse, J.S., and Senser, D.W. "Constant-tension Thermocouple Rake Suitable for Use in Flame Mode Combustio Studies." *Review of Sci. Instrum.*, 57 (1986): 1209-1210

6. Fristrom, R.M., and Webstenberg, A.A., *Flame Structure*, McGraw-hill, NY, (1965) p.145-174

7. Ho, Wen-Pin, Barat, R.B., and Bozzelli, J.W. "Thermal Reactions of CH2Cl2 in H2/O2 Mixtures: Implications for Chlorine Inhibition of CO Conversion to CO2."*Combustion and Flame*, 88 (1992): 265-295

8. Janssen, J.M., and Senser, D.W. "Incipient Soot Formation in Dichloromethane-Methane-Air Premixed Flame." *Combustion & Flame*, 84 (1991): 265-276

9. Karim, H., Personal Communication (1992)

10. Karra, S.B. and Senkan, S.M. "Chemical Structures of Sooting CH3Cl/CH4/O2/Ar and CH4/O2/Ar Flames." *Combust. Sci. and Tech.*, 54 (1987): 333-347

11. Kassem, M., and Senkan, S.M. Chemical Structures of Fuel-Rich, Premixed, Laminar Flames of 1,2-C2H4Cl2 and CH4." *Combustiom and Flame*, 83 (1991): 365-374

12. Kee, R.J., Grcar, J.F., Smooke, M.D., and Miller, J.A. A Fortran Program for Modeling Steady Laminar One-dimensional Premixed Flames." *Sandia Report SAND85-8240*, Sandia National Laboratoties, Livermore, CA (1985)

13. Pauwels, J.F., Carlier, M., Devolder, P. and Sochet,L.R. "Influence of Equivalence Ratio on the Structure of Low-Pressure Premixed Methane-Air Flames." *Combustiom and Flame*, 82 (1990): 163-175

14. Senser, D.W., Cundy, V.A., and Morse, J.S. "Chemical Species and Temperature Profiles of Laminar Dichloromethane-Methane-Air Flames." *Combust. Sci. and Tech.*, 51 (1987): 209

15. Valeiras, H., Gupta, A.K., and Senkan, S.M. "Laminar Burning Velocities of Chlorinated Hydrocarbon-Methane-Air Flames." *Combust. Sci. and Tech.*, 36 (1984): 123

16. Wilson, W.E. "Structure, Kinetics, and Mechanism of a Methane-Oxygen Flame Inhibited with Methyl Bromide." *10th Symposium (International) on Combustion*, The Combust. Institute, (1965) p.47